Catenary Action in Steel Framed Structures with Autoclaved Aerated Concrete Infill & Buckling Restrained Braces

by

Haitham A. Eletrabi

A dissertation submitted to the Graduate Faculty of
Auburn University
in partial fulfillment of the
requirements for the Doctor of
Philosophy

Auburn, Alabama
December 13, 2014

Keywords: catenary action, steel frames, AAC infill, BRB braces, concrete slab, progressive collapse

Approved by

Justin D. Marshall, Chair, Associate Professor
Robert W. Barnes, Associate Professor
Mary L. Hughes, Lecturer

Abstract

The progressive collapse of structures is considered a major concern for designers since the Ronan Point incident. Preventing and mitigating progressive collapse has become a serious issue for all types of buildings. Progressive collapse is disproportionate failure of the structure due to the failure of a relatively small part of it. This may result in either damage to a large portion or collapse of the whole structure. Collapse of portions of a structure generates lateral force demand in the lateral frames. Catenary action is a load mechanism that is developed to resist the additional loads as a result of sudden column loss and prevent disproportionate collapse. The beams above the removed column will resist the loads by flexural action until plastic hinge formation. Subsequently, the beam resists the loads by catenary action. The developed catenary (axial) forces in steel beams play a big role in the resistance of progressive collapse along with the adjacent lateral load resisting system. OpenSees (Open System for Earthquake Engineering Simulation), a software developed by the Pacific Earthquake Engineering Research (PEER) Center of the University of California at Berkeley, was used to analyze the models.

Autoclaved aerated concrete (AAC) infilled walls have shown superior resistance to axial loads compared to other infill materials. Previous research has focused on the impact of AAC on the seismic behavior of steel frames when subjected to lateral loads. Infilled steel frames have shown remarkable performance in resisting earthquake loads. The impact of AAC infill on the performance of steel frames subjected to lateral seismic

forces suggests that AAC infill might affect steel frames that are subjected to progressive collapse loads as well. Detailed study on the impact of AAC infill on the catenary action demands in steel framed structures was conducted. Results showed that AAC infilled frames had a higher load carrying capacity compared to bare steel frames.

Buckling restrained braces (BRBs) have been widely adopted as a dependable lateral load mechanism since the early 1990s. BRBs are particularly popular in highly seismic regions due to their superior performance in resisting earthquake loads compared to regular braced frames. The impact of BRBs on the performance of steel frames subjected to lateral seismic forces suggests that BRBs might also be beneficial to steel frames that are subjected to progressive collapse loads. A study on the impact of BRBs on the catenary action demands in steel framed structures was carried out. Results showed that buckling restrained braced frames can increase the resulting axial forces in steel beams.

The contribution of the concrete slab to catenary action development was also investigated. The results indicate that accounting for the concrete slab significantly increases the load-carrying capacity of the steel frame at earlier stages of deflection. A change in the concrete slab thickness affects the contribution of the slab in the axial force development in the beams. The results of this dissertation will help designers and code developers around the world understand the impact of AAC infill, BRBs and concrete slabs on the catenary action demands in steel structures.

Acknowledgments

First of all, I would like to thank my father, Ahmed, and my sister, Dalia, for their emotional and financial support. Without their encouragement and reassurance, I wouldn't have been able to do it.

I would also like to thank Dr. Marshall for his knowledge, time and guidance. His valuable input was crucial to my success. He inspired me to become more optimistic and enthusiastic. I am also particularly grateful to Dr. Hughes for her advice and continuous support. Dr. Barnes provided me with useful information in the course I have taken with him. I appreciate his time and feedback on this project.

Finally, I would like to acknowledge my friends here in Auburn and my fellow graduate students. Their support and encouragement throughout my time in Auburn made me eternally grateful.

Table of Contents

List of Tables

List of Figures

Chapter 1: Introduction

1.1 Motivation

By definition, progressive collapse or disproportionate collapse results in damage that is disproportionate to the original damaged element. The catastrophic losses in property and lives draw a lot of attention to the possible ways of mitigating or addressing progressive collapse. The U.S. General Services Administration (GSA) and National Institute of Standards and Technology (NIST), among others, developed reports and documents addressing the issue in order to reduce the likelihood of progressive collapse.

Technically, any structure in the world can suffer from progressive collapse. The loss of a column in a building, bridge or even a water tank can have disastrous effects on the structure. One of the main problems of addressing progressive collapse is that there are many factors and variables that can impact the outcome. Connections, existence of a slab, and overall structural integrity are just a few examples of those factors.

Based on the literature review, it is evident that the significance of this research arises from the fact that there is insufficient data on the impact of different structural elements like BRBs, AAC infill or concrete slabs on the catenary action demands in steel frames. This research is aimed to help understand the significance of accounting for those elements in the progressive collapse design of steel structures.

1.2 Research Objectives

The objectives of this research project are as follows:

- Evaluate the development of catenary action in steel beams and the corresponding structural behavior in steel structures.
- Illustrate the impact of AAC infill on the catenary action demands in steel frames.
- Understand the effect of buckling restrained braces on the load carrying capacity of the steel frame and catenary action development in the beams.
- Evaluate the contribution of the concrete slab in the overall load carrying capacity of the structure and how it affects the axial forces generated in beams.

1.3 Scope and Approach

The focus of this research is the structural members of the steel structures. Other types of buildings, like concrete structures, were not investigated. The scope of the different models involved the impact of AAC infill, BRBs and concrete slabs on the catenary action development in steel structures and the overall load carrying capacity.

A direct design method (Alternate Path Method) was adopted to investigate axial forces generated in the frame with different placement scenarios, building heights, and loading types. OpenSees (Open System for Earthquake Engineering Simulation) was used to develop and analyze the different models.

1.4 Dissertation Organization

This dissertation is organized into seven chapters. Chapter 1 gives an introduction, presents the research objectives, and clarifies the scope of the research. Chapter 2 provides a literature review on progressive collapse and the different factors that affect the catenary action development. The current design guidelines are also discussed. Chapter 3 gives details of the finite element modeling of the steel frames. The material models used for AAC infill, BRBs and concrete slabs are demonstrated. Chapter 4 discusses the impact of AAC infill on catenary action development. Different building heights and AAC infill placement scenarios are illustrated. Chapter 5 provides the results of the steel frames with buckling restrained braces. The load carrying capacity of the steel frame with and without the BRBs are shown. Chapters 6 studies the contribution of the concrete slab in the catenary action development and overall load carrying capacity. Finally, Chapter 7 provides a summary of the research, presents conclusions based on the analyses, and also includes final recommendations regarding catenary action development in steel frames.

Chapter 2: Background and Literature Review

2.1 Overview

In this chapter, background information focusing on progressive collapse and catenary action in steel buildings is outlined. A literature review of relevant research and current design guidelines discussing progressive collapse is presented.

2.2 Current Design Guidelines

2.2.1 Overview

This section highlights the current design guidelines that address progressive collapse of structures. Since the focus of this research is steel framed structures, other guidelines and design codes regarding other types of structures, like reinforced concrete structures or load bearing structures, are not covered.

2.2.2 US General Services Administration (GSA 2003):

The General Services Administration published *Progressive Collapse Analysis and Design Guidelines* in order to help save lives and protect federal buildings. The guideline helps to achieve that goal by mitigating the risk of progressive collapse in new federal buildings and assessing and upgrading existing federal buildings.

Section three in the guideline defines which buildings can be exempted from consideration for progressive collapse. The criterion used are the probability of risk and the details of human occupancy. Section five in the guideline deals only with steel frame analysis and design. The buildings are classified into two categories, new construction

and existing construction. The new construction follows the flowchart shown in Figure 2-1.

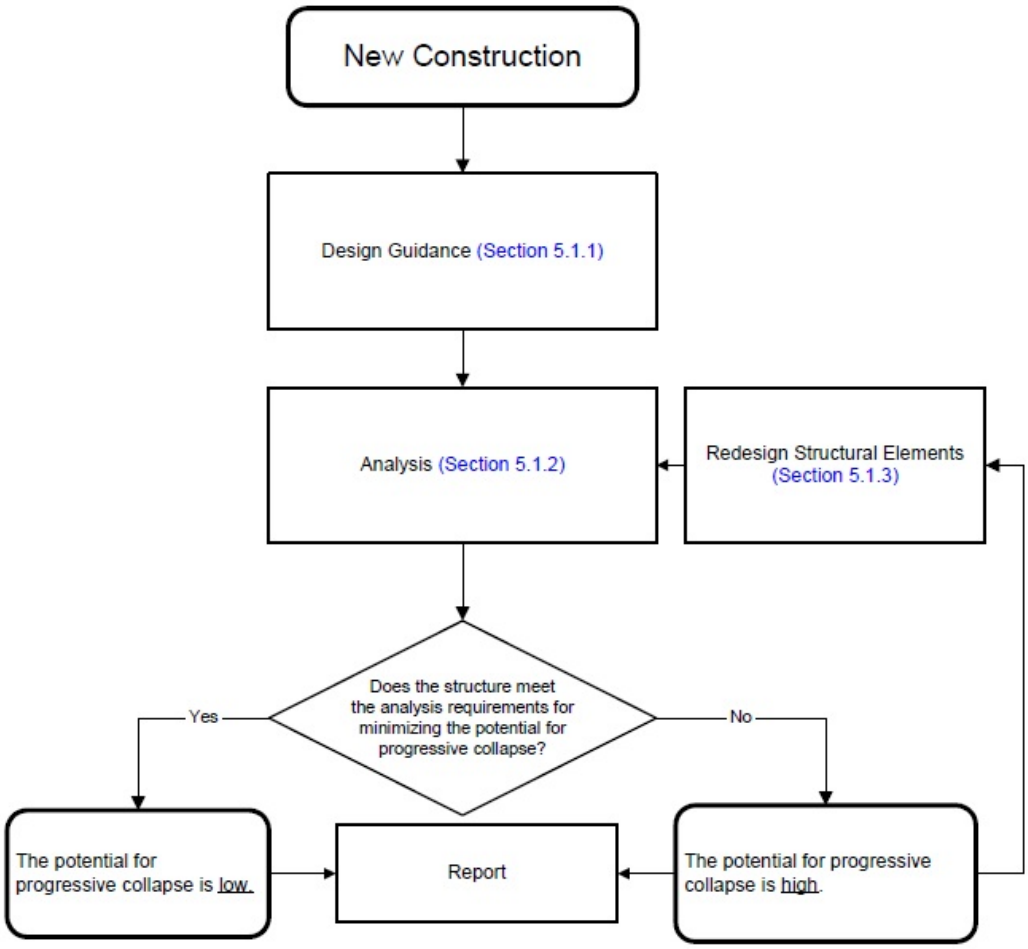

Figure 2-1: New Construction Flow Chart (GSA 2003)

The same analysis approaches and acceptance criteria that are applied to new construction should be applied to existing construction in order to determine whether it meets the requirements to mitigate the potential for progressive collapse or not.

The design guide includes local considerations like discrete beam-to-beam continuity, connection resilience, connection redundancy and connection rotational capacity. The global consideration (global frame redundancy) is as well a part of the

design guide. The analysis step which follows the guideline involves analysis techniques, procedure, analysis considerations and loading criteria, analysis criteria, material properties and modeling guidance. Analysis considerations depend on the structural configuration (whether it is typical or atypical), and whether the structures are framed structures or shear wall structures. Also, there are external and interior considerations. The acceptance criteria (part of analysis criteria) for structural components is defined as:

$$\mathrm{DCR} = \frac{Q_{UD}}{Q_{CE}} \qquad [2.1]$$

where:

DCR is the Demand-Capacity Ratio

Q_{UD} is the demand in the component or the joint

Q_{CE} is expected ultimate capacity of the component or joint (un-factored)

The limits of the acceptance criteria are defined in the guidelines. If the acceptance criteria limits are not met, redesign of the structural elements remains as an option for the designer.

However, the document has not been updated for a while, similar to the other design guidelines. It is likely that the GSA (2003) will be ultimately replaced by UFC 4-023-03. (UFC 2010)

2.2.3 Unified Facilities Criteria (UFC)

The Department of Defense's Unified Facilities Criteria (UFC) published *Design of Buildings to Resist Progressive Collapse* (UFC 4-023-03) in order to provide guidelines for progressive collapse design within the United States (UFC 2010). The

document defines the progressive collapse phenomenon and points out that the goal is not to prevent local/initial damage but to minimize the risk of mass casualties. UFC 4-023-03 classifies design approaches as "indirect" and "direct" design approaches. The direct design approaches are the Alternate Path (AP) method and the Enhanced Local Resistance (ELR) method. There is one indirect design approach called the Tie Force (TF) method. The decision of which approach to be used is based on the occupancy category (OC) of the structure. The occupancy categories and design requirements are shown in Table 2-1 and Table 2-2.

Table 2-1: Occupancy Categories (UFC 2010)

Nature of Occupancy	Occupancy Category
• Buildings in Occupancy Category I in \1\ Table 2-2 of UFC 3-301-01. /1/ • Low Occupancy Buildings[A]	I
• Buildings in Occupancy Category II in \1\ Table 2-2 of UFC 3-301-01. /1/ • Inhabited buildings with less than 50 personnel, primary gathering buildings, billeting, and high occupancy family housing[A,B]	II
• Buildings in Occupancy Category III in \1\ Table 2-2 of UFC 3-301-01. /1/	III
• Buildings in Occupancy Category IV in \1\ Table 2-2 of UFC 3-301-01. /1/ • Buildings in Occupancy Category V in \1\ Table 2-2 of UFC 3-301-01. /1/	IV

Table 2-2: Occupancy Categories and Design Requirements (UFC 2010)

Occupancy Category	Design Requirement
I	No specific requirements
II	Option 1: Tie Forces for the entire structure and Enhanced Local Resistance for the corner and penultimate columns or walls at the first story. **OR** Option 2: Alternate Path for specified column and wall removal locations.
III	Alternate Path for specified column and wall removal locations; Enhanced Local Resistance for all perimeter first story columns or walls.
IV	Tie Forces; Alternate Path for specified column and wall removal locations; Enhanced Local Resistance for all perimeter first and second story columns or walls.

The tie forces approach is based on enhancing the ductility and continuity of the existing structural elements. There are two types of ties, horizontal and vertical ties. The horizontal tie forces are divided into longitudinal, transverse and peripheral tie forces (Figure 2-2).

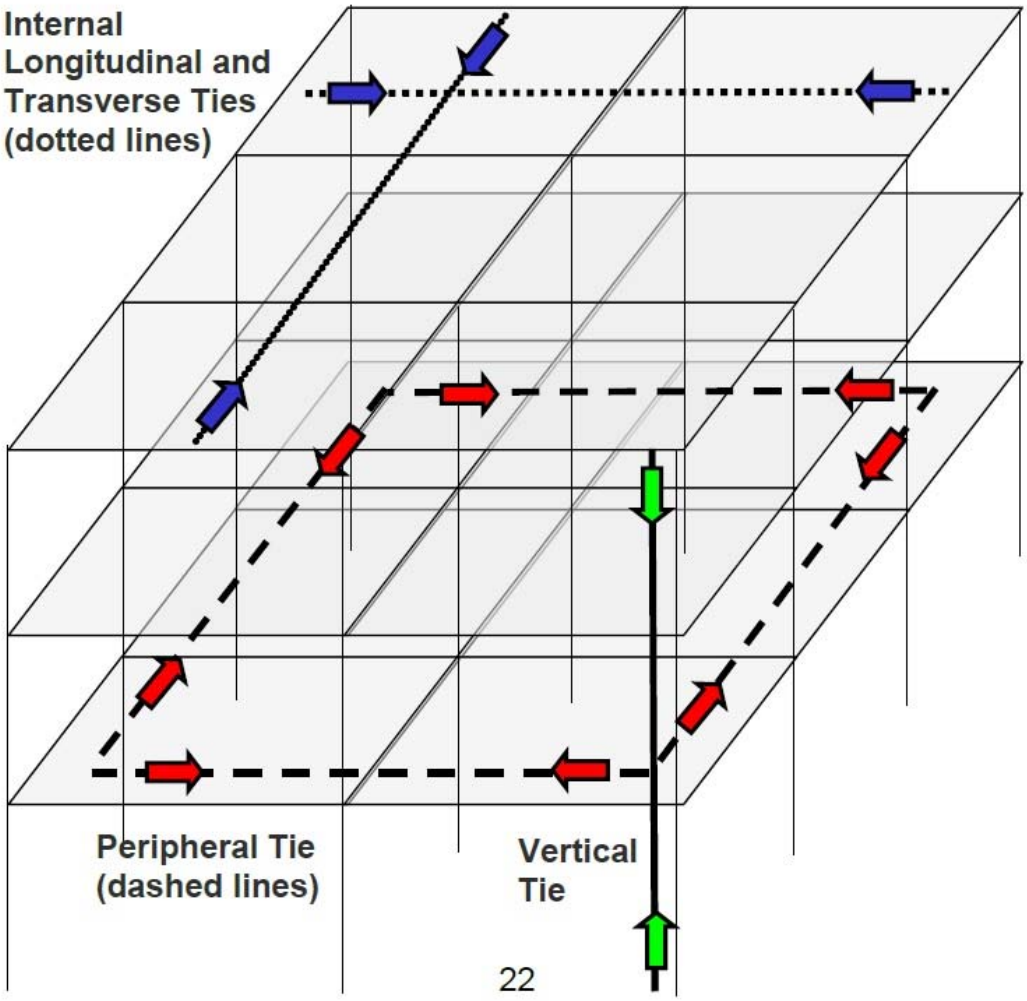

Figure 2-2: Tie Forces in a Frame Structure (UFC 2010)

Uniform floor loads are used to determine the required tie strengths as calculated by Equation 2.2.

$$W_F = 1.2D + 0.5L \quad [2.2]$$

Where W_F = Floor Load (lb/ft^2 or kN/m^2)
D = Dead Load (lb/ft^2 or kN/m^2)
L = Live Load (lb/ft^2 or kN/m^2)

The document also considers non-uniform loading like concentrated loads, load variations and cladding and façade loads. The floor system is supposed to provide the required longitudinal and transverse tie resistance along with other structural members like beams and girders if those members and their connections satisfy the limit. The UFC states that unless the structural members and the connections are capable of carrying the horizontal tie force while undergoing rotations of 0.2 rad, the horizontal tie forces are to be carried by the floor and roof system. The columns and load bearing walls are expected to carry the required vertical tie strength.

The Alternate Path Method (AP) is used in two cases. Firstly, when a vertical structural element cannot provide the required tie strength, the AP is used to check if the structure can bridge over the removed element. The second case is when a specific vertical load bearing element is removed (Figure 2-3). There are three analysis procedures that can be adopted, Linear Static (LSP), Nonlinear Static (NSP) and Nonlinear Dynamic (NDP).

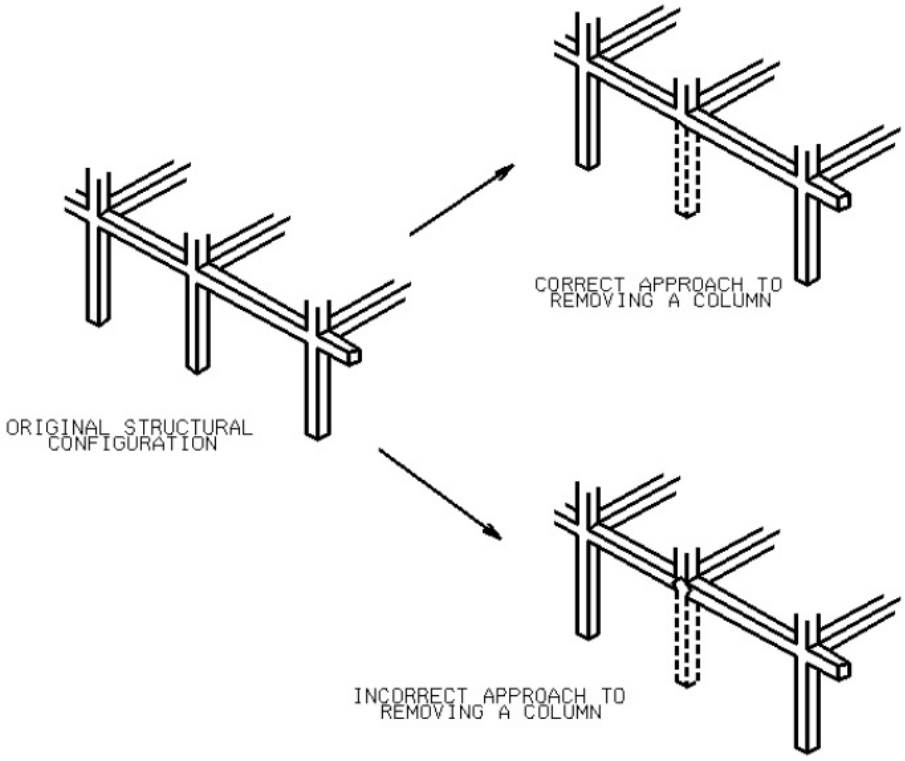

Figure 2-3: Removal of Column from Alternate Path Method (UFC 2010)

UFC 4-023-03 classifies all the structural elements that participate in resisting collapse as primary, while all the other elements as secondary. In order to consider the building structurally adequate, all of the primary, secondary elements, components or connections should be within the acceptance criteria defined in the UFC.

The Enhanced Local Resistance Method is provided through specific flexural and shear resistance of perimeter building columns at certain locations based on which occupancy category is chosen. The same classification applies to the calculation of both flexural and shear resistance.

2.2.4 Minimum Design Loads for Buildings and Other Structures (ASCE 7-10)

Minimum Design Loads for Buildings and other Structures (ASCE 2010) provides some guidance regarding general structural integrity and progressive collapse mitigation. Section 1.4 is the section in the ASCE standard that discusses the general structural integrity of the structure. The standard sets guidelines to ensure a minimum level of continuity through the main structural components. For example, load combinations for extraordinary events are required in order to ensure a continuous load path. Additionally, a load path connection between separation joints in the structure must be enforced and the effect of static lateral forces applied to the structure should be analyzed. Finally, providing connection to supports and anchorage of structural walls are necessary to ensure general structural integrity.

The commentary of section 1.4 defines the progressive collapse phenomenon and describes why general structural integrity is important to mitigate the phenomenon. However, the standard points out that it does not intend to provide specific design criteria to minimize the risk of progressive collapse. Also, the standard clarifies the distinction between general collapse and limited local collapse. Additionally, it lists a couple of past incidents and shows how different factors like lack of continuity, minimal factor of safety and missing structural integrity contributed to the damage propagation. The standard lists a number of ways to fulfill the integrity requirements like good plan layout, load bearing interior partitions, catenary action of floor slab, redundant structural systems and ductile detailing.

Section 2.5 provides load combinations for extreme load scenarios to check the capacity of the structure when subjected to an extreme load and to check the residual capacity of the structure after being subjected to that load.

2.2.5 International Building Code (IBC 2012)

There is a specific section (Section 1614 – Structural Integrity), in the International Building Code (IBC 2012) that outlines design guidelines that apply to special structures (high-rise buildings or Occupancy category III or IV). This section defines requirements for bearing wall structures, concrete frame structures and structural steel structures. In this dissertation, only steel structures are considered.

The code requires that a column splice shall be designed to resist the transferred design dead and live load between the column above and the column below. For beams, the end connections of beams and girders should have a minimum axial tensile strength equal to the required vertical shear strength for allowable stress design (ASD) or two thirds of the required shear strength for load and resistance factor design (LRFD) but not less than 44 kNs. The code states that the shear force and the axial force do not have to act simultaneously.

Proposed revisions to these requirements based upon UFC specifications were presented to the Structural Code Development Committee, but were rejected in 2008 (CPNI 2011).

2.2.6 Eurocode 1: Actions on Structures (BSi 2006)

Accidental Actions (Part 1-7) is the guideline released by the Eurocode to deal with structures subjected to accidental actions like progressive collapse. The purpose of

this section is to provide guidelines and strategies to mitigate failure of those structures. The Eurocode has two strategies for design to accidental actions. The first strategy is based on specific accidental actions (like explosions or impact) and the second strategy is based on limiting the extent of localized failure from an unspecified cause (Figure 2-4).

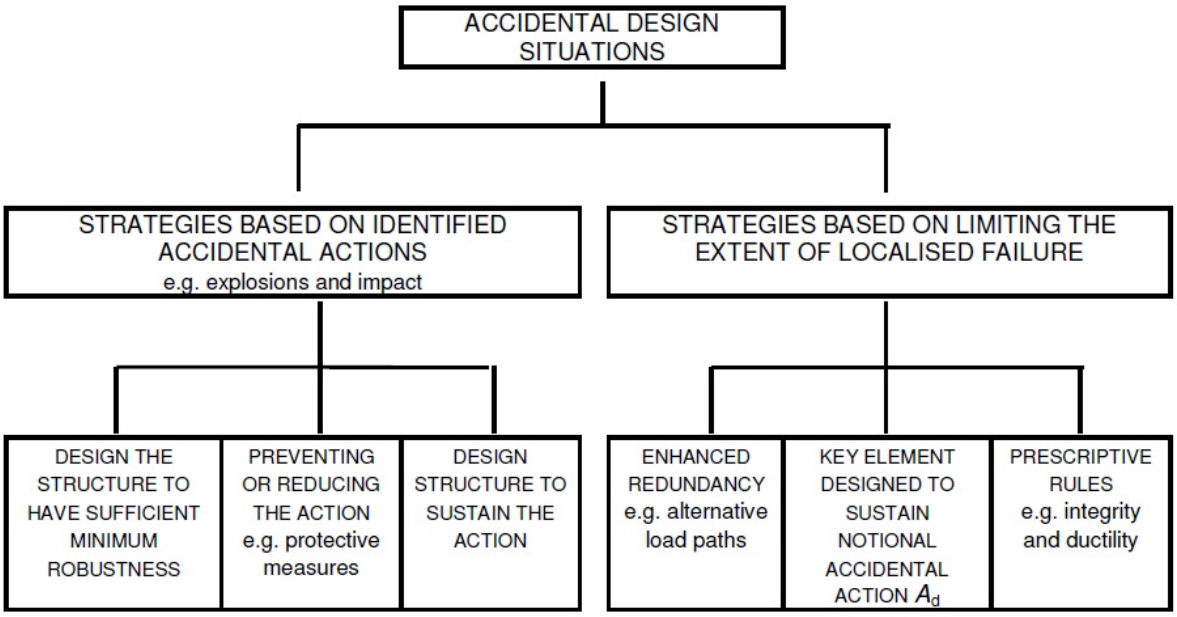

Figure 2-4: Strategies for Accidental Design Situations (BSi 2006)

The requirements of the two strategies are based on the classification of the buildings/occupancies. The Eurocode defines three consequence classes:

- Low consequences of failure (CC1)
- Medium consequences of failure (CC2)
- High consequences of failure (CC3)

Some examples of those consequence classes are presented below:

- CC1 class: single occupancy houses and agricultural buildings.
- CC2 class: Five story single occupancy houses and hotels not exceeding fifteen stories.

- CC3 class: Stadia accommodating more than 5000 spectators and buildings containing hazardous substances.

The course of action to take based on identified accidental actions (e.g. explosions and impact) depends on many factors. Some example are public perception, level of risk, probability of occurrence and consequences of failure due to accidental action. A localized failure might be accepted as long as it doesn't affect the overall stability of the structure.

Many requirements should be met to mitigate the impact of accidental actions, for example:

- Preventing the accidental action itself or reducing its probability
- Protecting the structure from the actions (e.g. protective bollards or safety barriers)
- Designing the structure with sufficient robustness

There are various methods that are used to achieve sufficient robustness; a few examples are listed below:

- Designing key elements for additional load
- Designing structural members to have sufficient ductility
- Implementing sufficient redundancy in the structure
- Applying accidental actions simultaneously with the other loads
- The safety of the structure post the accidental action should be taken into account

Ties are required in certain cases in order to satisfy the strategy requirements based on the categorization of structures. There are two types of ties: horizontal and vertical.

Horizontal ties should be placed around the perimeter of each floor in order to tie the columns and the wall elements to the structure. Continuity of the ties should be ensured. The ties could be rolled steel sections, steel bar reinforcement in concrete slabs, or steel mesh reinforcement and profiled steel sheeting in composite steel/concrete floors. They could also consist of a combination of the above types. Ties should be able to resist design tensile load for accidental limit state.

The vertical structural element should be tied continuously throughout the whole height to act as a vertical tie of the structure. It also should be able to resist the maximum design accidental tensile force applied to the column.

2.2.7 Blast and Progressive Collapse (AISC)

The American Institute of Steel Construction (AISC) has published *Facts for Steel Buildings Number 2: Blast and Progressive Collapse* (Marchand & Alfawakhiri 2004). The document provides basic guidance and information for engineers, architects, developers and owners of commercial and industrial buildings that are subjected to extraordinary loads. The document does not provide detailed analysis or design recommendations. The document is divided into eight sections: general science of blast effects, threats and acceptable risk, resistance of steel structures to blast and extreme loads, mitigation of progressive collapse in steel structures, best practices to mitigate blast load effects, best practices to mitigate progressive collapse effects, a history on blast

and collapse events, and a discussion on current research and future needs (Marchand & Alfawakhiri 2004). Sections four and six are the sections that are concerned with steel structures. The fourth section focuses on mitigating progressive collapse in steel structures, the difference between direct and indirect design and explanation of the tying approach in guidelines like ASCE 7, UFC and GSA. Section six highlights the specific design guides (GSA and UFC) and their approaches of mitigating blast effects and progressive collapse. The document is mainly used to introduce the basic concepts of progressive collapse to the reader and to introduce the available design guides that deal with progressive collapse.

2.3 Literature Review

Catastrophic disproportionate failures of structures around the world have triggered research to develop a better understanding of progressive collapse. Connections, beam behavior and slab contribution were studied to find potential solutions for the lack of structural integrity. Catenary action was studied as a load carrying mechanism that can be a potential solution to arrest progressive collapse of steel structures. Experimental and analytical investigations were carried out in order to understand this mode of failure. This section presents a review of the research that is relevant to the dissertation topic of catenary action in steel building structures.

The literature review in this chapter is divided into three categories. The first category covers the research on progressive collapse of steel structures, connections and concrete slabs. The second category covers the relationship between infill walls and seismic behavior that reflects the potential role that AAC infill can play in improving the

load carrying capacity of the structure. The third category covers the relationship between braced frames and seismic behavior and catenary action and how the adjacent lateral load resisting systems can impact the development of axial forces in beams and the overall structure.

2.3.1 Progressive Collapse of Steel Structures

Byfield & Paramasivam (2007) addressed the catenary action approach and the tie force method in steel framed structures. The tie force method attempts to enhance the general integrity of the building through internal ties. The authors investigated the sufficiency of the rotation capacity of beam-column connections. They calculated the factor of safety for three different scenarios to evaluate the impact of connection ductility on catenary action. Results yielded factors of safety less than one. The authors suggested that insufficient ductility is the main reason behind the limited factors of safety. Therefore, they concluded that catenary action alone won't be able to prevent progressive collapse. They pointed out that increasing the connection strength and robustness might solve the problem. However, such improved connections might increase the risk of a process known as "drag down", where the additional tying could widen the range of progressive collapse.

Khandelwal et al. (2009) considered two popular types of braced frames; special concentrically braced frames (SCBF) and eccentrically braced frames (EBF). The authors used LS-DYNA software to analyze the frames and generate results. They applied the Alternative Path Method (AP) on a 10-story prototype building. Macro-models were used to model the structural response to accurately simulate the behavior. Results showed that an EBF is less vulnerable to progressive collapse than a SCBF. Also, placement of the seismic system at the building perimeter improved the performance of both systems.

Finally, the authors suggested that the reason EBFs performed better than SCBFs is the improved system layout rather than ductile seismic detailing.

Kim and An (2009) studied the effect of catenary action of steel framed structures. The analysis was conducted according to the AP method outlined in GSA (2003). The authors used Opensees to analyze braced and non-braced frames. Nonlinear static and dynamic analyses of three and six story frames were considered. The results showed that catenary action increased with increase of lateral restraints (braced frames). However, the variation of the number of the stories had no effect on catenary action. Finally, they found that the maximum deflection decreased when catenary action was taken into consideration.

Tan & Astaneh-Asl (2003) conducted experimental work on the impact of using steel cables to resist progressive collapse of floors. They performed tests on new and existing buildings. Cables were placed inside the floor slab for new buildings and were placed on the web of the façade beams for existing buildings. They noticed that some technical issues, such as shear tab strength and shear connection rotation capacity might limit the effectiveness of the cables. However, the cables provided additional strength and stiffness against progressive collapse.

Khandelwal et al. (2008) investigated the progressive collapse resistance of seismically designed steel moment frames. They concluded that moment frames designed for high-seismic behavior have better resistance to progressive collapse than the ones designed for moderate seismic behavior. They attributed this improvement to the general layout and general system rather than improved ductile detailing. Khandelwal and Tawil (2007) conducted a computational simulation to investigate catenary action in moment resisting steel frames. The authors used a numerical model that employed a calibrated

micromechanical model for steel to investigate the catenary behavior of a number of steel subassemblies. Results indicated that the out-of-plane pulling action had limited impact on the subassemblage structural behavior. Moreover, it was observed that increasing beam depth and yield-to-ultimate strength ratio had a significant influence on the connection ductility and strength.

Izzuddin & Nethercot (2009) compared the use of the ductility-centred approach for progressive collapse assessment versus a design oriented approach. The ductility-centred approach is based on calculating the maximum load that can be sustained under sudden column loss without exceeding the ductility limit. The authors suggested that the ductility-centred approach will be more practical and applicable than the load factor approach. Difficulties in prescribing the dynamic increase factor (DIF), without taking into consideration the nonlinear static response, were pointed out. The authors stated that, in some cases, the DIF might be underestimated by about 30%. This might lead to unsafe design of structures. On the other hand, the ductility-centred approach allows easy and quick evaluation of the dynamic ductility demand of different structural forms.

Kwasniewski (2010) performed progressive collapse analysis of an existing 8-story steel framed structure. The author used the program LS-DYNA with explicit time integration to run nonlinear dynamic simulations of progressive collapse. Although the explicit method took advantage of parallel processing on multiprocessor computers, the analysis required large computational resources. The author verified the simulations using a hierarchical verification with four levels of complexity. Global analyses of three cases of column removal scenarios were investigated. The author concluded that detailed modeling can provide a realistic approximation of structural collapse.

An important area of progressive collapse is the behavior of steel connections during collapse. Sadek et al. (2009) conducted an experimental and analytical investigation of two steel beam-column assemblies under monotonic loading conditions. Kim et al. (2010) studied the collapse resistance of steel moment connections originally designed to resist gravity loads. Kim & Kim (2009) investigated the progressive collapse potential for different steel frames using linear static and nonlinear dynamic analysis. They observed that steel frames that were designed for lateral loads were less vulnerable to progressive collapse than the frames that were designed for gravity loads only. Semi-rigid and simple shear connection behavior under progressive collapse conditions has been also investigated. Examples of this research include: Gong (2010), Pirmoz et al. (2011), and Xu et al. (2011). Other researchers like Main et al. (2009) and Alashker et al. (2011) used three dimensional nonlinear dynamic micro models to analyze structural systems.

Kim et al. (2009) investigated the impact of various factors on the progressive collapse resistance of steel moment frames using two-dimensional nonlinear static finite element analyses. The factors examined were: number of bays in the lateral load resisting system, number of stories, span length of the beams, and intensity of design earthquake load. The results indicated that the progressive collapse resistance of the systems seemed to increase with the number of bays and the number of stories. Conversely, the collapse resistance seemed to decrease with increasing span length. Furthermore, the collapse-resistance of the studied structures was higher for those that were designed for higher earthquake loads. The study concluded that a nonlinear static pushdown analysis tends to

overestimate the collapse resistance of structures as compared to a nonlinear dynamic analysis.

Hayes Jr, et al. (2005) tried to answer the question of whether seismic design requirements can contribute to an improved resistance of the structures against blast loads and progressive collapse. The study was an analysis of the Alfred P. Murrah Federal building after adding three strengthening schemes as if the building was located in a seismically active region. The analysis showed that the pier-spandrel system, special concrete moment frame, and the re-detailed original system actually helped reduce the progressive collapse damage.

Kim et al. (2011) proposed a combined system of rotational friction dampers connected to high strength tendons to enhance the seismic and progressive collapse resisting capacity of structures. They performed static and dynamic analyses that showed significant improvement in the progressive collapse capacity of the structure. Khandelwal and El-Tawil (2011) investigated a variety of push-down methods for the evaluation of progressive collapse resistance for structures designed for moderate and high seismic activity. The investigation proposed implementing ‘fuses’ to prevent the propagation of collapse in the event that the structure in question loses its capacity to bridge over a damaged element.

2.3.2 Autoclaved Aerated Concrete Infill

In regard to infill walls and their impact on the seismic behavior of structures, Ravichandran & Klingner (2012) studied the behavior of steel moment frames with

autoclaved aerated concrete (AAC) infill (Figure 2-5). Bare steel frames (without AAC infill) and frames with AAC infill were subjected to lateral loads. Experimental testing and analytical models were used to determine the stiffness, strength, and hysteretic behavior of the frames. They concluded that the stiffness determined from experiments was in good agreement with the stiffness predicted by the Masonry Standards Joint Committee, MSJC (2008).

Figure 2-5: Autoclaved Aerated Concrete Infill (AAC)

Liu & Li (2004) conducted tests on four steel frames with and without AAC infill. Based on their experimental work and theoretical analysis, they concluded that the stiffness of the AAC infilled steel frames was 50% higher than the bare steel frame. Ravichandran (2009) concluded that AAC infill can be designed to improve the seismic performance of steel frames without changing the seismic design factors of the bare steel frame. Humar et al. (2001) investigated the performance of buildings during the 2001 Bhuj, India earthquake. The authors observed that reinforced concrete framed structures with masonry infill performed better than frames without masonry infill, provided that the infill was uniformly distributed throughout the height of the building.

Mehrabi et al. (1996) remarked that masonry infill had a beneficial influence on the performance of reinforced concrete frames that are subjected to lateral loads. Escalera (2011) studied the effectiveness of thin infill steel plates in mitigating progressive collapse

in steel buildings. The study showed that the plates improved the progressive collapse resistance of the steel frames. Tsai & Huang (2009) investigated the effect of brick-infill partitions on the progressive collapse of reinforced concrete buildings. They concluded that the brick infill had a positive impact on decreasing the demand-to-capacity ratio of the beam end moment. However, they pointed out that it can increase the axial force in the beam bridging over the removed column.

Literature has focused on the impact of AAC infill on seismic behavior in steel frames. Also, there has been research addressing progressive collapse and catenary action in steel frames. However, there is no previous research that addresses the impact of AAC infill on catenary forces in steel frames.

2.3.3 Buckling Restrained Braces

In regard to braced frames and their impact on seismic behavior of structures, Sabelli (2001) analyzed a series of three and six story braced framed buildings that were designed for a site in metropolitan Los Angeles. The buckling restrained braces (BRBs) (Figure 2-6) were designed and modeled as an unbonded yielding steel core inside a mortar filled steel tube. Inputs to the models were selected to represent a range of earthquake events that might occur at the building location over a long period of time. The results indicated that the buckling restrained braces performed better than special concentric braces. BRBs provided significant benefits compared to the conventional braced frames and moment-resisting frames. Kim & Choi (2004) investigated the energy dissipation capacity and earthquake response of steel structures with buckling restrained braces. They also presented a simple design procedure to meet a given target displacement. The authors

analyzed five and ten story steel frames to study the seismic response of structures with BRBs. They concluded that as the stiffness of the BRB increases, the equivalent damping ratios of BRB-braced SDOF structures generally increase. Another finding was that the use of low strength steel for BRB reduces structural damage. The reason is that the low strength steel undergoes large plastic deformation and dissipates more energy that high strength steel.

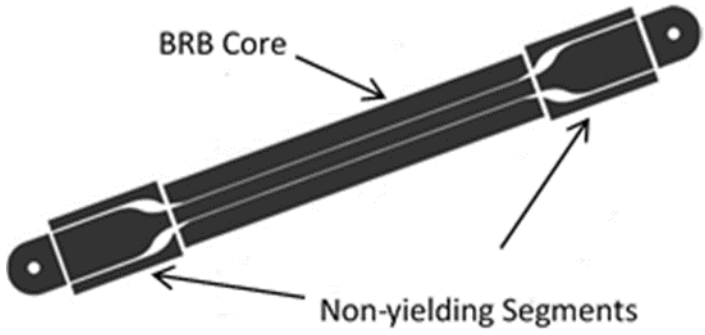

Figure 2-6: Buckling Restrained Brace (BRB)

Mahin et al. (2004) performed large-scale tests on buckling restrained braced frame subassemblies to assess their seismic performance. They investigated the behavior of a one story, beam-column frame with unbonded braces with three different buckling restrained brace designs. The authors concluded that the three buckling-restrained braced frame subassemblies performed well as seismic lateral systems. The hysteretic and elongation behavior of the braces appeared not to be influenced by the combined axial and flexural loading of the subassemblies. Sabelli et al. (2003) investigated the seismic demands on steel braced frame buildings with buckling-restrained braces. The authors analyzed three and six story concentrically braced frames utilizing buckling-restrained braces. The results showed that the buckling-restrained braces can potentially solve many problems associated

with special concentric braced frames. The authors also found that the response appears to be sensitive to structural proportioning, which suggests that further improvements in response may be obtained by better estimation of a structure's dynamic properties.

Mashhadiali and Kheyroddin (2013) assessed the progressive collapse-resisting capacity of a new hexagrid structural system for tall buildings. The hexagrid structure is an innovative tube-type system. The authors studied 28-story and 48-story frames using nonlinear static and dynamic analysis methods. The results showed that the hexagrid has enough potential for force redistribution to resist progressive collapse using its special configuration. The results also showed that the structural system's performance in mitigating progressive collapse improved when buckling was restrained. Kim et al. (2011) examined a combined system of rotational friction dampers connected to high strength tendons to enhance both seismic and progressive collapse resisting capacity of existing structures. The authors designed the friction dampers using the capacity spectrum method to satisfy given performance objectives against seismic load. The nonlinear static and dynamic analysis results showed that the non-seismic-designed model collapsed when a column was suddenly removed. On the other hand, the model with the frictional dampers remained stable after the column was suddenly removed.

Chen et al. (2012) investigated the contribution of horizontal bracing to the resistance of a steel moment frame against progressive collapse. The authors used nonlinear dynamic analyses of two three-dimensional steel frames with and without horizontal braces to study the effect of the horizontal bracings. They concluded that the displacements and rotational angles were much smaller for the braced model compared to the bare steel frame model due to the horizontal tie provided by the horizontal bracing. Another finding was

that horizontal bracing can actually enhance the resistance of the steel moment frame. Tsai (2012) studied a performance-based design approach for retrofitting regular building frames with steel braces. The approach was developed based on a pseudo-static response analysis of an idealized elastic-plastic, single degree of freedom system. The author verified the accuracy of the approach with incremental dynamic analysis. The results indicated that the column-loss response of the braced frames is reasonably conservative and approximated to the performance target. Hence, the approach is actually feasible for practical applications.

Mazzolani et al. (2009) investigated the impact of steel dissipative bracing systems on the seismic behavior of reinforced concrete structures. The authors carried out experimental tests on two-story, one-bay reinforced concrete structures braced with eccentric and buckling restrained braces. The experiments showed that in the case of eccentric braces, large over-strength of short links with respect to the first yielding shear and consequent danger of connection failure was noticed. For the BRBs, the braces improved the lateral stiffness, strength and displacement capacity of the structure.

Past research projects have focused on the impact of buckling restrained braces on seismic behavior in steel frames. Furthermore, there has been research addressing progressive collapse and catenary action in steel frames. However, there is no research addressing the impact of BRBs on catenary forces in steel frames.

In addition to the previous research, there have been many other investigations into various aspects of progressive collapse. Since these investigations relate somewhat more remotely to the subject of this dissertation, they will be discussed in brief.

In order to better understand the behavior of actual structures, Song et al. (2010) conducted experimental and analytical investigations of two steel structures undergoing collapse. Vlassis et al. (2009) studied the impact of falling floors on the progressive collapse of multi-story structures. Kim et al. (2011) studied the sensitivity of different design parameters of steel buildings. The effect on structural fires on the progressive collapse resistance of structures was explored by Quiel and Marjanishvili (2012). Finally, Gerasimidis and Baniotopoulos (2011) examined the impact of wind load on the dynamic disproportionate collapse analysis of steel frames.

2.4 Summary

In this chapter, current design guidelines addressing progressive collapse, structural integrity and catenary action were presented. A literature review of the previous research regarding catenary action development in steel structures, the contribution of AAC infill and BRBs on the seismic performance of steel buildings, and concrete slab participation in progressive collapse resistance were investigated. The next chapter will cover the models and the platform that was used in the current project to design, develop and analyze steel frames in order to study catenary action development in steel framed structures.

Chapter 3: FE Modeling

3.1 Introduction

Finite element (FE) models in this dissertation were developed using the *Open System for Earthquake Engineering Simulation* (OpenSees). OpenSees is an open source finite element software package, developed by the Pacific Earthquake Engineering Research (PEER) Center of the University of California at Berkeley (McKenna & Fenves 2000). OpenSees was a natural choice because of its modeling capabilities. Tools like discretization of a section into fibers, corotational transformations and zero length elements are essential for analyzing the models developed in this study. This section will cover the different aspects of the finite element modeling. The material models, geometric transformations and boundary conditions will be discussed and explained.

3.2 Material Models

OpenSees offers a variety of material models which include materials that were contributed by individual authors. For this research five uniaxial materials will be discussed. Those models are elastic, elastic-perfectly plastic (EPP), elastic-no tension (ENT), bilinear hysteretic model (Steel02), and zero tensile strength concrete (Concrete01) materials.

The elastic material is defined by an elastic modulus of 29,000 ksi. The elastic-perfectly-plastic (EPP) steel material (Figure 3-1) is defined by an elastic modulus of 29,000 ksi and a yield stress of 50 ksi. The EPP material was used to define the steel frames.

The ENT material was used to define the AAC infill. The elastic-no tension material is defined by an elastic modulus of 296 ksi. The modulus of elasticity of the ENT material is based on the compressive strength of AAC.

The Steel02 material (Figure 3-2) is a Giuffre-Menegotto-Pinto model with isotropic strain hardening defined by an elastic modulus of 29,000 ksi, a yield stress of 36 ksi and strain hardening ratio of 3%. The Steel02 material was used to define the yielding length of the BRB.

Finally, the Concrete 01 material (Figure 3-3) was used to define the concrete slab on top of the steel beam.

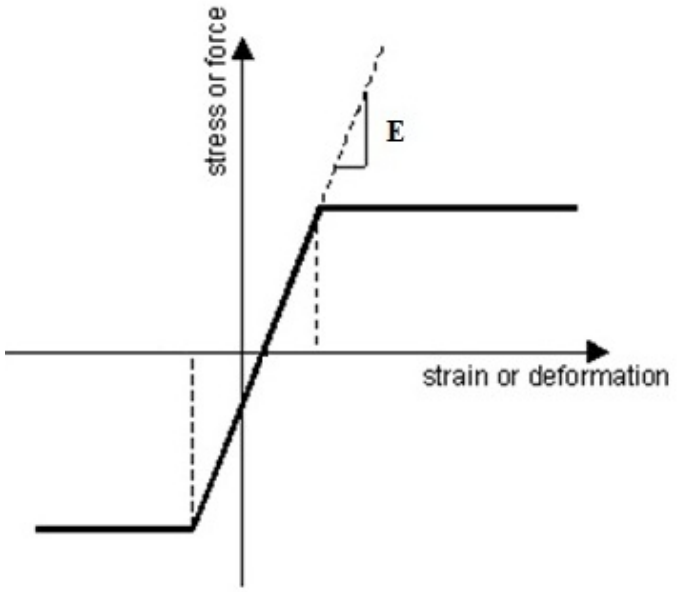

Figure 3-1: Elastic Perfectly-Plastic Material Model (McKenna & Fenves 2000)

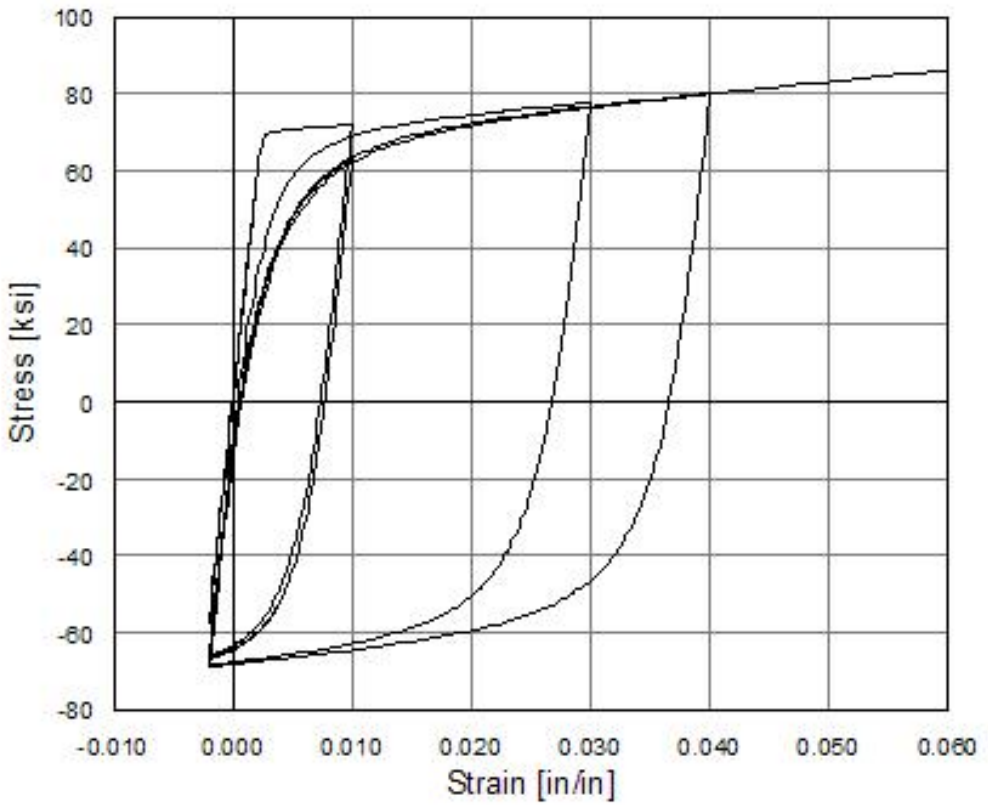

Figure 3-2: Steel02 Material Model (McKenna & Fenves 2000)

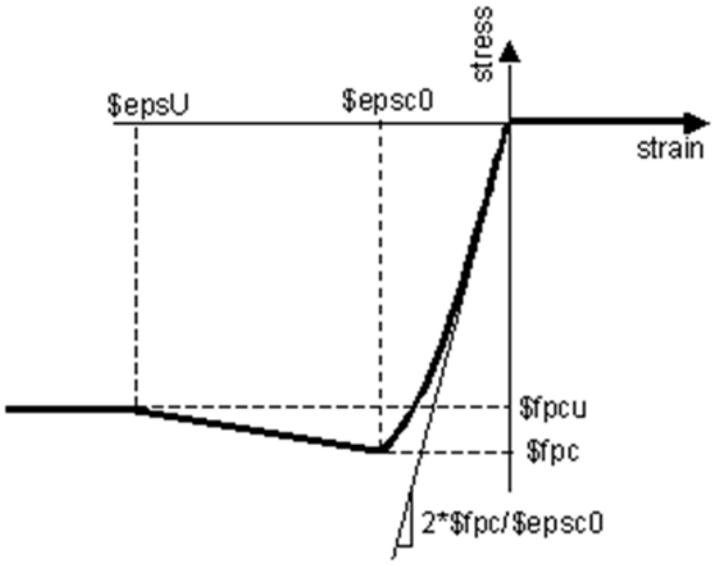

Figure 3-3: Concrete 01 Material Model (McKenna & Fenves 2000)

3.3 Element Types

Three types of elements were selected for the models in this study: elastic beam column elements, force-based nonlinear beam column elements and truss elements.

The elastic beam column element was utilized to define the side frame members and the non-yielding segments of the BRBs. Definition of this element type requires selecting a modulus of elasticity, cross-sectional area and moment of inertia (about the major axis of bending).

Force-based nonlinear beam column elements were used for the middle span beam and column elements. Unlike the elastic beam-column element, section and integration points need to be specified in the definition of the force-based nonlinear beam-column element. Neuenhofer & Filippou (1998) proposed the force-based nonlinear beam column element in order to utilize force interpolation functions for varying internal forces due to transverse displacements and to explicitly satisfy equilibrium in the deformed shape. The force-based nonlinear beam-column element considers the spread of plasticity along the length of the element and is capable of considering equilibrium in the deformed shape.

Finally, the AAC infill was modeled in OpenSees as equivalent struts (Figure 3-4). Those struts were defined as truss elements with the ENT material. The BRB core was also modeled in OpenSees as a truss element.

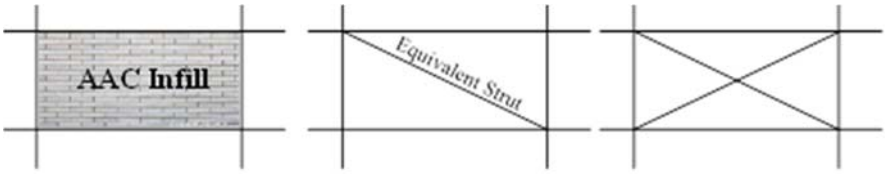

Figure 3-4: AAC Infill Equivalent Struts

The area of the AAC infill had to be calculated in order to define the truss properties. The Masonry Standards Joint Committee, (MSJC) (2008), developed draft design provisions for masonry-infilled frames. The draft MSJC design provisions for infill, idealized the infill as an equivalent strut. The provisions provided equations 3.1 through 3.6 to define the width and area of the equivalent strut.

$$E_{AAC} = 6500 * (f_{AAC})^{0.6} \quad [3.1]$$

$$\theta = tan^{-1}(h_{st.}/l_{bay}) \quad [3.2]$$

$$H_{infill} = h_{st.} - t_{beam} \quad [3.3]$$

$$\lambda_{strut} = \sqrt[4]{\frac{E_{AAC} * t_{infill} * sin\,2\theta}{4 * E_{col} * I_{col} * h_{infill}}} \quad [3.4]$$

$$\omega_{strut} = \frac{0.3}{\lambda_{strut} * cos\,\theta} \quad [3.5]$$

$$A_{strut} = t_{infill} * \omega_{strut} \quad [3.6]$$

where:

E_{AAC} is the modulus of elasticity of the AAC infill

f_{AAC} is compressive strength of AAC

h_{st} is the story height

l_{bay} is the bay length

θ is angle between the diagonal of the infill panel and the beam

t_{beam} is the depth of beam

h_{infill} is AAC infill height

t_{infill} is the thickness of infill

E_{col} and I_{col} are the modulus of elasticity and moment of inertia of confining columns.

λ_{strut} is the relative stiffness parameter for the equivalent strut

ω_{strut} is the width of the equivalent strut, perpendicular to the beam width

A_{strut} is the area of the equivalent strut.

Finally, the number of the elements along the length of the middle span beam models was taken as one hundred throughout the study.

3.4 Section Definitions

There are different sections available in OpenSees that can be utilized with the appropriate element types to represent specific behavior of a material or an element. Elastic and fiber sections were used for all the models in this study. Fiber sections have a general geometric configuration formed by discretizing the section into smaller regions (fibers). Those fibers are integrated to keep track of propagation of yielding through the cross section. This is necessary in order to capture the transition from flexural to catenary behavior. The quadrilateral patch command shown in Figure 3-5 was chosen as a discretization method. Thickness of the fibers was consistently taken as 0.005 inches and fillets were neglected for all the steel sections.

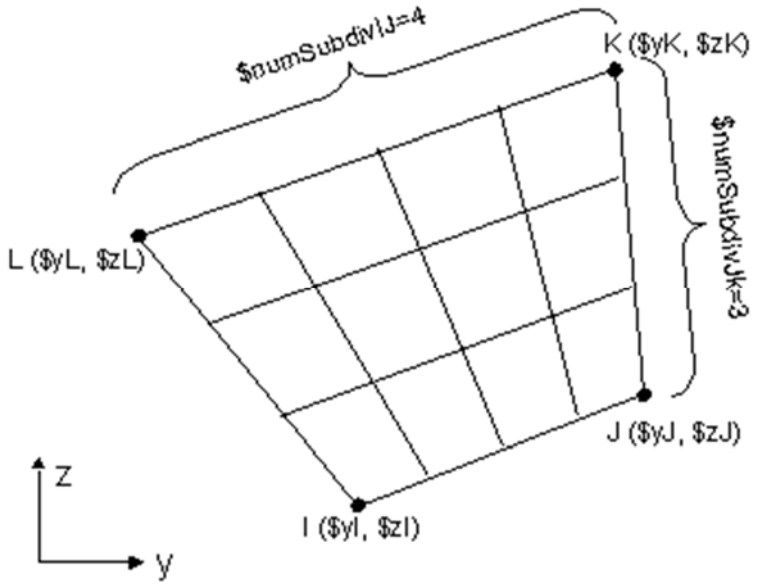

Figure 3-5: General Quadrilateral Patch (McKenna et al. 2000)

3.5 Geometric Transformations

The geometric transformation command in the OpenSees is used to transform beam element stiffness and forces from the base system to a global coordinate system. In this research, two geometric transformations were utilized: "linear transformation" and the "corotational transformation".

Linear transformation performs linear geometric transformation of beam stiffness and forces from the reference system to global coordinate system. Linear transformation assumes that the rotations and displacements are considered infinitesimal. Consequently, linear transformation is limited to small deformation applications, and thus it was assigned to the adjacent side frames.

Corotational transformation accounts for arbitrarily large rotations and displacements by attaching a coordinate system that will rotate and displace along with the

element. Rigid body motion is then separated from element deformations. In this manner, the transformation can handle arbitrarily large rigid and deformable motions. Consequently, it is possible to consider problems that include large rotations and displacements. However, this approach does not account for large strains along an element. According to De Souza (2000), this problem may be solved by dividing the element into smaller elements. Hence, corotational transformation was used to account for geometric nonlinearity for the AAC and the middle span steel beams (the beams above the removed column) and columns.

3.6 Loads and Analysis

In OpenSees, applying the loads requires two steps. First, a load pattern must be defined. Secondly, the analysis features need to be defined.

OpenSees offers three types of patterns: plain pattern, Uniform Excitation pattern and Multiple Support pattern. In this research, the plain pattern was used to define nodal loads for the concentrated and distributed loading.

The different models in this study used centerline analysis. Panel zone behavior wasn't considered. It was assumed that the behavior was fully ductile; therefore, connection failure and instability were ignored. The slab contribution in load carrying capacity was not taken into consideration when initially studying the effects of AAC infill and BRBs on catenary action development, but were considered in the final stage of the study.

3.7 Summary

In this chapter, the different material models, cross section types, and element types that were used in this research were presented. The geometric transformations that were used for the different models and sections were explained. In the next three chapters, the impact of AAC infill, BRB and concrete slabs on catenary action development in steel frames will be covered.

Chapter 4: Catenary Action in Steel Framed Buildings with Autoclaved Aerated Concrete Infill

4.1 Introduction

The local damage of structural elements due to extreme events that results in global collapse of a structure is called progressive collapse. Design to prevent progressive collapse of buildings can be addressed either through direct or indirect design methods. The U.S. General Services Administration, GSA, (2003) proposed the Alternate Path Method (APM), which is a direct design method. APM is commonly referred to as the "missing column scenario." After a column is removed, the double-span beam above it resists the resulting additional loads. This causes the beam to transition from flexural action to catenary action in order to sustain the additional loads. In this study, APM was adopted to investigate the progressive collapse and development of catenary action in infilled steel frames. Previous research has shown that infilled walls can have a significant impact on the performance of steel structures subjected to lateral loads. An autoclaved Aerated Concrete (AAC) infilled steel frame is a hybrid structural system in which a steel frame is filled with a panel of AAC material. In this chapter, analytical results from models including three building heights, four infill placement scenarios and three loading types are described. The impact of AAC infill on generated forces in the frames adjacent to the double-span beam suffering from column removal are highlighted. Comparisons are made between the developed catenary action in the steel frames with and without the AAC infill. Finally, the implications of the different building heights, infill placement scenarios and loading types are discussed.

4.2 AAC-Infilled Frame

An eight-story steel frame was designed using the commercial software package SAP2000 (Habibullah 2013). The frame shown in Figure 4-1 was designed for Seismic Design Category A (Atlanta, GA) with S_{DS} equal to 0.1447 and S_{D1} equal to 0.056. The design loads for the frame were determined based on the Minimum Design Loads for Buildings and Other Structures, ASCE (2010). W16x26 sections were chosen for all the beams in the frame to rule out the impact of beam variation on the development of catenary action along the height of the frame.

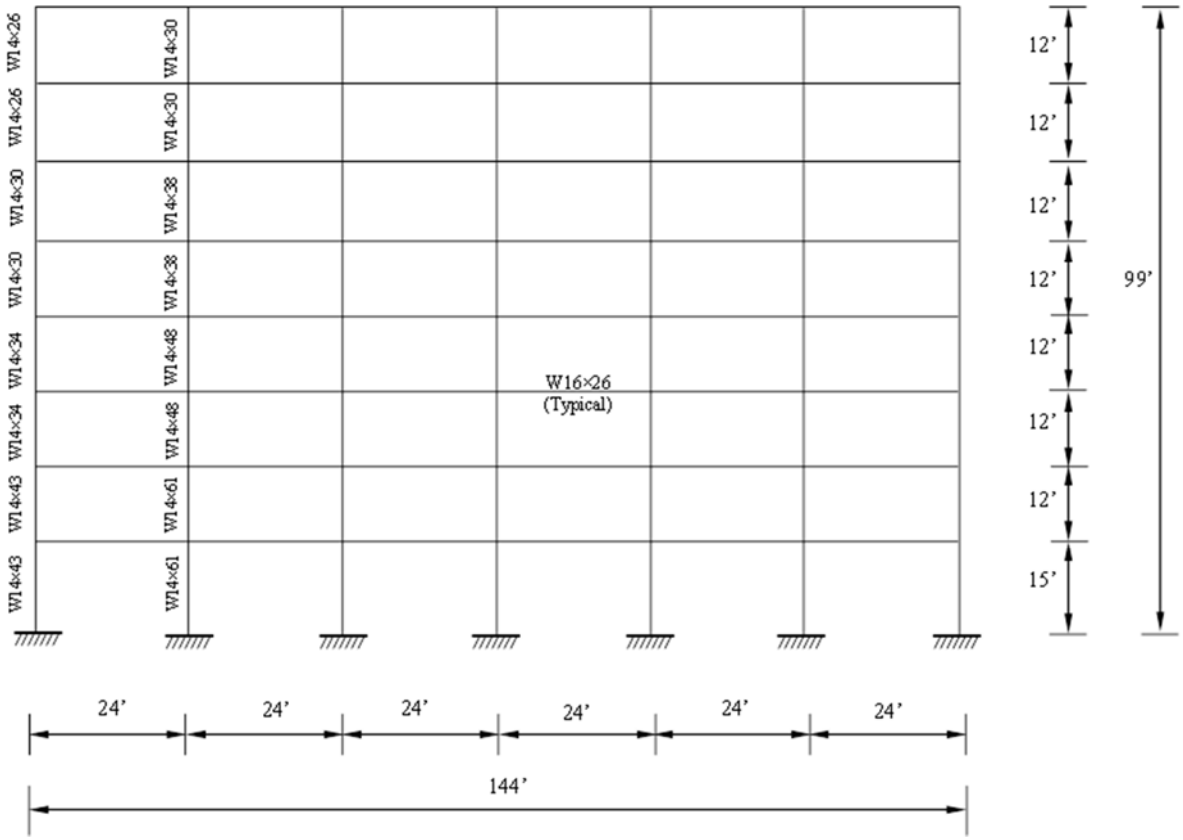

Figure 4-1: Eight-Story Steel Frame Elevation

In order to study the impact of AAC infill on the catenary action demands in steel frames, two steel frames were analyzed using OpenSees. One was a bare steel frame while the other was a steel frame with AAC infill. Figure 4-2 shows elevation of views the steel frame with and without AAC infill. In order to address progressive collapse, an interior bottom-story column was removed to simulate the missing column scenario. The two frames were subjected to a concentrated load at point "A" and were analyzed to study the difference between the cases with and without AAC infill. The AAC infill was placed everywhere in the frame except in the double span area suffering from a column loss. It was assumed that the extraordinary event that resulted in losing the column, would remove the surrounding AAC infill as well. In Figure 4-2, point "A" is right above the removed column (mid-point of the double span beam at the first floor). Point "A" was highlighted because some of the data discussed in the following sections was measured at this point.

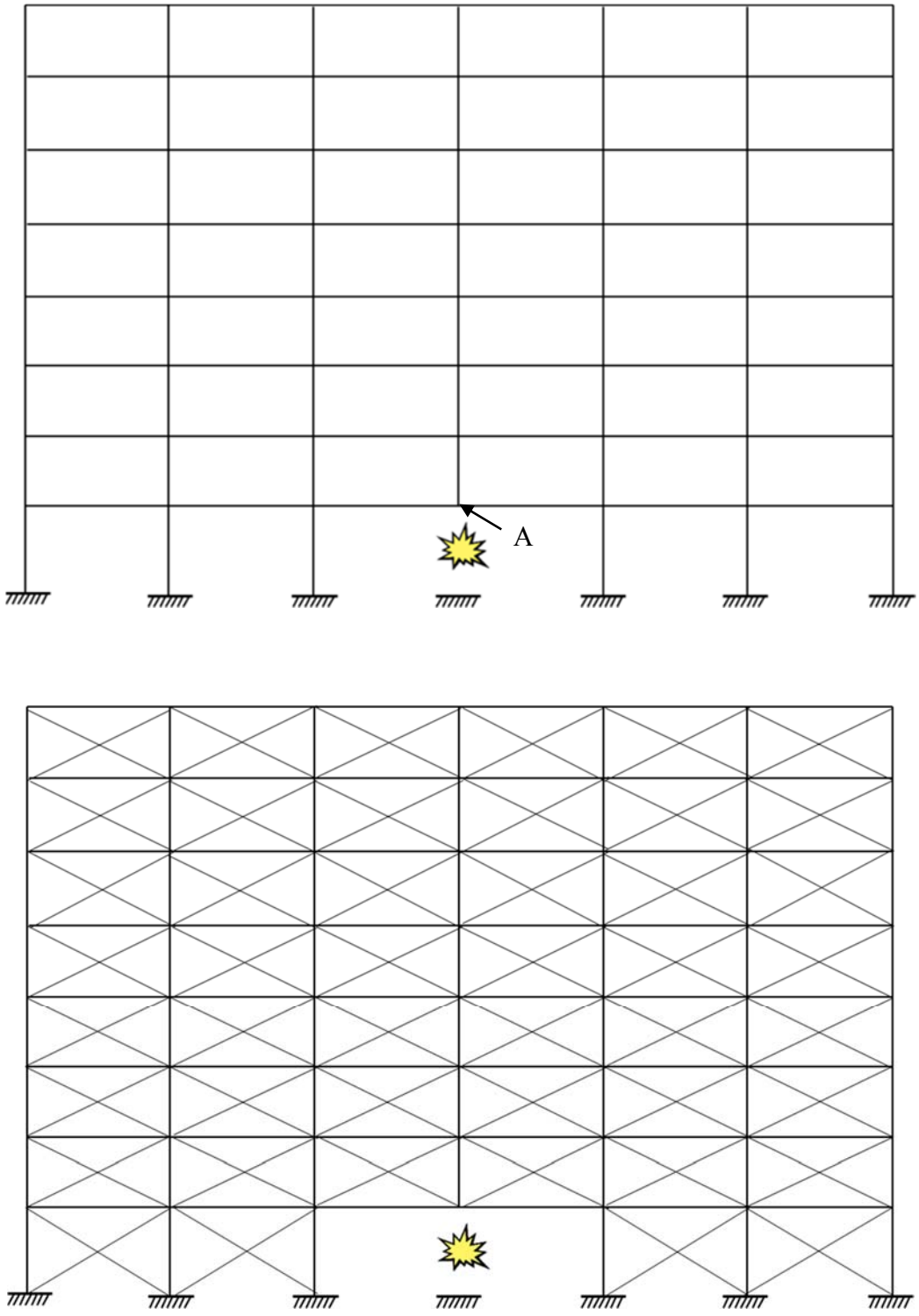

Figure 4-2: Eight Story Steel Frame without and with AAC Infill

4.2.1 Analysis Results

Figures 4-3 through 4-8 show normalized plots of vertical load P, at point A, axial force N and bending moment M at the double span beam end. P, N and M were chosen at those locations in order to determine the load carrying capacity of the structure and the demand on the adjacent lateral load resisting system. Vertical deflection Δ was measured at point A as shown in Figure 4-2. In Figures 4-3 and Figure 4-4, the vertical load is normalized with respect to the flexural plastic collapse load, P_c, given as:

$$P_c = \frac{4M_P}{L} \tag{1}$$

where L is the span of a single bay in the steel frame and M_p is the plastic yielding moment of the beam's steel section. The axial force and moment are normalized with respect to plastic axial force N_p and plastic bending moment M_p, respectively. The vertical deflection is normalized with respect to the section depth, d.

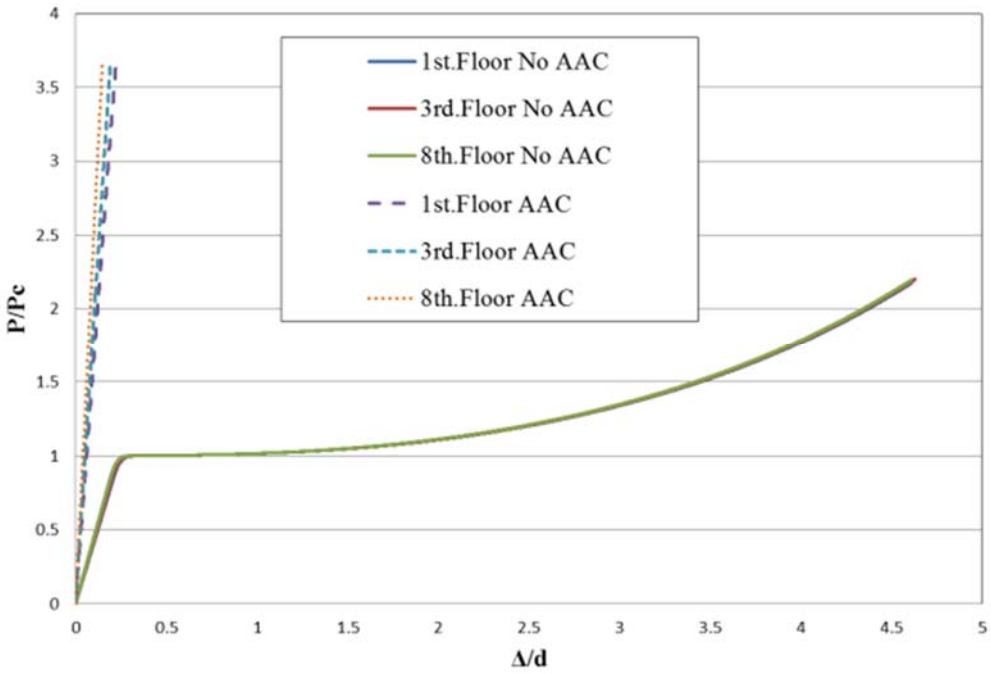

Figure 4-3: Effect of AAC Infill - Vertical load with & without AAC

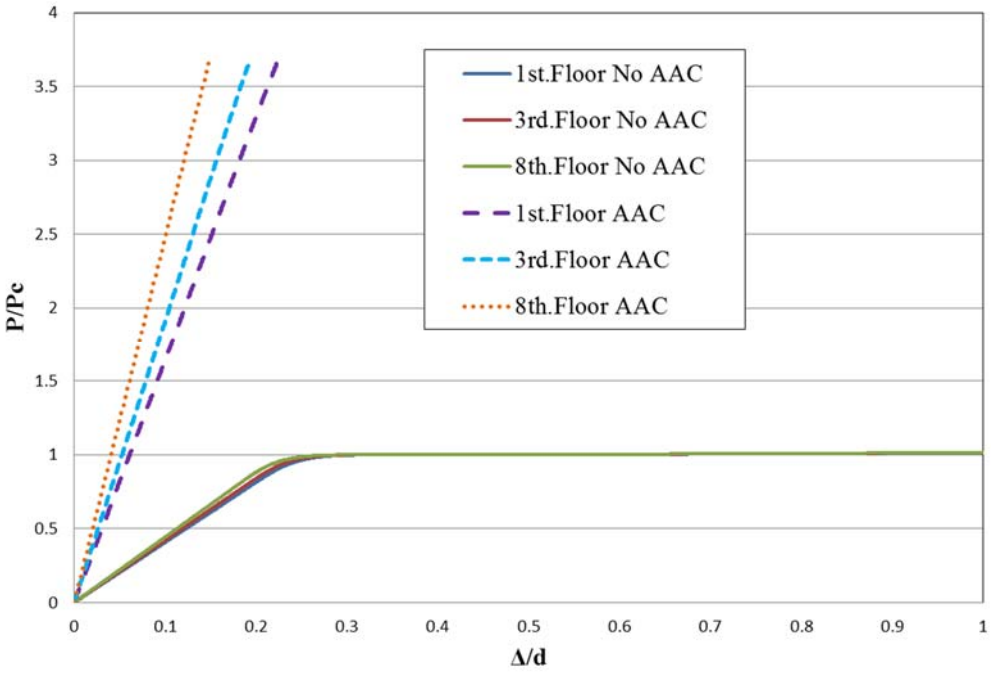

Figure 4-4: Vertical load with & without AAC - Expanded View

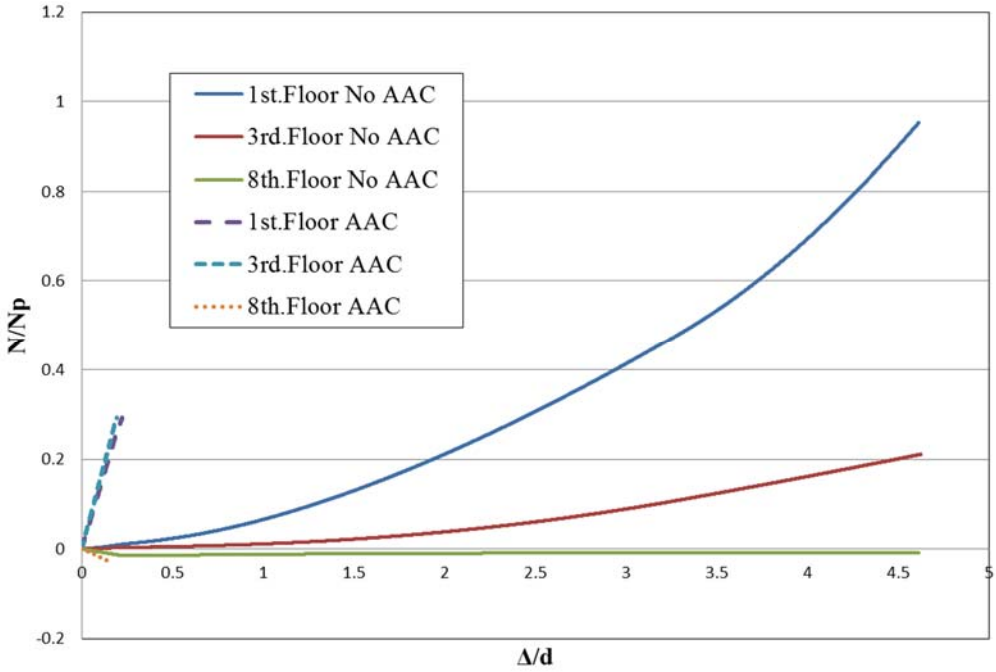

Figure 4-5: Axial force with & without AAC

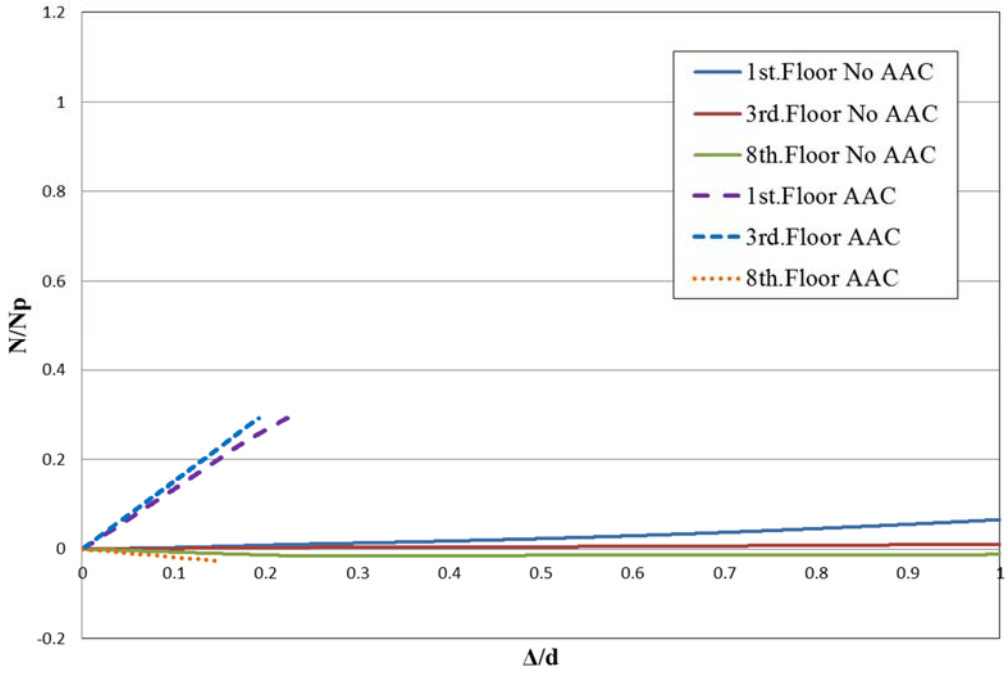

Figure 4-6: Axial force with & without AAC - Expanded View

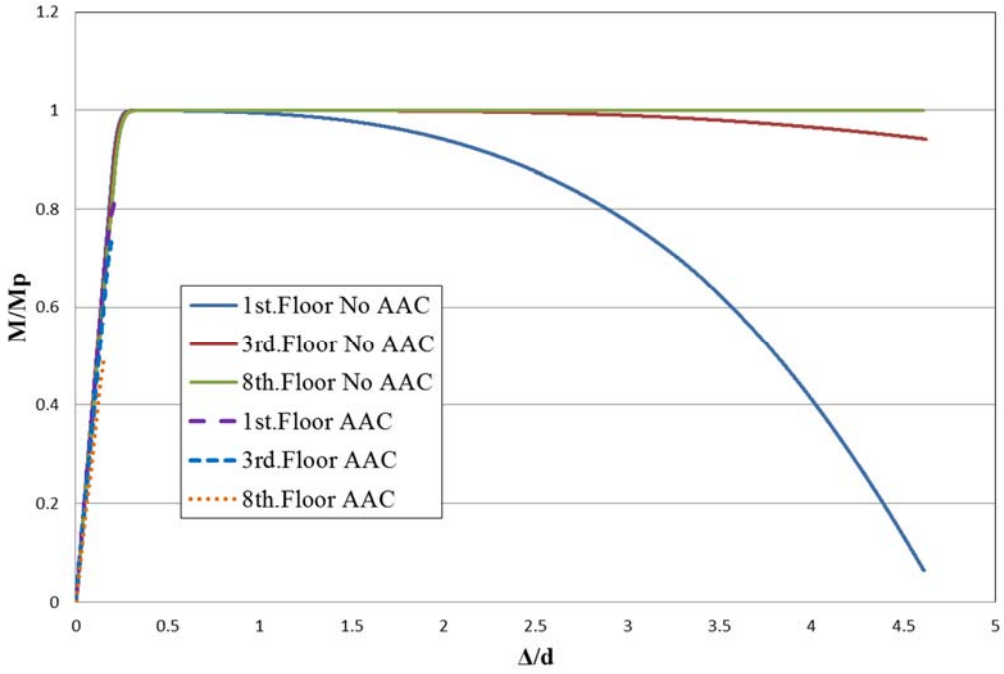

Figure 4-7: Moment versus Deflection with & without AAC

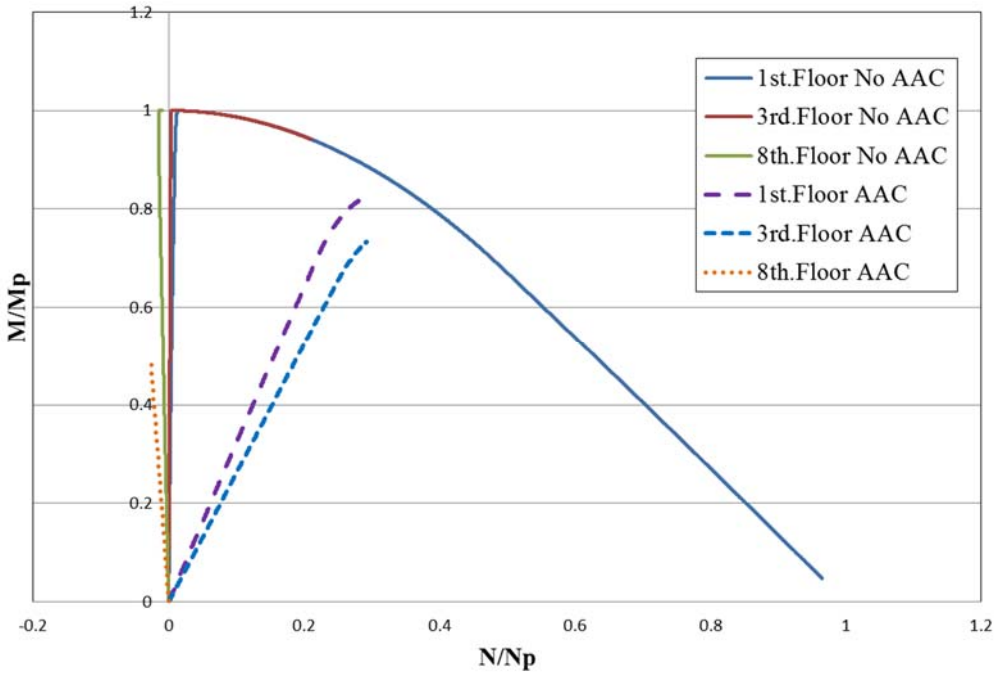

Figure 4-8: Moment versus Axial Force with & without AAC

Figures 4-3 through 4-8 show a comparison between bare steel frame and frame with AAC infill. To clarify the impact of the AAC infill, the results of the 1st, 3rd and 8th floors for the two frames were presented in three sets of figures. Figure 4-3 and Figure 4-4 plot the vertical load P versus deflection at point "A" with different ranges of deflection. Figure 4-5 and Figure 4-6 plot the axial force at beam end versus deflection at point "A". Figure 4-7 and Figure 4-8 plot the moment at beam end versus deflection at "A" and axial force at beam end. In order to highlight the difference in behavior of the three floors of the AAC infilled frame, Figure 4-4 and Figure 4-6 were generated to focus on the AAC infilled frame beams.

Figures 4-3 through 4-8 show that the behavior of the steel frames without AAC is significantly different from steel frames with AAC. Figure 4-3 shows that the 1st, 3rd and 8th floors of bare steel frame behave similarly. The three cases reach the plastic collapse load at a relatively low vertical deflection of about 0.2d. Afterwards, a transition from flexural behavior to catenary behavior starts occurring, leading to significant vertical deflection in the beams. The beams reach $2P_c$ at a midspan vertical deflection of about 4.5d. Figure 4-3 shows that the beams of the steel frame with AAC can sustain higher load carrying capacity compared to the cases without AAC (about 1.75 times). Additionally, those high levels of load carrying capacity are achieved at very low deflection levels (about 0.2d). It was observed that the 1st floor with AAC had a higher vertical deflection at midspan for the same load carrying capacity compared to the 3rd and 8th floors respectively as shown in Figure 4-4.

Figure 4-5 and Figure 4-6 showed that the bare steel frame behaves differently from the AAC infilled steel frame. However, unlike the load carrying capacity plot, there is a

difference between the three floors of the steel frame without AAC. For the 1st floor bare steel frame, the beam develops an axial force of about N_p at 4.5d, while for the 8th floor it hardly develops any axial force at 4.5d. On the other hand, the steel frame with AAC behaves in a different way. While the 1st and 3rd floor develop axial force of about ($0.3N_p$) the 8th floor develops compression rather than tension. This can be attributed to the contribution of AAC infill in the steel frame. When the first floor double span beam starts deflecting, the beams of the other stories start deflecting at the same rate. As a result, the AAC infill (modeled as struts) starts developing axial forces. As the forces move up the frame, the impact of AAC starts building up, leading to development of compression rather than tension on the top floor.

Figure 4-7 and Figure 4-8 verify the earlier remarks. They show that while the steel frame without AAC infill starts developing catenary action at relatively small deflections and actually reaches pure catenary action when M=0 and $N=N_p$, the steel frame with AAC floors can't achieve similar axial forces or get to M_p (plastic hinge formation). It can be observed that while steel frames without AAC achieve pure catenary action (in some floors), the AAC infilled steel frame not only achieves higher load carrying capacity but due to the fact that it reaches it at relatively low deflections, it is likely in reality to be able to sustain more loads than the bare steel frame due to the ductility and connections' limitations.

Figure 4-9 is a close up of the eight story frame. It shows the double span beam, the columns and the struts at this specific joint. Figure 4-10 reveals the contribution of each strut and shows how their location affects the axial force distribution among them. For example, Strut 1 gets the maximum axial force compared to the other two struts due to the

fact that it is located right above the missing column. In other words, the additional loads are redistributed among the catenary action in beams and AAC struts. On the other hand, Strut 3 is not subjected to compression, and can't withstand tension. This results in zero axial force strut.

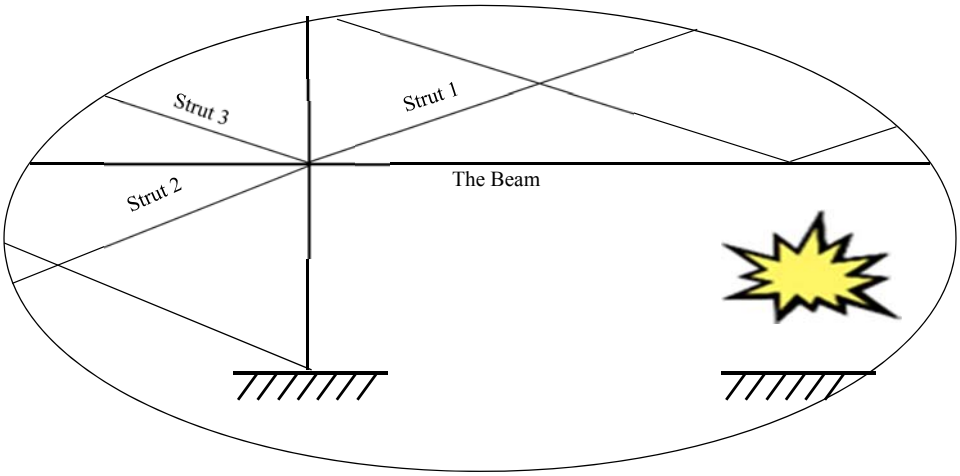

Figure 4-9: Close up of the struts & the beam

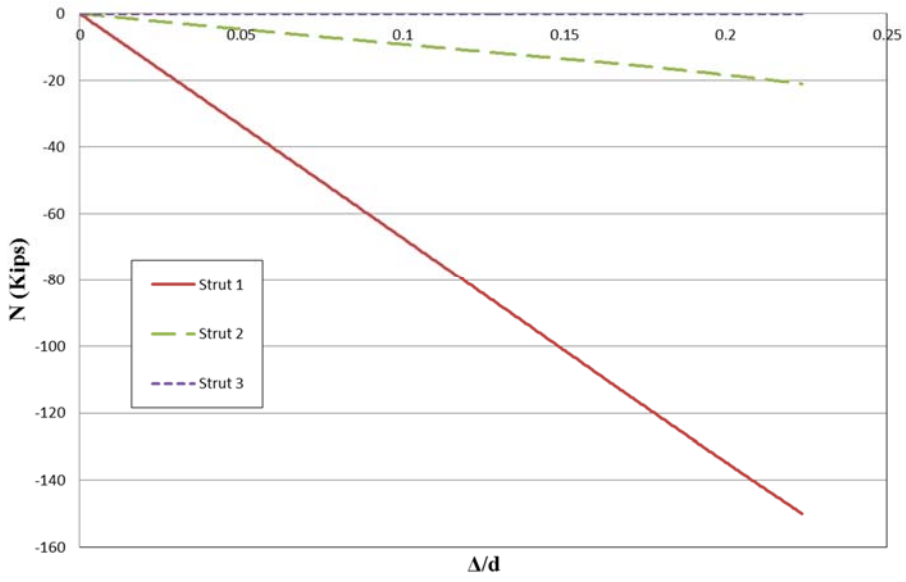

Figure 4-10: Forces in AAC struts - Axial forces versus midspan deflection

4.3 Effect of Building Height

Three steel frames with the AAC infill were analyzed in order to study the impact of building height on the results. The eight, five and three story AAC infilled frames that were chosen are shown in Figure 4-11. The steel sections for the three and the five story steel frames are presented in Figure 4-12.

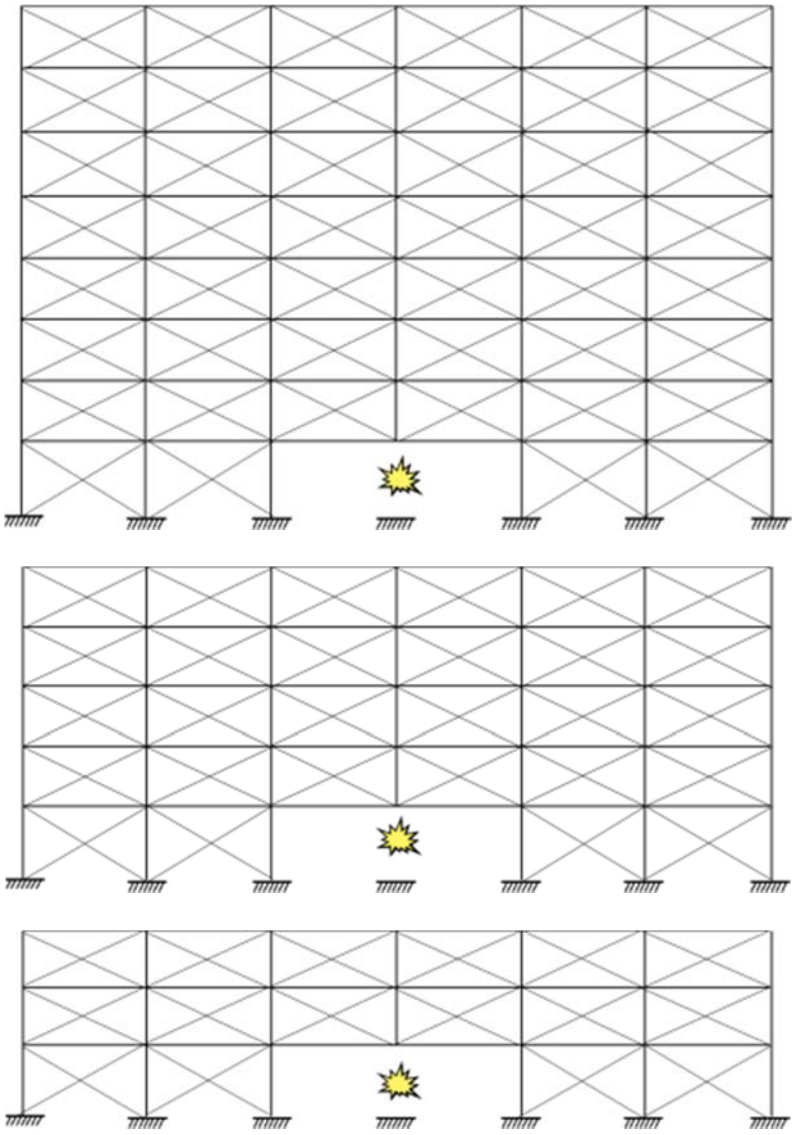

Figure 4-11: Eight, Five and Three Story Frames with AAC Infill

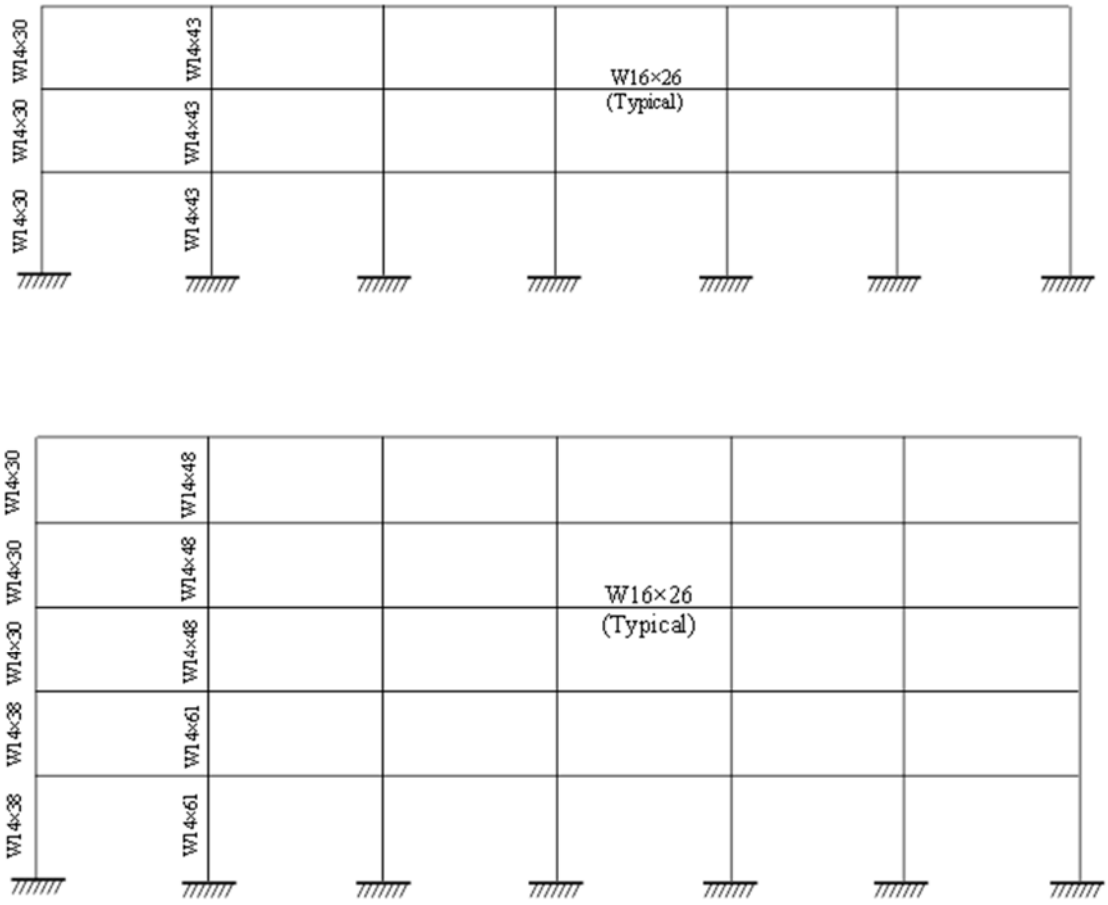

Figure 4-12: Three & Five Story Steel Frames Elevations

Due to the fact that the story height is not identical throughout the frame height (the first floor height is different from the rest of the floors) and the column size change from one frame to the other, the AAC infill struts' width and area are different. Table 4-1 shows the different sizes of the AAC infill struts that were used for the different frames. The three frames were modeled in OpenSees and subjected to a concentrated load at midspan of the first story beam. The behavior of the first story beams of each frame were

presented and compared with each other. The axial force and moment at the ends of the first story beams are presented in Figure 4-14 through 4-15.

Table 4-1: AAC Infill Struts Dimensions

	Three Stories		Five Stories		Eight Stories	
	1st. Floor	**Typical Fl.**	**1st. Floor**	**Typical Fl.**	**1st. Floor**	**Typical Fl.**
ω_{strut} (in)	14.97	14.36	16.35	15.88	16.52	15.88
Area(in^2)	119.7	114.9	130.8	127.1	132.2	127.1

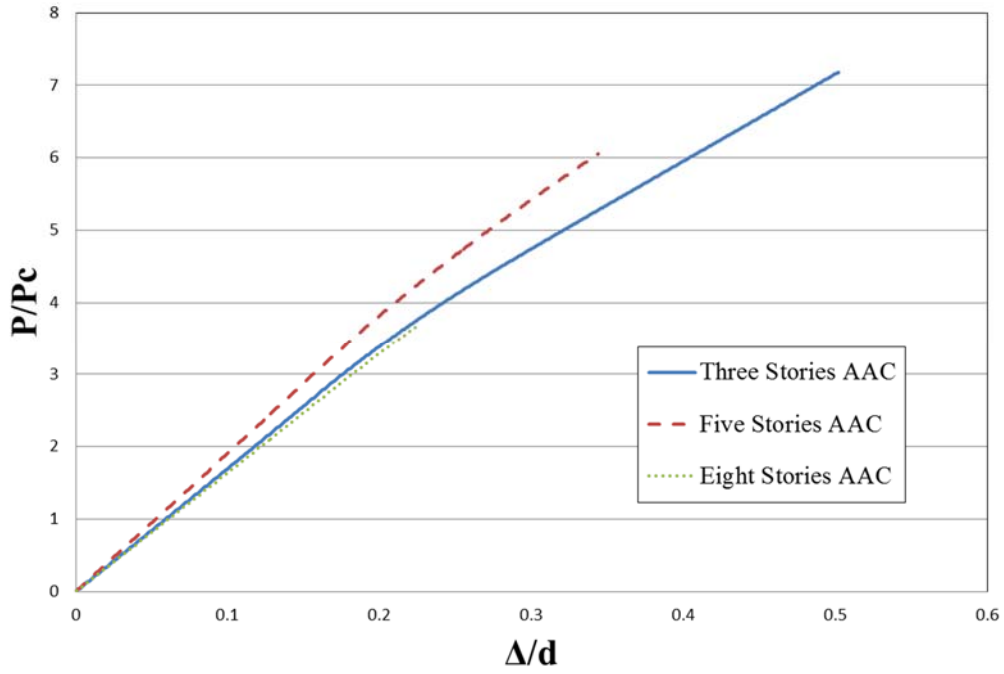

Figure 4-13: Effect of Building Height - Vertical Load versus Deflection

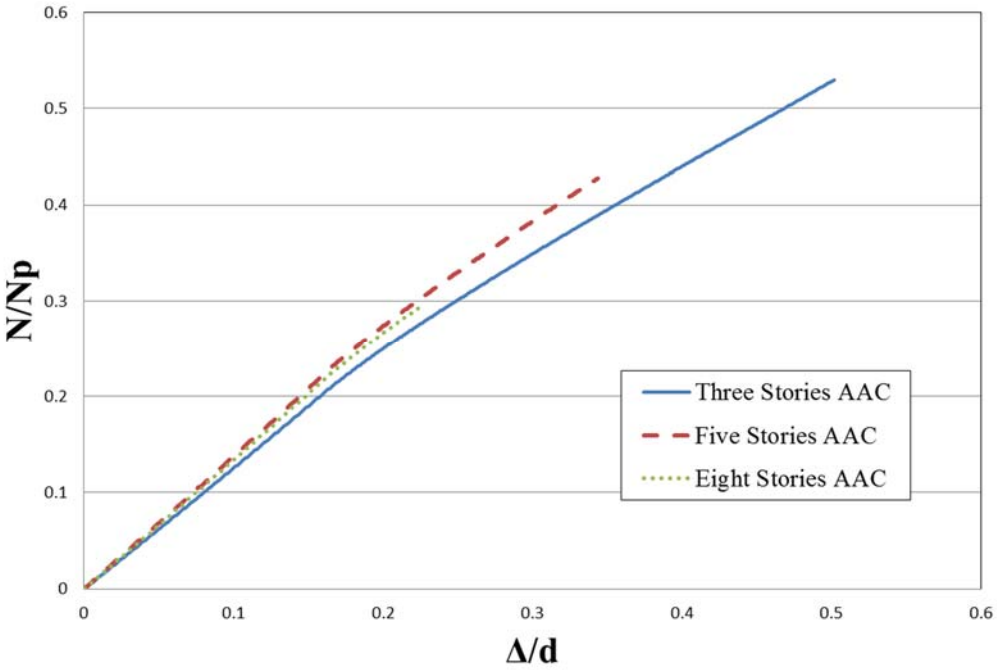

Figure 4-14: Effect of Building Height - Axial Force versus Deflection

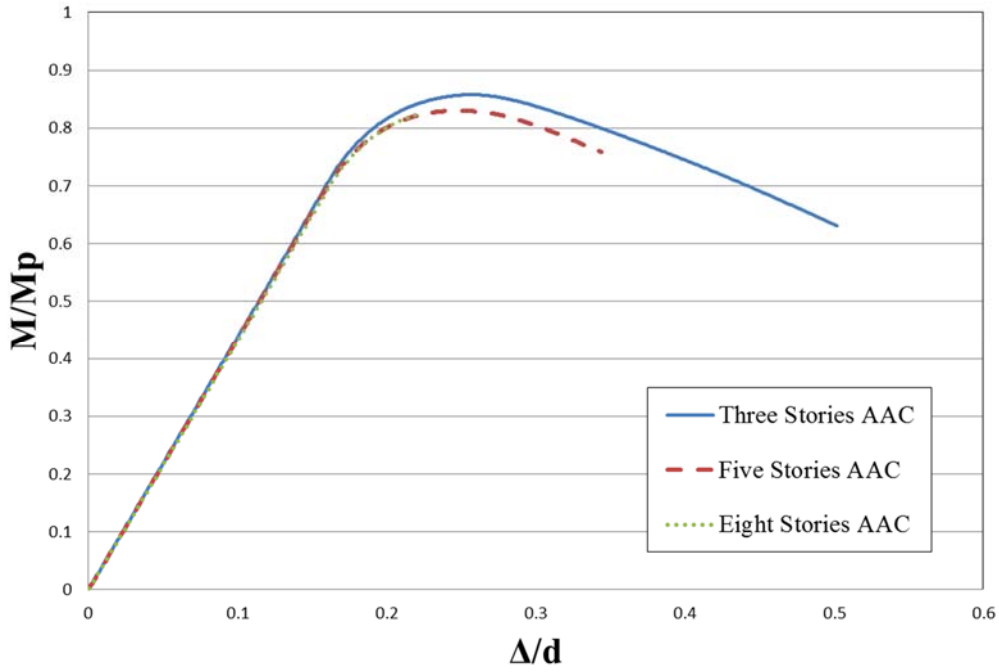

Figure 4-15: Effect of Building Height - Moment versus Deflection

Figure 4-13 shows the load carrying capacities of the different frames based on the behavior of the first floor beam in each frame. It can be observed that the load carrying capacity (as a fraction of the actual collapse load of the frame) decreases as the frame height increases. In other words, the three story AAC infilled frame performed better than the eight story AAC infilled frame. It is also noted that the five story frame seems to resist loads at a rate higher than the three and the eight story frames. The slight difference in the rate can be attributed to the change in lateral resistance of the side frames. The AAC infill is the main contributor of lateral resistance for the three story frame as the AAC infill struts act as bracing for the frame. On the other hand, the AAC impact is limited at the eight story frame, where the framing action is the main contributor to the lateral resistance. In the five story frame, both AAC infill struts and the framing action are contributing more evenly and this might explain why the five story frame has a slightly higher rate of load carrying capacity.

In Figure 4-14 and Figure 4-15, the first floor beams of the three, five and eight story frames developed axial forces and moments at the beam ends. Although none of them were able to achieve full catenary action (where N gets to N_p and M gets to zero), the beams still generated significant catenary forces in the adjacent lateral load resisting frames. The generated catenary forces ranged between 0.3 N_p for the eight story frame to 0.53 N_p for the three story frame. Those results are in agreement with the load carrying capacities of the frames from the previous plot. The impact of the AAC diminishes as the height of the frame increases due to the fact that the column sections are bigger and stiffer for the eight story frame compared to the three story frame. As a result, the

contribution of the AAC infill as bracing decreases as the height increases because of the increased role of the framing action of the steel frame.

The ability of the first floor beam to generate axial forces in the adjacent lateral load resisting frame is crucial in order to enhance the load carrying capacity of the whole frame. The results had shown that the axial forces generated in the beam ends are concentrated mainly in the first few stories. Thus, the load carrying capacity of the frame is greatly affected by the ability of the first floor beam to generate axial forces in the adjacent lateral load frame.

4.4 Effect of AAC Infill Placement

To account for the impact of AAC placement scenarios, three additional placement scenarios for the five story steel frame plus the original infill placement were considered. Each of the different placement scenarios are shown in Figure 4-16 through 4-19. Scenario 2 represents the case where there is AAC infill everywhere except the bays above the removed column. Scenario 3 is identical to scenario 2, except that there is AAC infill in the top story. Finally, scenario 4 is the case where there is AAC infill in the middle bays only (above the removed column).

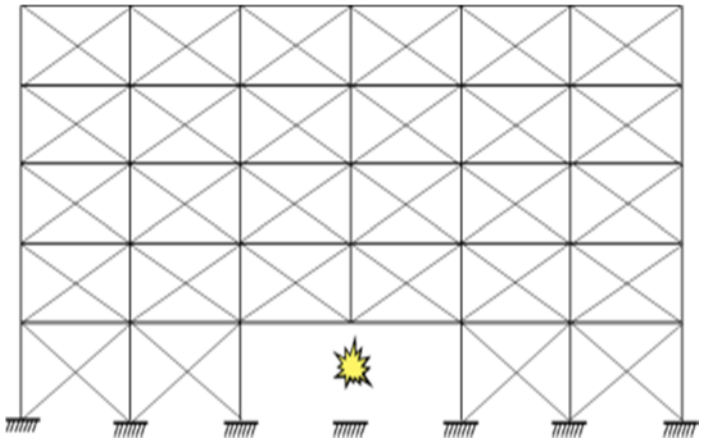

Figure 4-16: The Original Placement Scenario – Scenario 1

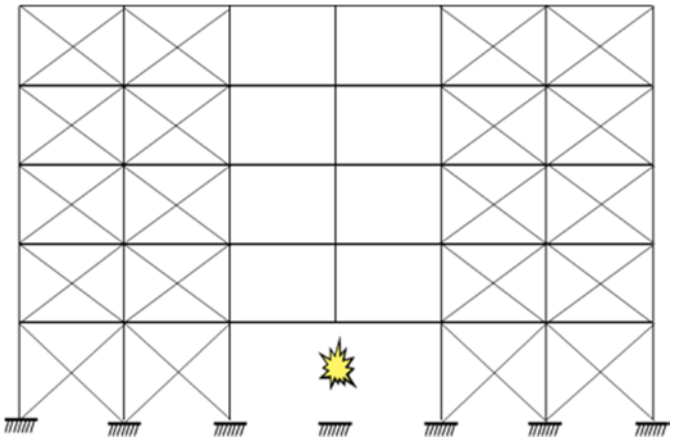

Figure 4-17: The Additional Infill Placement Scenarios - Scenario 2

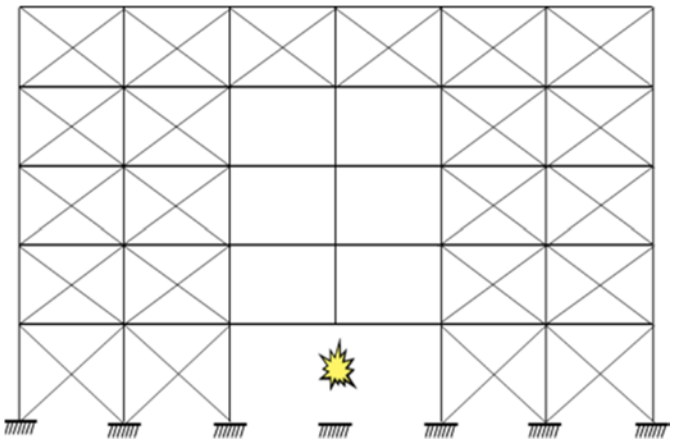

Figure 4-18: The Additional Infill Placement Scenarios - Scenario 3

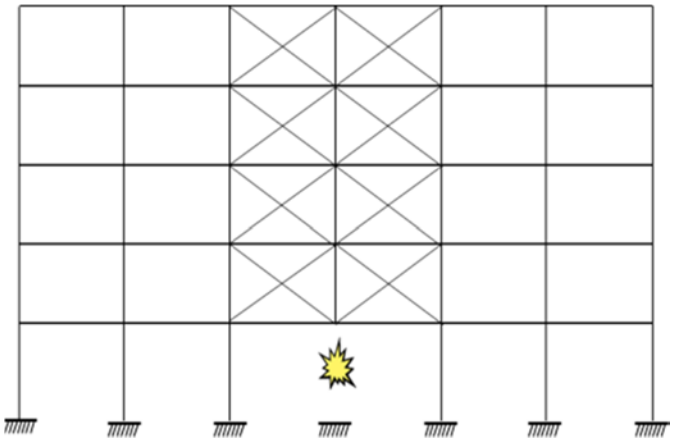

Figure 4-19: The Additional Infill Placement Scenarios – Scenario 4

The three infill placement scenarios plus the original infill placement were analyzed in OpenSees to understand the impact of infill placement on the results. The results of the first story double span beams from the four scenarios and the bare steel frame are plotted in Figure 4-20 through Figure 4-23.

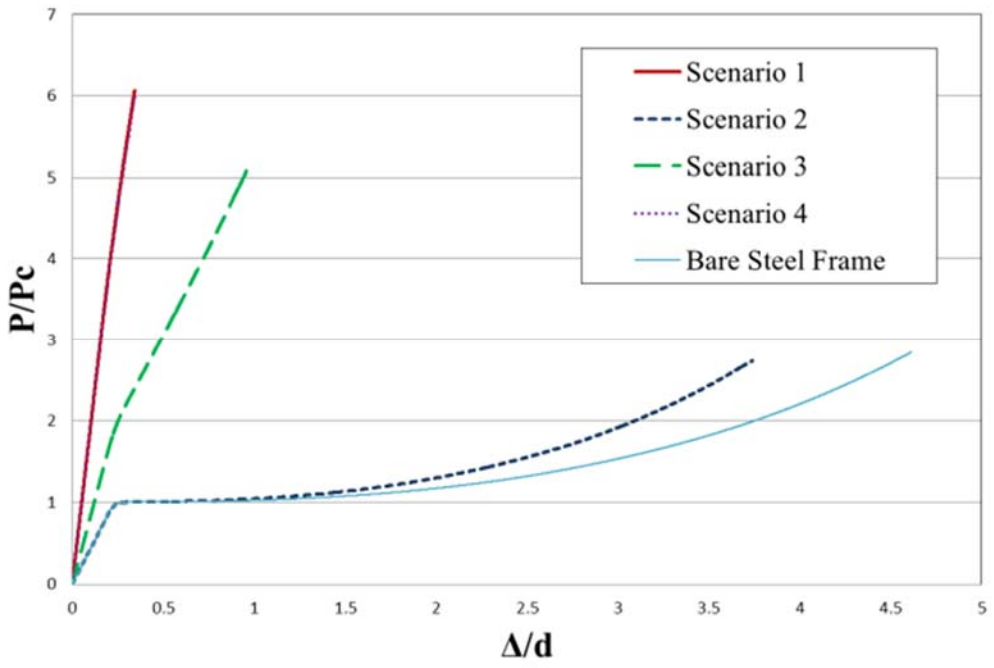

Figure 4-20: Effect of AAC Infill Placement - Vertical Load versus Deflection

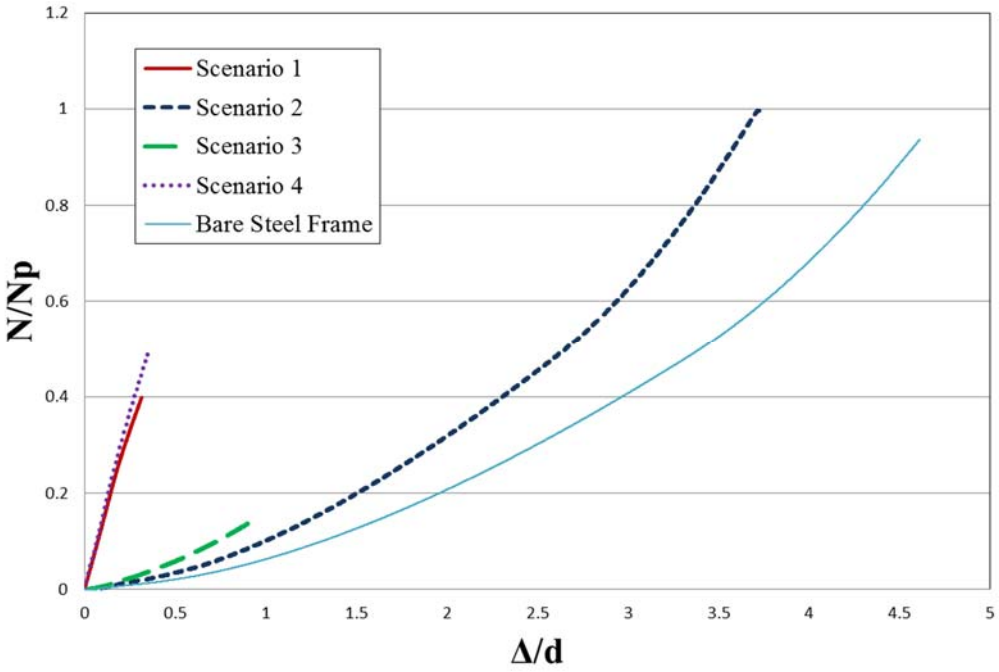

Figure 4-21: Effect of AAC Infill Placement – Axial Force versus Deflection

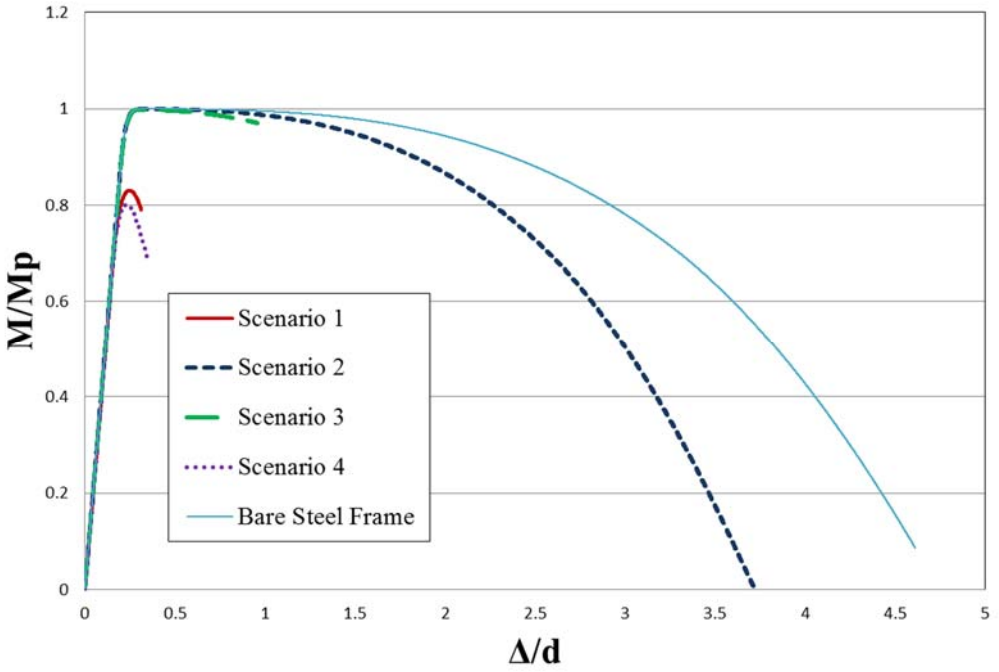

Figure 4-22: Effect of AAC Infill Placement – Moment versus Deflection

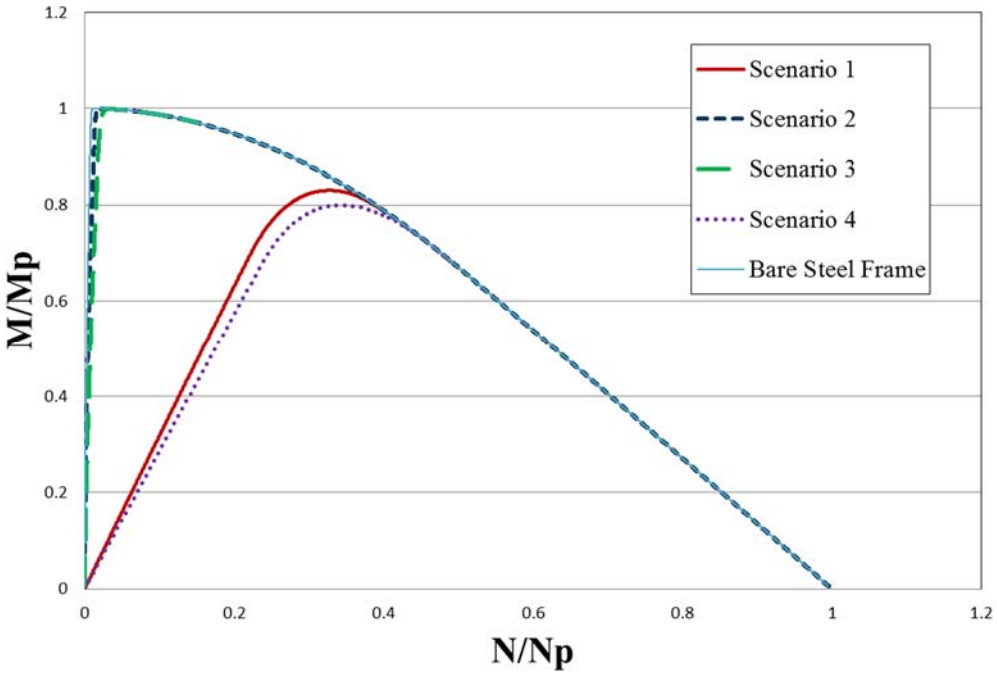

Figure 4-23: Effect of AAC Infill Placement - Interaction Diagram

Figure 4-20 shows the load carrying capacity of the four steel frames with the different AAC infill scenarios and the bare steel frame. It shows that the beams behave significantly different based on the location of the AAC infill. Scenario 1 reaches load carrying capacity of 6 P_c at a midspan deflection of about 0.5d while scenario 2 gets to about 2.75 P_c at a midspan deflection of about 3.75d. This wide range of results highlights the impact of AAC infill placement on the overall frame behavior. The difference between the two scenarios can be attributed to the role played by the AAC struts on top of the double span beam. Those struts that are designed to resist compression were resisting the additional loads resulting from the column loss and transferring the loads to the lateral load resisting system. Therefore, removing those struts (in the middle bay) limited the ability of the frame to carry loads (about 45% of the load carrying capacity of the first scenario). However, the second scenario was more flexible

than the first one (i.e. higher midspan deflections). The third scenario exhibited results in between the first two scenarios. The AAC infill struts at the top story of the frame managed to bring the load carrying capacity of the frame close to the second scenario. Finally, the fourth scenario is actually plotted right on top of the first scenario. This can be explained using the same logic from before. The middle bay struts continued to resist the additional loads and to distribute them among the other struts and the overall frame. This observation leads to the conclusion that the AAC infill placed directly above the damaged or removed column has a far greater impact on the overall frame resistance than placing the AAC infill in other bays. This conclusion can be reinforced by the fact that the second scenario was the closest to the bare steel frame case.

Figures 4-21 through 4-23 show the generated axial forces and moments at the beam ends of the first floor beam for the four scenarios. Examining the rate of axial force development in the side frames inferred from Figure 4-21 helps to interpret the beam behavior. The second scenario achieved full catenary action; this can be attributed to the removal of AAC struts above the double span beam. It can be reasoned that the removed struts were playing a part in resisting the additional loads. Therefore, the additional loads were transmitted to the side frames by developing catenary forces in the double span beams. The first and the fourth scenarios behave similarly because there is AAC infill throughout the middle bay resulting in similar constraints on the frame. The additional loads are carried by the AAC struts on top rather than significant catenary action in the beams and thus putting less demand on the side frames. The third scenario behaves initially in a similar fashion to the second scenario. However, the third scenario failed to generate equivalent catenary forces (it stops at 0.19 N_p) because after a certain lateral

displacement of the side frame, the AAC struts in the top frame started participating in the resistance of loads.

Figure 4-22 and Figure 4-23 are intended to focus on the generated moment at the beam ends versus the midspan deflection and the interaction diagram at the beam end. The plots show that the second scenario achieved full catenary action, and the third scenario initially behaved similarly however it couldn't achieve catenary action due to the presence of AAC struts on the top story, as explained earlier. Finally, the fourth scenario behaves in a manner similar to the first scenario in that it fails to get to plastic hinge formation due to the presence of the AAC struts in the middle bays.

4.5 Effect of Loading Type

In order to model the missing column scenario in the steel frame, a concentrated load was applied to the midspan point of the double span beam. In this section, two additional loading types were investigated. The two techniques are distributed loading and a combination of concentrated and distributed loading. The distributed loading was applied to the middle double span beam. ASCE 7-10 specifies 1.2 times the dead load plus 0.5 times the live load as a proper loading combination for extraordinary events, which applies to this case. For the concentrated load case, the plastic collapse load of the double span beam was applied. Finally, a combination of distributed and concentrated loading was applied as well. For this type of loading, a combination of the distributed and concentrated loads previously described were applied.

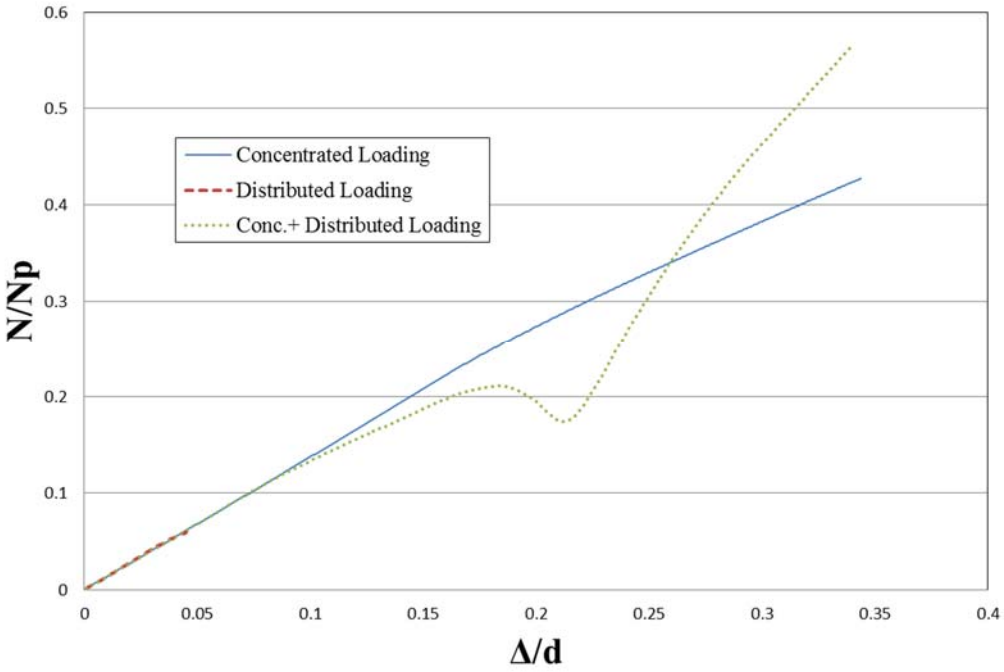

Figure 4-24: Effect of Loading Type - Axial Force versus Deflection

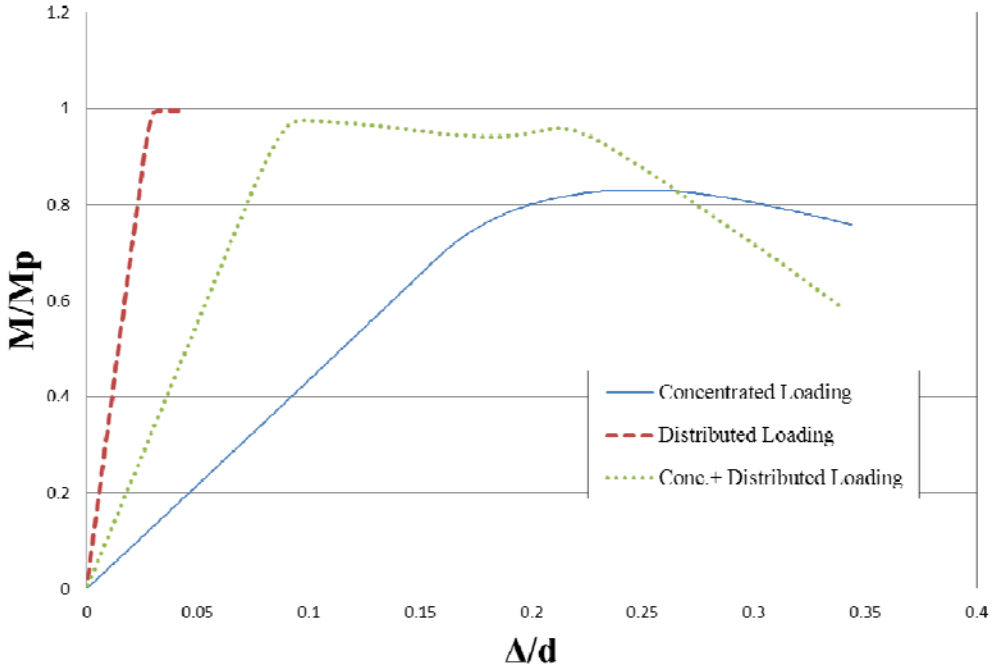

Figure 4-25: Effect of Loading Type - Moment versus Deflection

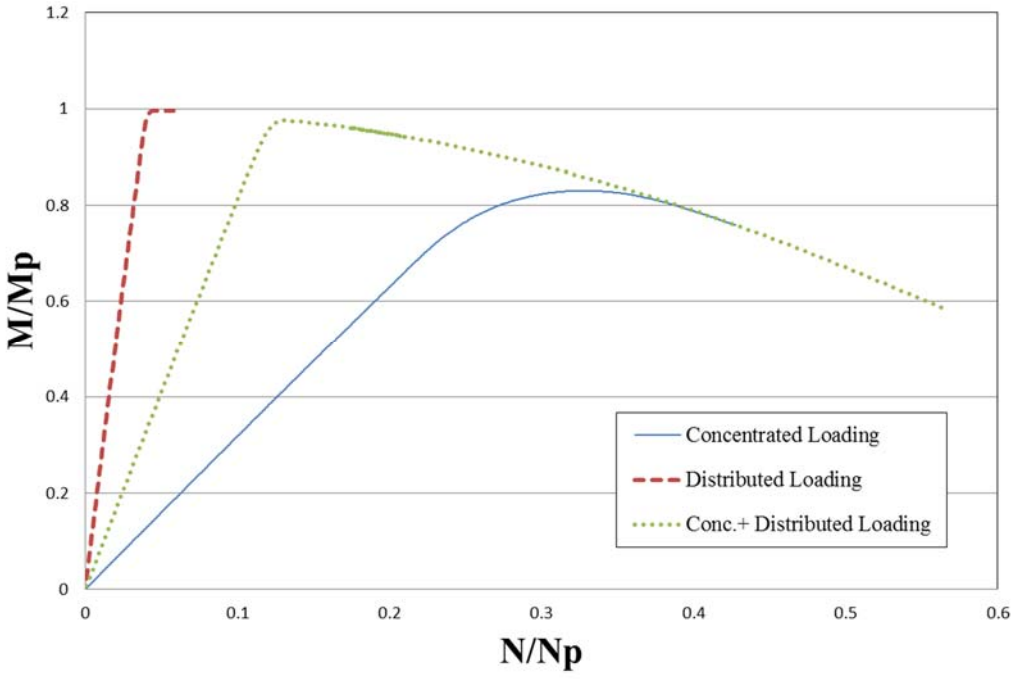

Figure 4-26: Effect of Loading Type - Interaction Diagram

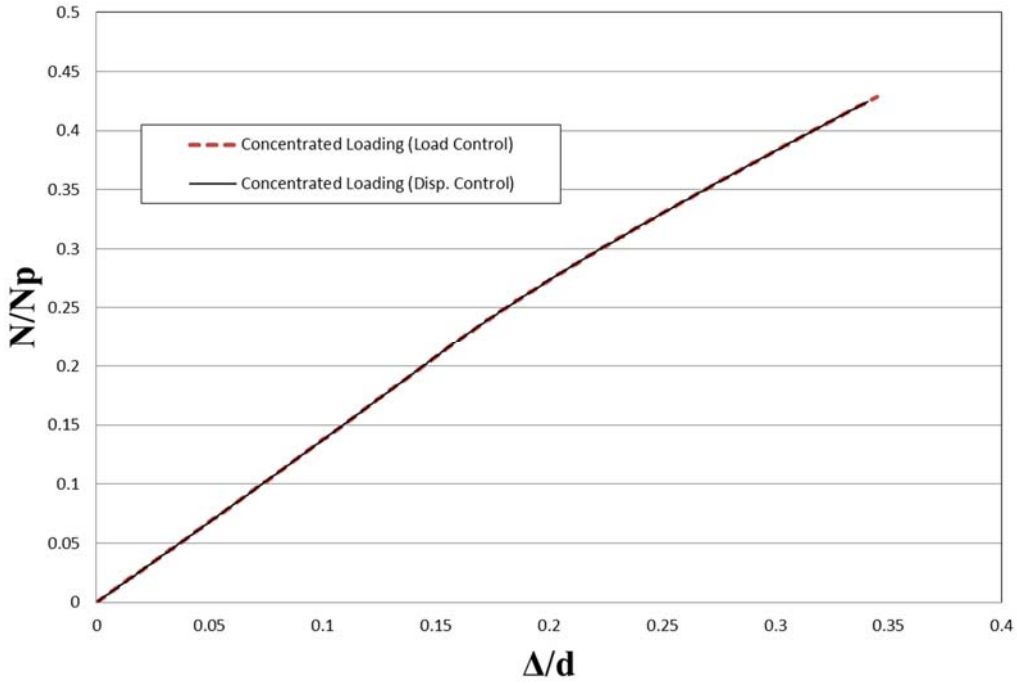

Figure 4-27: Load Control versus Disp. Control

The results of the three loading types for the five story steel frame are presented in Figures 4-24 through 4-26. For all of these models, displacement control analysis was adopted. In order to rule out the impact of analysis type, load control analysis was performed and compared to the displacement control analysis. Figure 4-27 shows a perfect match between the two types of analysis.

Figure 4-24 shows the generated axial forces at the beam ends for the three loading types. The three loading types generated axial forces at the same rate up to a midspan vertical deflection of about 0.05d. The distributed loading stoped developing axial force beyond this point. On the other hand, the concentrated loading continued to develop axial force up to $0.43N_p$ at a midspan deflection of 0.345d. The difference between the results can be attributed to the AAC struts' contribution. The distributed loading caused the AAC struts to start resisting loads at a rate faster than the concentrated loading.

Results of the combined loading exhibited a different behavior, the combined loading started developing axial forces in a manner similar to the distributed loading type, due to the fact that there are vertical loads close to the beam end. However, the combined loading didn't stop generating axial load as did the distributed loading. This was likely due to the existence of the concentrated load at midspan which continued to generate more axial load at the beam end. When the axial force got to $0.21N_p$, the AAC struts above the middle bay and the struts in the side frame started playing a role in resisting the loads, which explains the dip in the generated axial force for the combined loading case. As the vertical load and the midpan deflection increased, the beam end started picking up more axial force until it got to $0.56\ N_p$.

Figure 4-25 and Figure 4-26 show the generated moment and the interaction diagram at the beam end. The distributed loading case managed to get to plastic hinge formation point. However, the concentrated and the combined cases failed to get to M_p. The concentrated loading case got to $0.83M_p$ at a midspan deflection of 0.25d and then the moment at the beam end started declining from this point. The combined case got very close to plastic hinge formation at moment equal to $0.98M_p$ at 0.1d and an axial force of $0.13N_p$. All of the loading types failed to get to moment equal to zero or to achieve full catenary action ($N=N_p$).

4.6 Conclusions

The analyses presented in this chapter focused on understanding the impact of AAC infill on catenary action in steel frames and possible implications on the overall steel frame load carrying capacity. Push-down analyses of three, five and eight story steel frames with different configurations were performed. An eight story steel frame with AAC infill was compared to a bare steel moment frame. The load carrying capacity of the frames and the developed forces in the adjacent lateral load resisting frames were discussed. The role of building height and its effect on the results was studied. Finally, four different AAC placement scenarios and three loading types for a five story steel frame were considered to study the effect of infill placement and loading types on the overall results.

The comparison between the AAC infilled frame and the bare eight story frame indicated that the infilled frame had a higher load carrying capacity than the bare steel frame. It was also concluded that the infilled frame resulted in a lower demand on the

adjacent frame (i.e. developed lower axial forces at beam ends compared to bare steel frame) due to the presence of AAC struts. It was noticed that the change in building height had a significant impact on the results. Furthermore, after four AAC placement scenarios were compared, the beam behavior showed that the placement of AAC struts in the middle double span bay limits the developed catenary action forces in the steel frame. On the other hand, when AAC struts were removed from that bay only and were kept everywhere else in the structure, the side frames developed much higher catenary forces compared to the other case. However, having even one floor of AAC struts above the removed column ensures improved load carrying capacity of the frame compared to no AAC infill in that bay at all.

Finally, it was shown that the loading type and whether it is concentrated, distributed or a combined loading had a significant impact on the developed catenary forces.

In conclusion, the findings of this study highlight the importance of incorporating AAC struts when calculating the developed catenary action forces in the adjacent lateral load resisting systems. This will ensure more accurate and efficient design of the overall structure.

The conclusions of this study were based on the assumptions made in this study and on the limited number of building heights and AAC infill placement scenarios that were presented. Hence, the conclusions are limited to the scope of the study.

Chapter 5: Catenary Action in Steel Framed Buildings with Buckling Restrained Braces

5.1 Overview

In this chapter, the impact of the buckling restrained braces on catenary action demands is discussed. Previous research has shown that BRBs can have a significant impact on the performance of steel structures subjected to lateral loads. The superior performance of BRBs in resisting lateral loads is a strong indication of the potential role that BRBs can play in resisting the additional loads resulting from the missing column scenario. The buckling restrained braced steel frame is a structural system in which a steel frame is braced with buckling restrained braces. Buckling restrained braces (BRBs) are passive control devices that have superior ductility and energy dissipative behavior compared to other bracing systems. BRBs are composed of a steel core supported by a mortar-filled steel casing to eliminate buckling under axial loading. In this chapter, a study including analytical results for three building heights, four BRB placement scenarios and three loading types is described. The impact of BRBs on the generated forces in the adjacent frames to the double span beam suffering from column removal is highlighted. A comparison between the developed catenary action in the steel frames with and without the BRBs was conducted. Finally, the implications of the different building heights, BRB placement scenarios and loading types on structural behavior are discussed.

5.2 Buckling Restrained Braced Frame

Two eight story steel frames were designed using the commercial software package SAP2000 to determine the steel sections. The two frames are located in San Francisco, California and were designed for Seismic Design Category D with S_{DS} equal to 1.2683 and S_{D1} equal to 0.6451. The frames were located in San Francisco (high seismicity area) to justify the use of BRBs as a lateral load resisting mechanism. The design loads for the frame were determined based on the Minimum Design Loads for Buildings and Other Structures, ASCE (2010). The first frame, shown in Figure 5-1, was a bare steel frame (no bracing). The second frame was a buckling restrained braced frame (dual system) with diagonal BRBs in the second and fifth bays as shown in Figure 5-2. The areas of the BRBs core (A_c) and non-yielding (A_{ny}) segments are presented in Table 5-1.

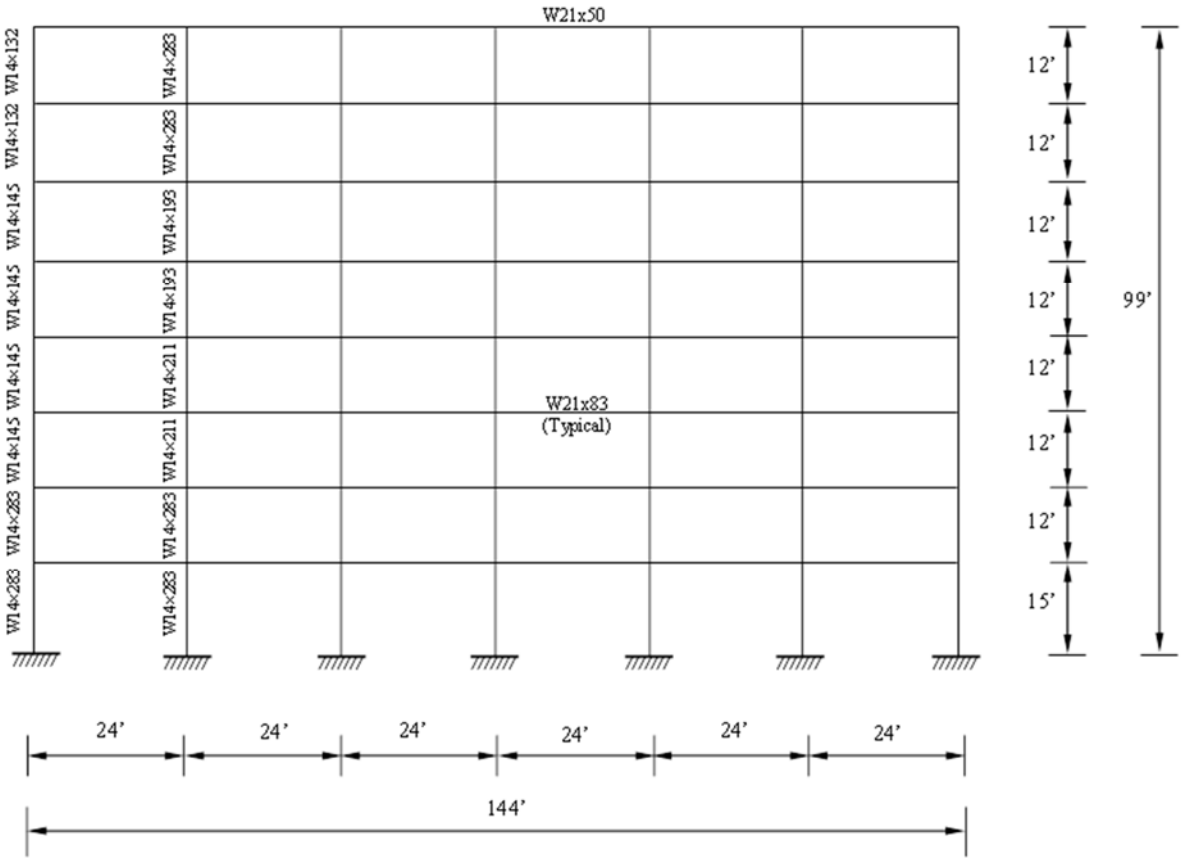

Figure 5-1: Eight Story Bare Steel Frame Elevation

Table 5-1: Areas of BRBs for Each Story

Brace	8th Floor	7th Floor	6th Floor	5th Floor	4th Floor	3rd Floor	2nd Floor	1st Floor
$A_c(in^2)$	1.00	1.50	2.00	3.00	3.00	3.50	4.00	4.50
$A_{ny}(in^2)$	5.00	7.50	10.00	15.00	15.00	17.50	20.00	22.50

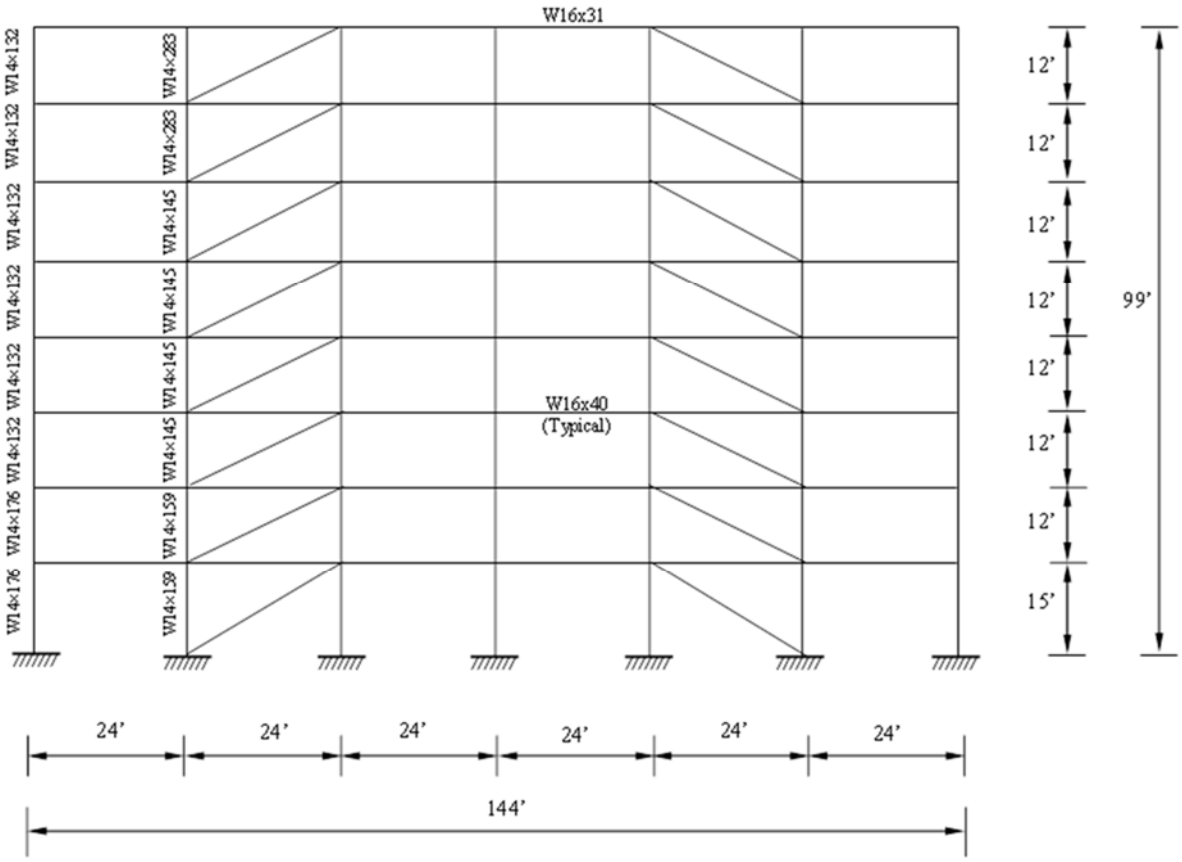

Figure 5-2: Eight Story Braced Steel Frame Elevation

Two steel frames were analyzed using OpenSees to study the impact of BRBs on the catenary action demands in steel frames. In order to address progressive collapse, an interior bottom-story column was removed to simulate the missing column scenario. The two frames were subjected to a concentrated load at the midspan point of the first floor "Point A" and were analyzed to study the difference between the cases with and without BRBs. Figure 5-3 shows the elevation of the steel frame with and without BRBs. In Figure 5-3, point "A" is directly above the removed column (mid-point of the double span beam at the first floor).

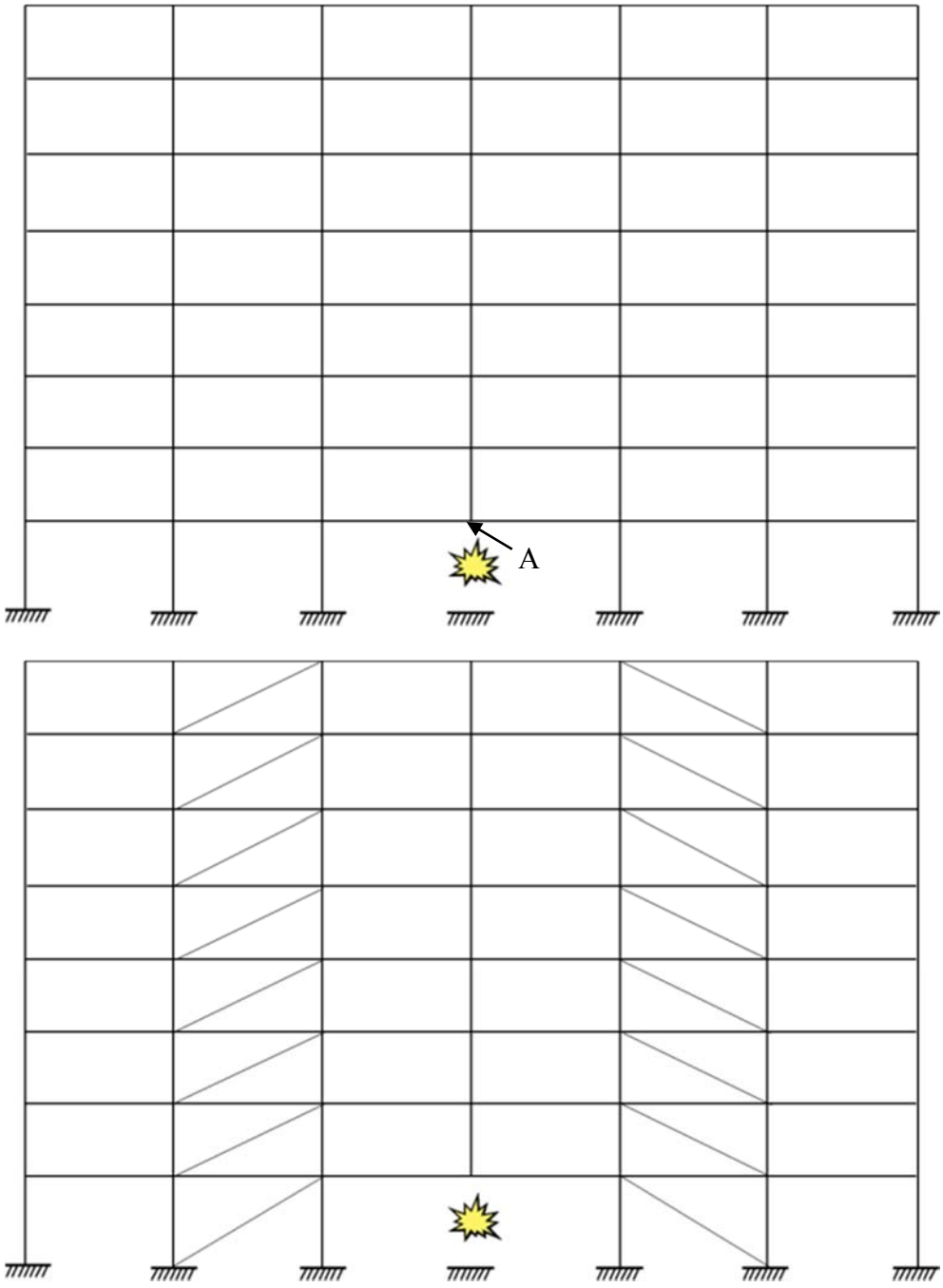

Figure 5-3: Eight Story Frames without and with BRBs

5.2.1 Analysis Results

Normalized plots of vertical load P, at mid-span, axial force N and bending moment M at the double span beam's end are shown in Figures 5-4 through 5-7. P, N and M were chosen at those locations in order to determine the load carrying capacity of the structure and the demand on the adjacent lateral load resisting system.

The axial force and moment are normalized with respect to the plastic axial force N_p (N_p is the area of the section times the yield strength of the steel section) and the plastic bending moment M_p, respectively.

To highlight the impact of the BRBs on the overall steel frame behavior and to demonstrate the steel frame behavior with and without BRBs, the results of the 1st, 3rd and 8th floors for the two frames are presented in Figures 5-4 through 5-7. Figure 5-4 plots the vertical load P versus deflection at midspan. Figure 5-5 plots the axial force at beam end versus deflection at point A. Figure 5-6 plots the moment at beam end versus deflection at A.

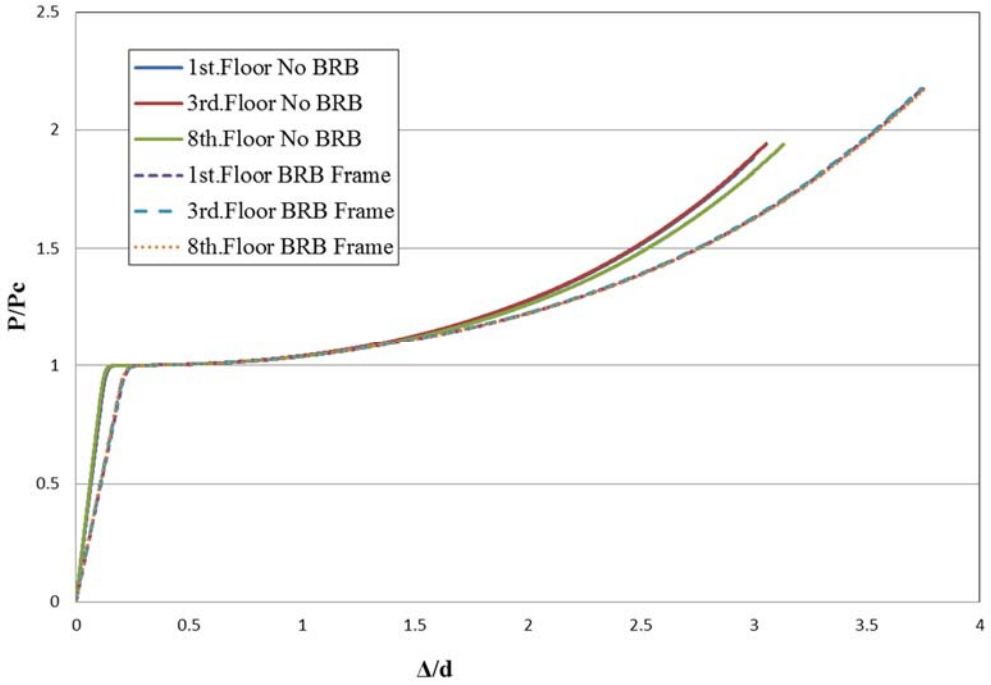

Figure 5-4: Effect of Buckling Restrained Braces - Vertical load versus Deflection

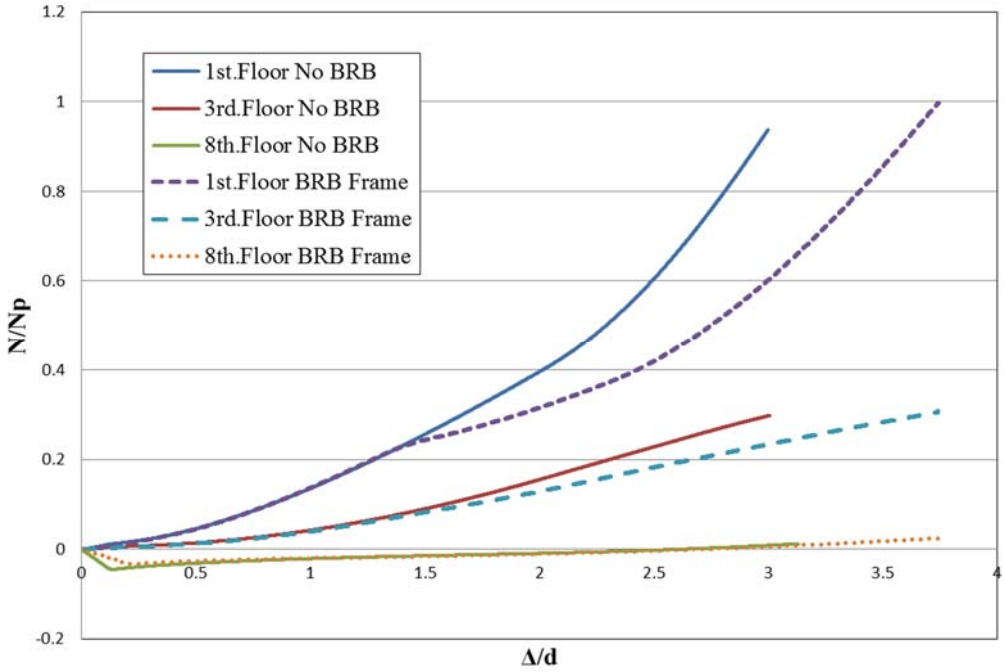

Figure 5-5: Effect of Buckling Restrained Braces - Axial force versus Deflection

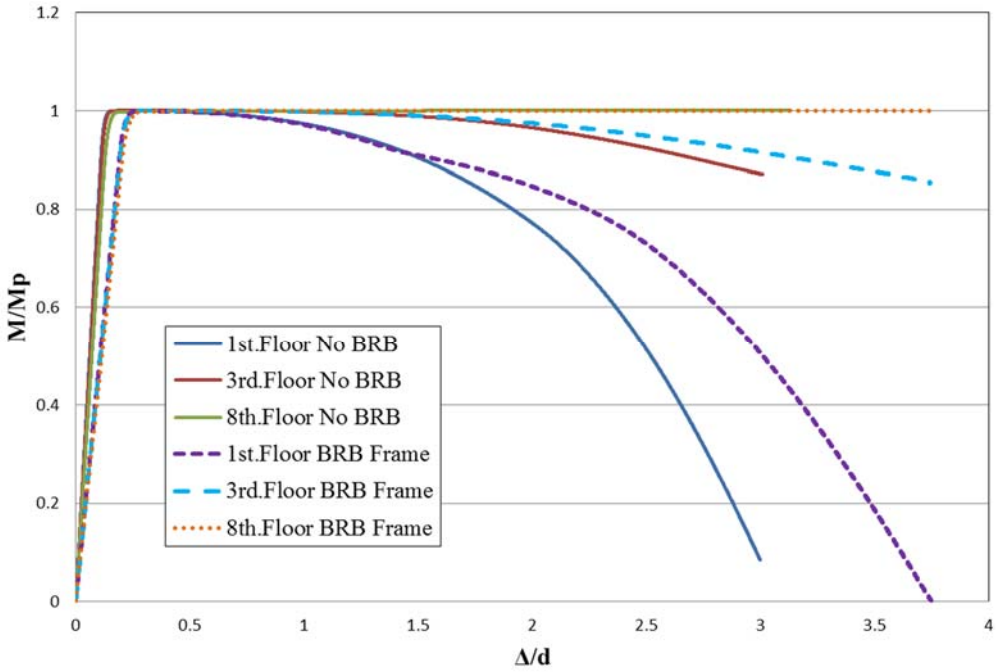

Figure 5-6: Effect of Buckling Restrained Braces - Moment versus Deflection

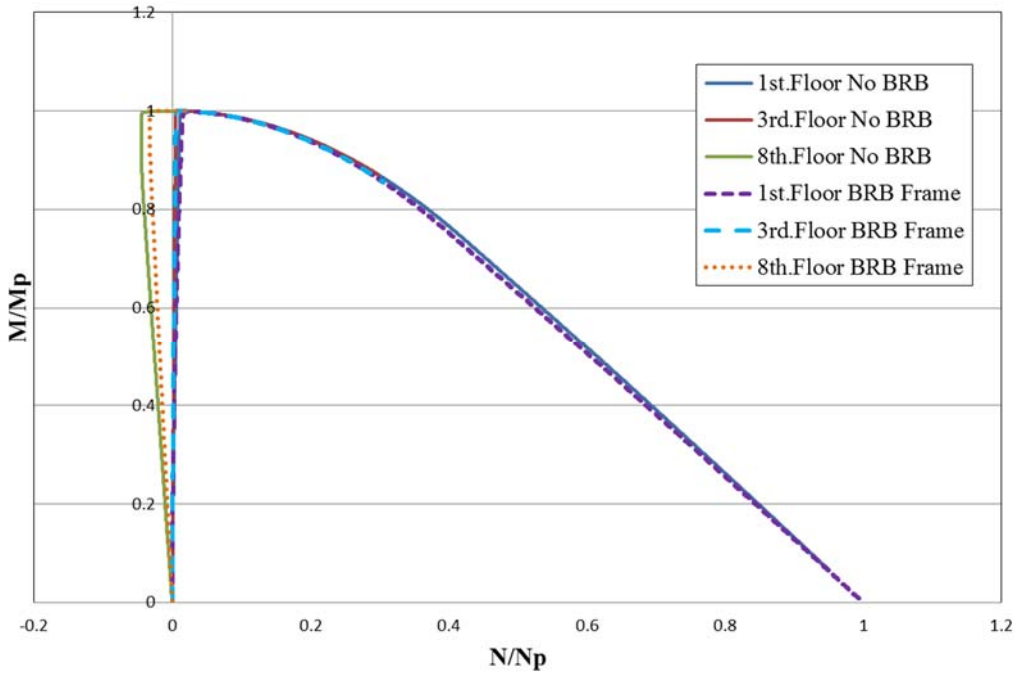

Figure 5-7: Effect of Buckling Restrained Braces - Interaction Diagram

The results reveal that the behavior of the steel frames without braces is different from that ofbraced steel frames. Figure 5-4 shows that the 1st, 3rd and 8th floors of the bare steel frame behave similarly. The three cases reach the plastic collapse load at a relatively low vertical deflection of about 0.2d. Afterwards, a transition from flexural behavior to catenary behavior starts occurring leading to significant vertical deflection in the beams. The beams reach $1.9P_c$ at a midspan vertical deflection of about 3d. Figure 5-4 shows that the beams of the braced steel frame can sustain higher load carrying capacity than the cases without BRBs (about 1.12 times). It was also noticed that the three beams of the braced frame behaved similarly. It was observed that the behavior of beams of the braced frames started deviating from that of the bare steel frame beams at a vertical deflection of about 1.5d, this is when the BRBs' contribution started impacting the overall load carrying capacity of the frame.

Figure 5-5 shows that the bare steel frame is behaving differently from the braced steel frame. However, unlike the load carrying capacity plot, there is a difference between the three floors of the bare steel frame. For the 1st floor bare steel frame, the beam develops an axial force of about $0.95N_p$ at 3d, while for the 8th floor it hardly develops any axial force at 3d. On the other hand, the steel frame with BRBs behaves in a different way. While the 1st floor develops an axial force of about N_p at 3.75d, the 3rd floor develops an axial force of about $0.3N_p$ at 3.75d. Finally, the 8th floor barely develops tension at all. This phenomenon can be attributed to the contribution of BRBs in the lateral steel frame. When the first floor double span beam starts deflecting, the beams of the other stories start deflecting at the same rate. As a result, the BRBs start developing axial forces. As the

forces move up the frame, the impact of BRBs starts building up, leading to development of compression rather than tension on the top floor.

Figure 5-6 and Figure 5-7 show similar trends. They show that while the 1st floor of the braced steel frame starts developing catenary action and actually reaches pure catenary action (when M=0 and $N=N_p$), the bare steel frame cannot achieve similar axial forces. It can be observed that only the first floors of the bare and braced steel frames came close to achieving pure catenary action. The other floors of the two frames did not come close to reach Np. This is due to the fact that the constraint from adjacent side frames decreases significantly with the height. The BRBs basically magnify this effect.

Figure 5-8 is a close up of the eight story frame. It shows the double span beam, the columns and the BRBs at these specific joints. Figure 5-9 shows the axial forces in the BRBs for each floor. The results indicate that the BRBs of the first and second floors get the most axial force when compared to the other struts due to the fact that those BRBs are subjected to the largest lateral force demands. On the other hand, the BRBs of the 8th floor are subjected to the least amount of lateral forces.

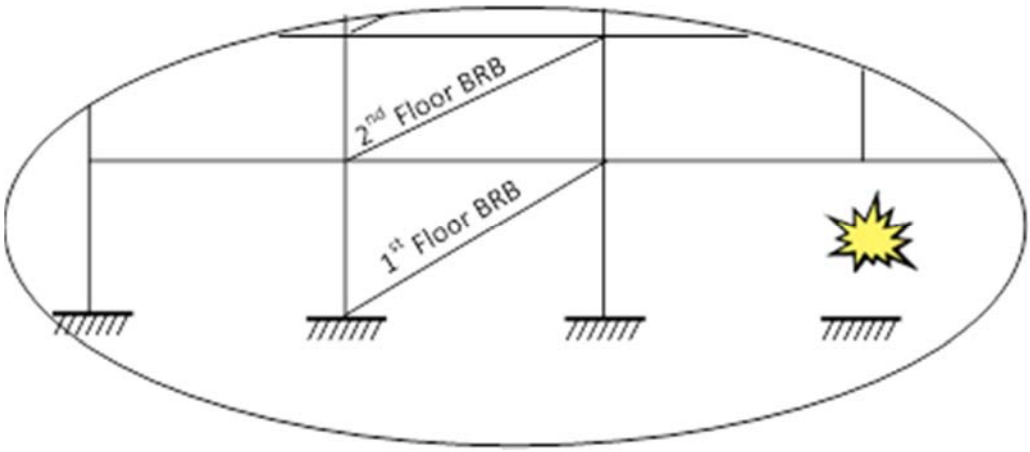

Figure 5-8: Close up of the BRBs & the Beam

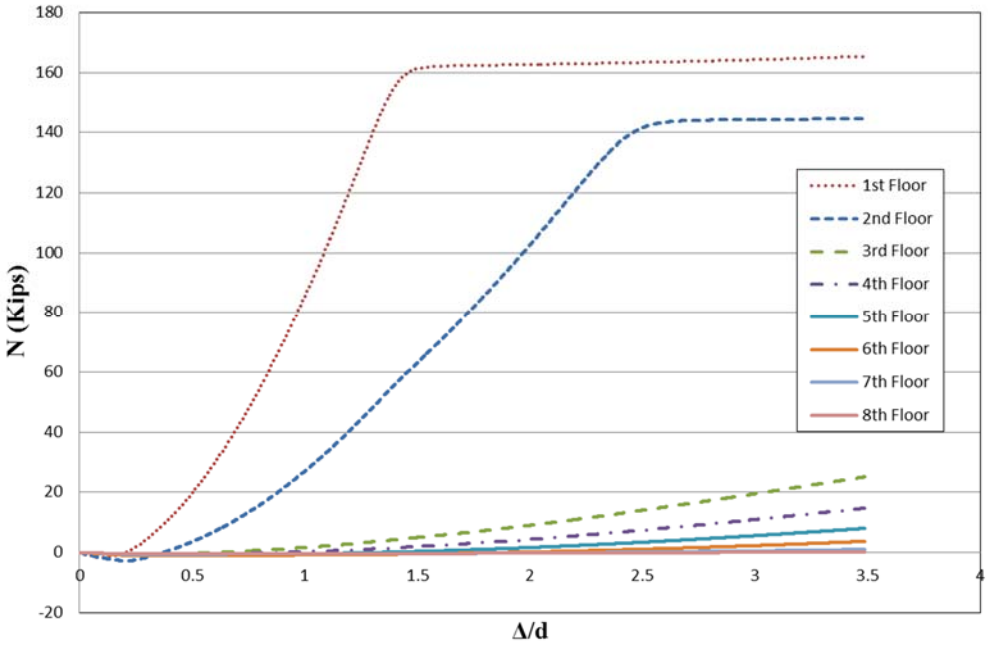

Figure 5-9: Forces in BRBs - Axial forces versus Mid-span Deflection

5.3 Effect of Building Height

Three, five, and eight story braced steel frames were analyzed in order to study the impact of building height on the results. The three steel BRB braced frames that were designed are shown in Figure 5-10. The steel sections for the three and the five story steel frames are presented in Figure 5-11. All the frames were designed for the same seismic hazard as the eight story frame.

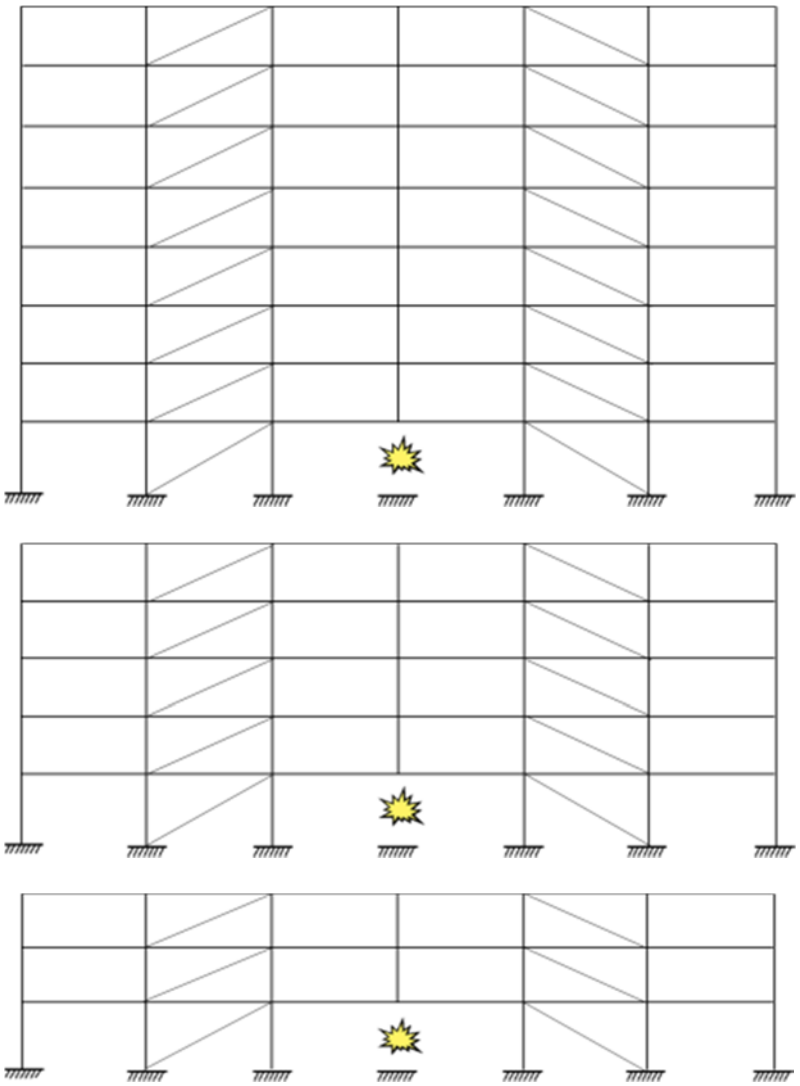

Figure 5-10: Eight, Five and Three Story Frames with BRBs

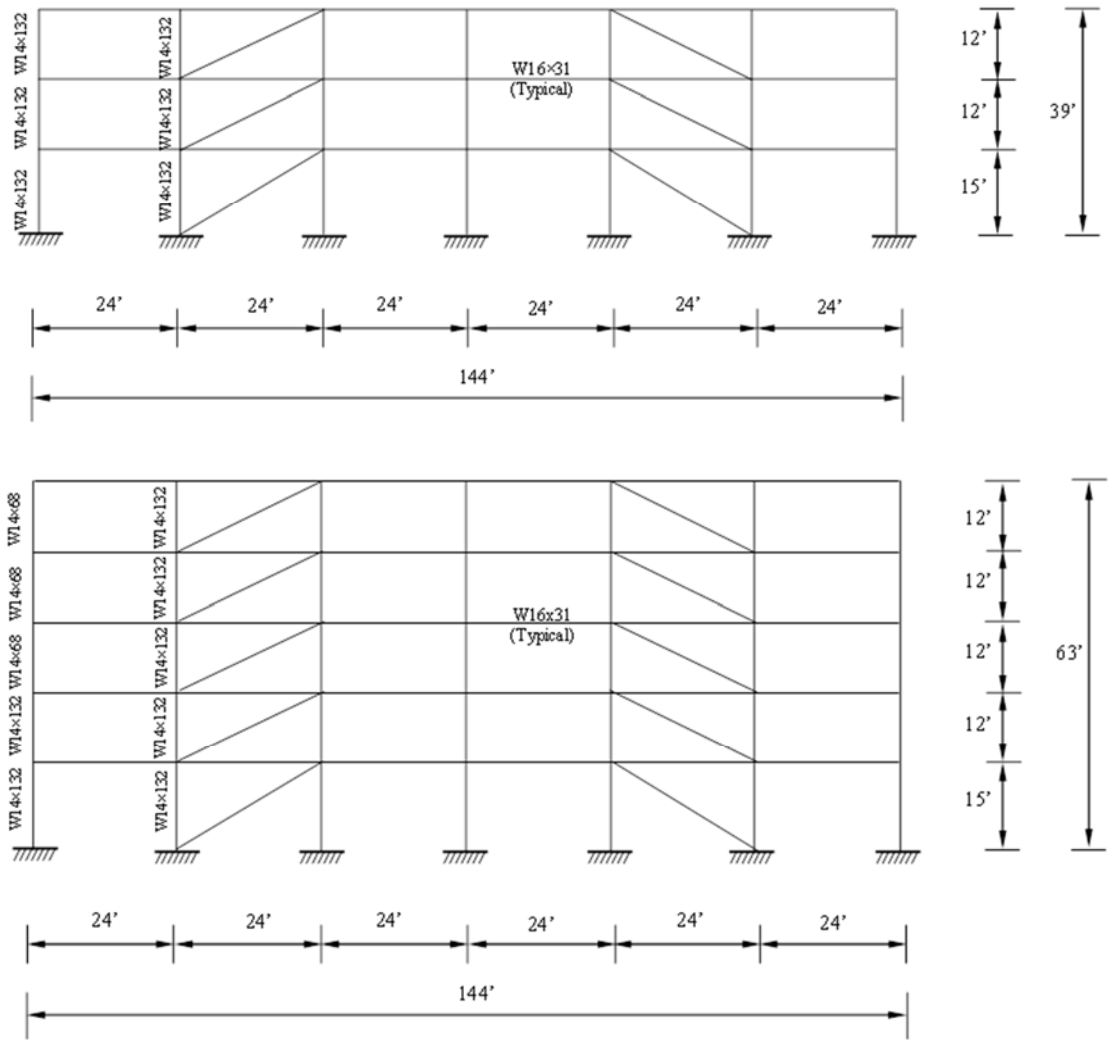

Figure 5-11: Three and Five Story Steel Frame Elevations

The story height is not identical throughout the frame height (the first floor height is different from the rest of the floors), and the column size changes from one frame to the other. Table 5-2 shows the areas of the BRB cores (A_c) and non-yielding (A_{ny}) segments that were used for the three and five stories frames. The three frames were modeled in OpenSees and were subjected to a concentrated load at midspan of the first story beam.

The behavior of the first story beams of each frame was monitored. The axial forces and moment at the ends of the first story beams are presented in Figures 5-13 through 5-15.

Table 5-2: Area of BRBs for the Three and Five Story Frames

	Three Story Frame		Five Story Frame	
Brace	**$A_c(in^2)$**	**$A_{ny}(in2)$**	**$A_c(in^2)$**	**$A_{ny}(in2)$**
5th Floor	-	-	1.00	5.00
4th Floor	-	-	2.00	10.00
3rd Floor	1.00	5.00	3.00	15.00
2nd Floor	2.00	10.00	3.50	17.50
1st Floor	2.50	12.50	4.00	20.00

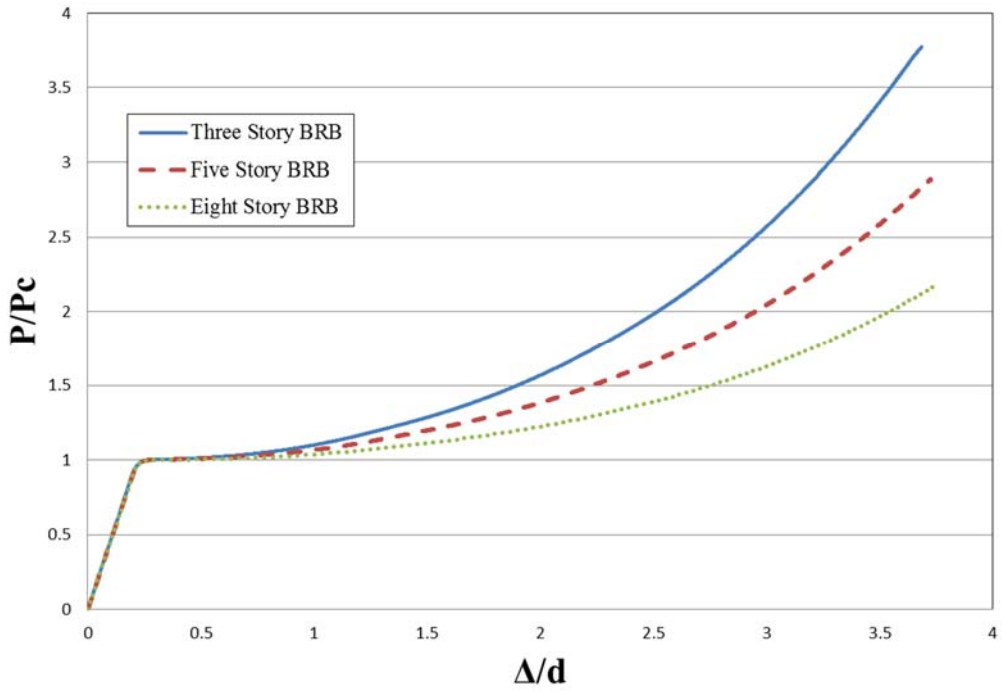

Figure 5-12: Effect of Building Height - Vertical Load versus Deflection

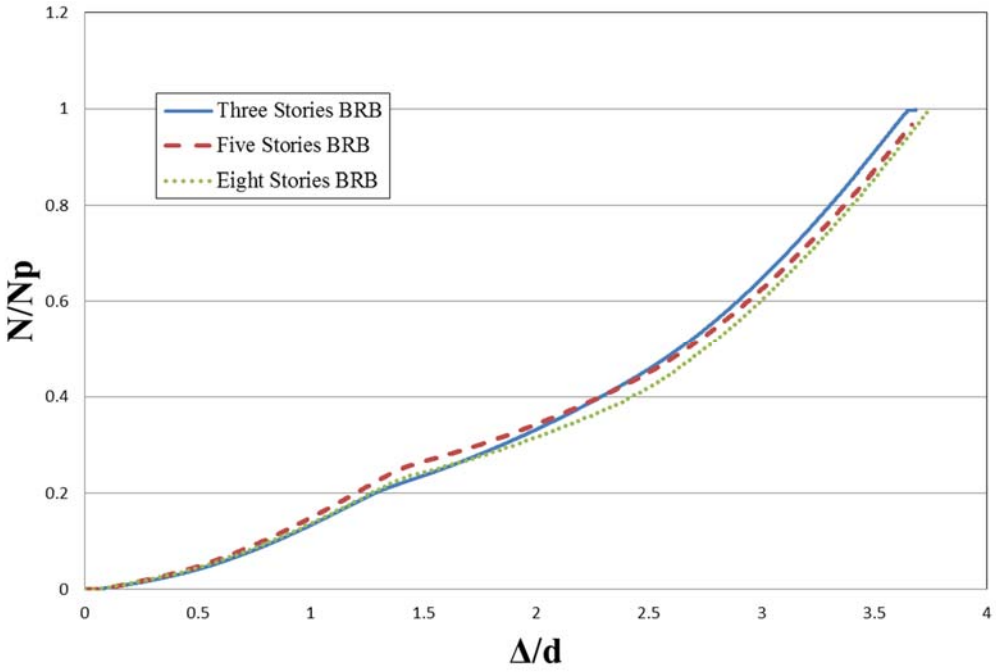

Figure 5-13: Effect of Building Height - Axial Force versus Deflection

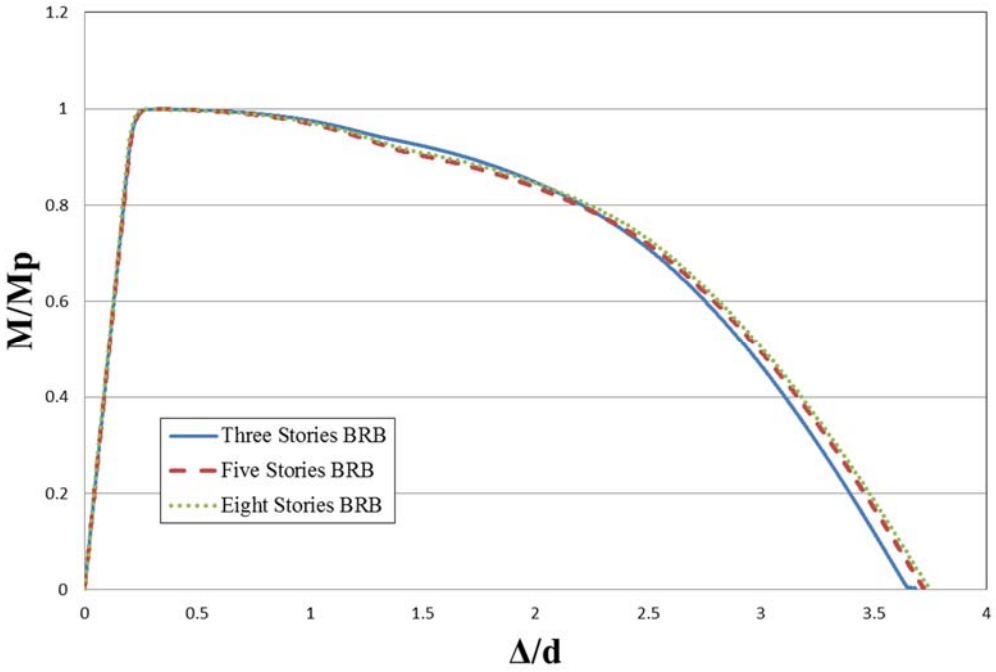

Figure 5-14: Effect of Building Height - Moment versus Deflection

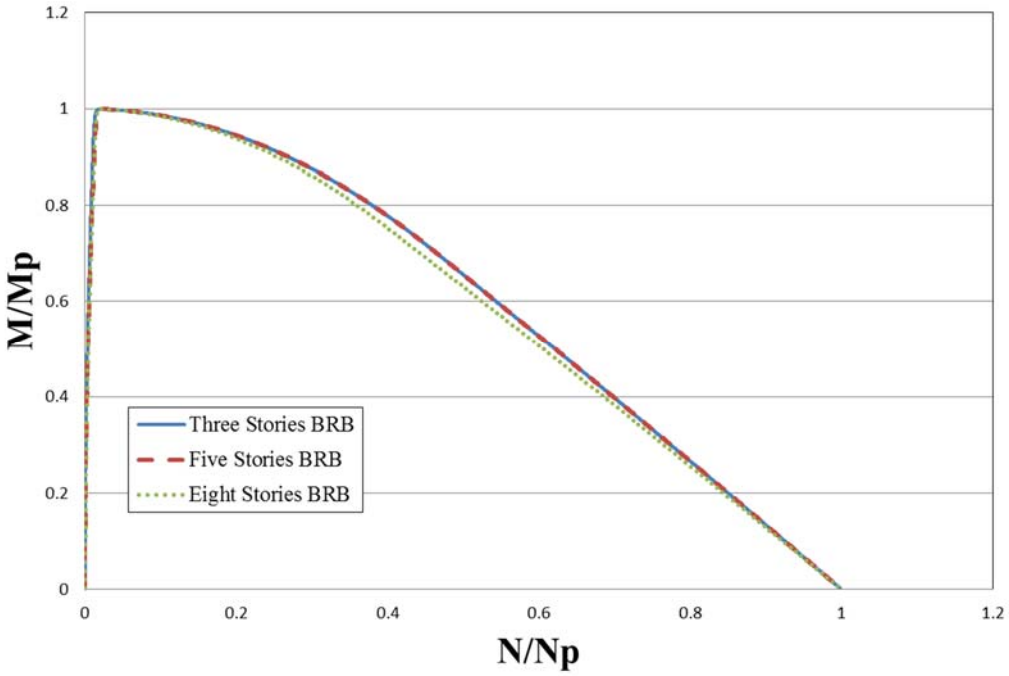

Figure 5-15: Effect of Building Height - Interaction Diagram

Figure 5-12 shows the load carrying capacities of the different frames based on the behavior of the first floor beam in each frame. It can be observed that the load carrying capacity (as a fraction of the flexural plastic collapse load of the frame) decreases as the frame height increases. It is also noted that all the frames shared similar load carrying capacities in the beginning. However, as the deflection increased, the three frames started behaving differently due to the impact of the side frames and BRBs. So, as the frame height increased, the impact of the adjacent lateral load resisting frame and BRBs became less significant.

Figure 5-13 and Figure 5-14, showed the generated axial forces and moments at the beam ends of the first floor beams of the three, five and eight story frames. The first floor beams for all the frames were able to achieve full catenary action (i.e. N gets to N_p and M gets to zero). This means that the beams generated significant catenary forces in the

adjacent lateral load resisting frames. The plots show that the beams of the three frames behave similarly. This suggests that the frame height did not have a significant impact on the developed axial forces and moments at the beams ends. Figure 5-15 shows the interaction diagram at the beam ends of the first floor beam in the three frames. The results are in agreement with previous plots. The three frames behave in a similar manner as they get to plastic hinge formation at the same point ($M=M_p$), and then get to full catenary action together.

5.4 Effect of BRB Placement

To account for the impact of BRB placement, two additional scenarios for the five story steel frame, and the original BRB braced frame, were considered. The three different scenarios are shown in Figures 5-16 through 5-18. Scenario 1 represents the case where there are BRBs in the second and fifth bays only. Scenario 2 represents the case where there are BRBs in the all the bays except the bays above the removed column. Scenario 3 is the case where there are BRBs in the middle bays only (above the removed column). In the third scenario, there were no BRBs in the ground floor because it was assumed that the damage will destroy the column and the braces. The three frames were designed for the same base shear.

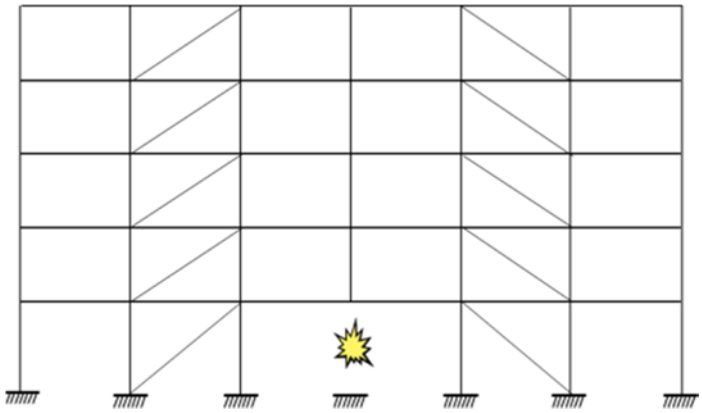

Figure 5-16: BRB Placement Scenarios – Scenario 1

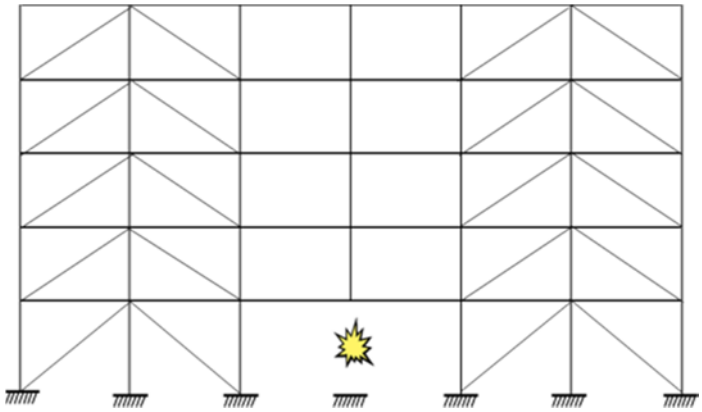

Figure 5-17: BRB Placement Scenarios – Scenario 2

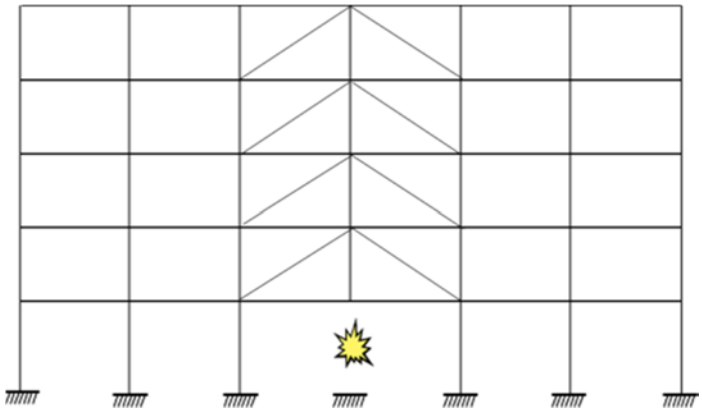

Figure 5-18: BRB Placement Scenarios – Scenario 3

The three BRB placement scenarios were analyzed in OpenSees to understand the impact of BRB placement on the results. The results of the first story double span beams from the three scenarios, and the bare steel frame, are plotted in Figure 5-19 through 5-22.

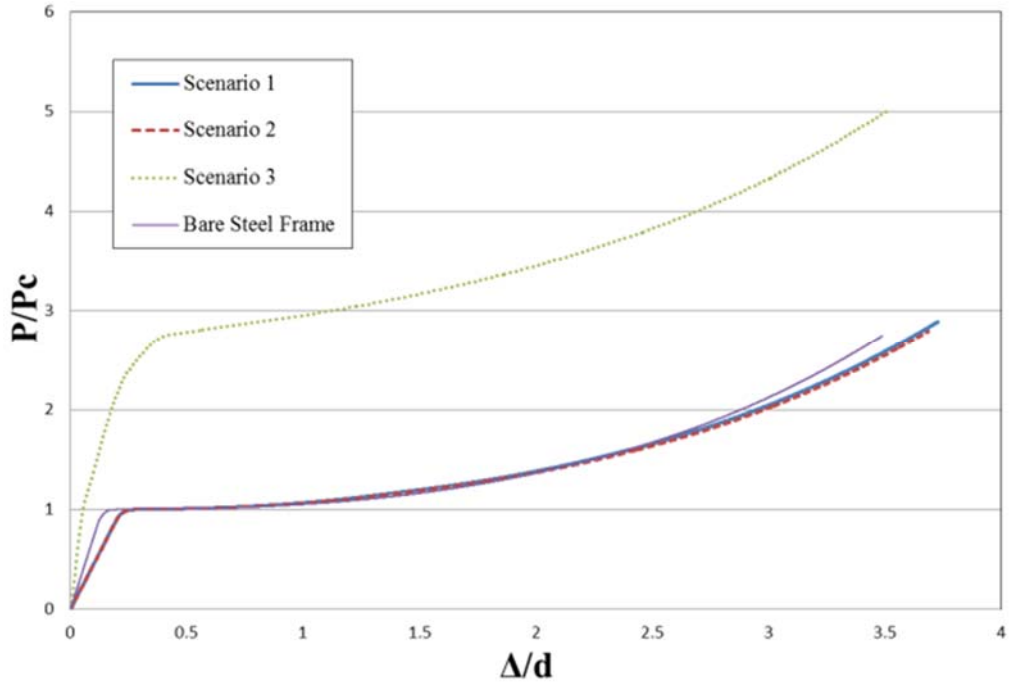

Figure 5-19: Effect of BRB Placement - Vertical Load versus Deflection

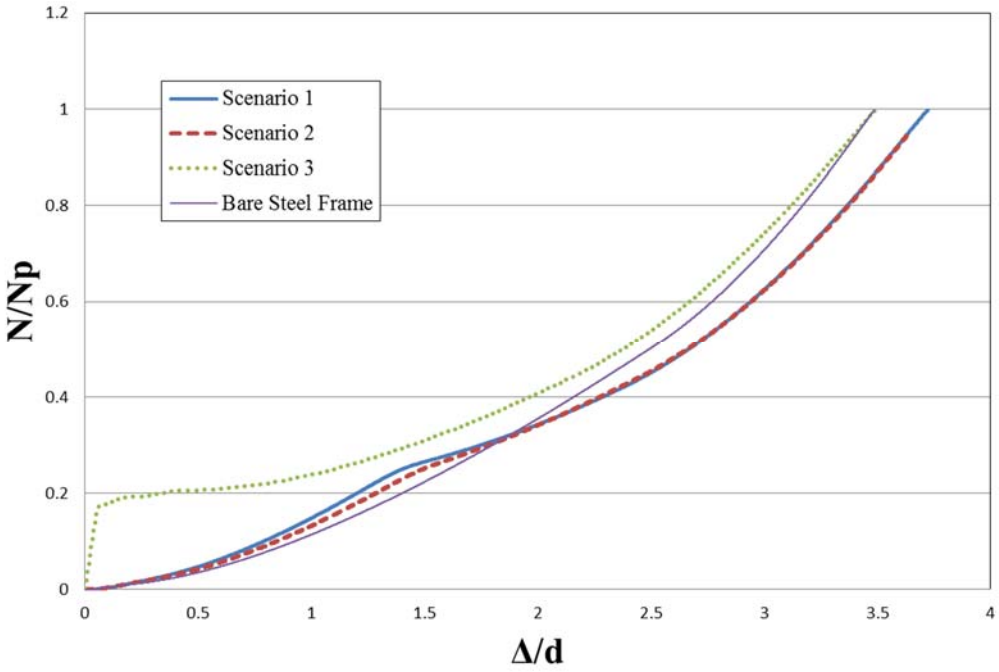

Figure 5-20: Effect of BRB Placement - Axial Force versus Deflection

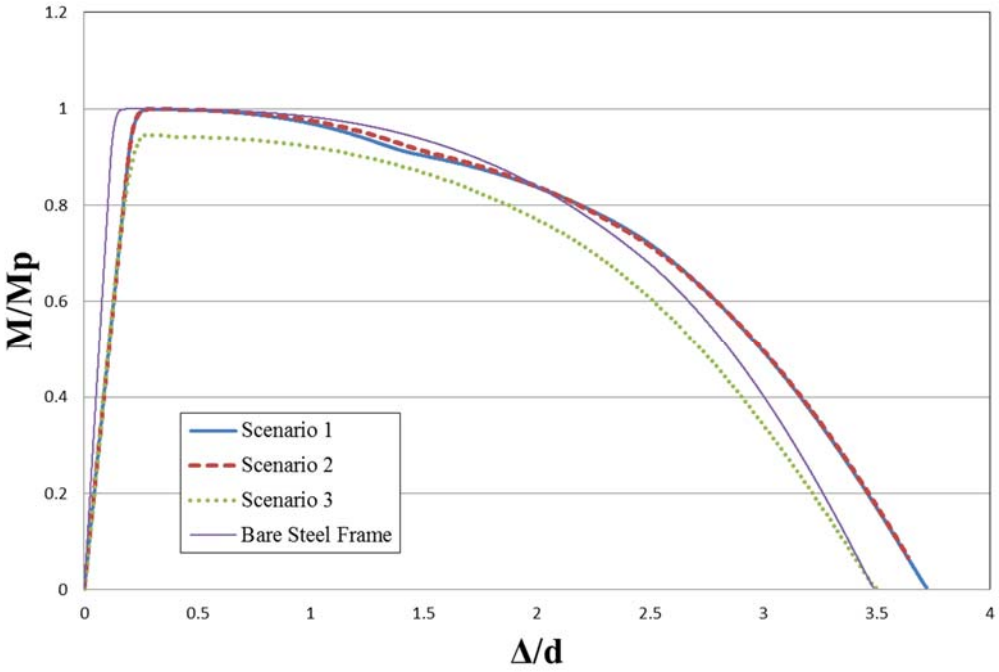

Figure 5-21: Effect of BRB Placement - Moment versus Deflection

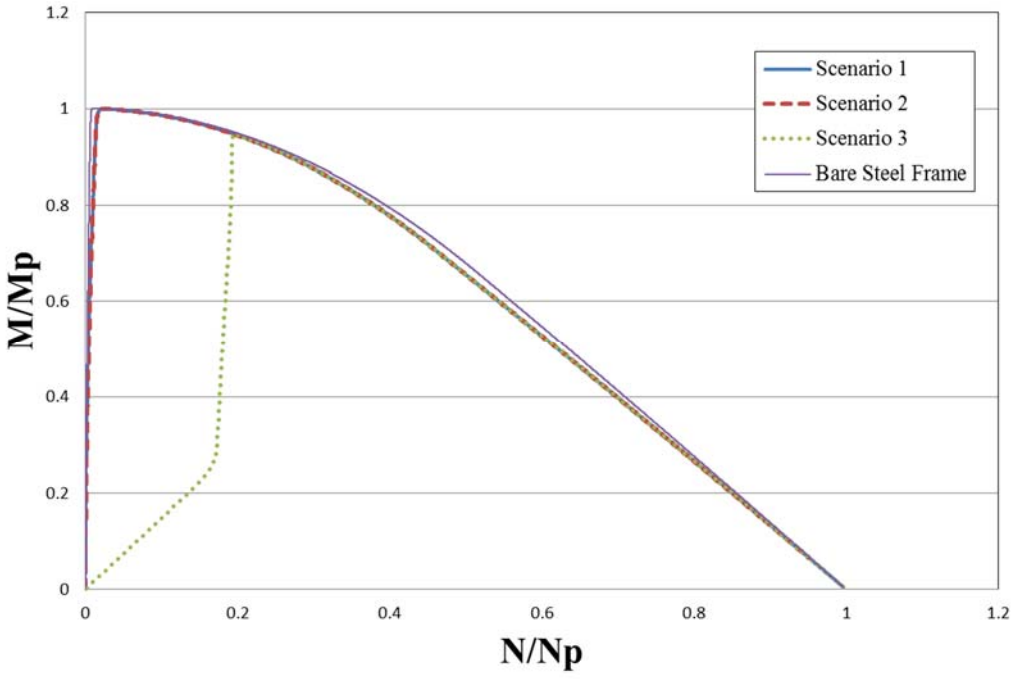

Figure 5-22: Effect of BRB Placement - Interaction Diagram

Figure 5-19 shows the load carrying capacity of the three steel frames with the different BRB placements and that of the bare steel frame. It shows that the beams behave differently based on the placement of the BRBs. While the response of the first and second scenarios are almost identical, the third scenario has a different load carrying capacity from the other two scenarios. The first and second scenarios reach a load carrying capacity of about 2.8 P_c at a midspan deflection of about 3.6d, while the third scenario reaches about 5 P_c at a midspan deflection of about 3.5d. This wide range of results highlights the impact of BRB placement on overall frame behavior. The difference between the scenarios can be attributed to the role played by the BRBs above the double span beam. Those BRBs resisted the additional loads resulting from the column loss and transferred the loads to the lateral load resisting system. Therefore, removing those BRBs (in the middle bay) limited the ability of the frame to carry loads (Adding BRBs in the middle bay increased the load

carrying capacity of the frame by about 44%). However, the first and second scenarios were slightly more flexible than the third scenario (i.e. had higher midspan deflections). These observations lead to the conclusion that placing BRBs above the damaged or removed column has a far greater impact on the overall frame resistance than placing the BRBs in other bays. This conclusion is reinforced by the fact that the first and second scenarios behaved similarly to the bare steel frame case, as shown in Figure 5-19.

Figures 5-20 through 5-22 show the generated axial forces and moments at the beam ends of the first floor beam for the three scenarios. Observations of the rate of axial force development in the side frames shown in Figure 5-20, helps to clarify the beam behavior. The first and third scenarios achieved full catenary action. However, the third scenario experienced a sudden and early increase in axial force at the beam ends compared to the other two scenarios. The other two scenarios experienced a steady increase in the axial force in the double span beam. The third scenario reached N_p at a midspan deflection of about 3.5d, and the first scenario reached N_p at a midspan deflection of about 3.7d. The second scenario failed to get to full catenary action (stopped at $N= 0.95N_p$). Finally, the bare steel frame started developing axial forces similar to the first and the second scenarios. However, the bare steel frame reached Np at the same midspan deflection of the third scenario. The response of the first and second scenarios was almost identical because there are no BRBs in the middle bay resulting in similar constraints on the frame. However, the fact that there were four bays of BRBs compared to two bays of BRBs in the first scenario explains why the second scenario failed to get to Np while the first scenario did. For the third scenario, the BRBs were located in the middle bays(on top of the double span beam) which is why, unlike the other two cases, the beam ends started picking up axial forces

right away. This result was presumably due to the fact that the BRBs were part of the axial response from the beginning. In other words, the presence of the BRBs in the middle bays led to early participation of the double span beams due to the truss action of the BRBs. However, the BRBs in the middle bays led to a limitation on the flexibility of the frame. The third scenario reached Np at a midspan deflection of 3.5d, unlike the first scenario that reached Np at a midspan deflection of 3.7d.

The bare steel frame behavior can be explained as well. As was observed from Figure 5-19, the bare steel frame beam behaved similarly to the first and the second scenarios, but as the axial forces increased in the beam the side frames offered lower restraint than that of the first and the second scenarios leading to full catenary action in the beam at vertical deflection of 3.5d.

Figure 5-21 and Figure 5-22 show the generated moment at the beam ends versus the midspan deflection and the interaction diagram at the beam end. The plots show that the first and second scenarios got to plastic hinge formation, and the third scenario was on the same track, however it couldn't get to the plastic hinge formation point due to the presence of BRBs in the middle bays as explained earlier. The same conclusions can be drawn from the interaction diagram.

5.5 Effect of Loading Type

In order to model the missing column scenario in the steel frame, a concentrated load was applied to the midspan point of the double span beam in all the previous models. The concentrated load was equivalent to the plastic collapse load of the double span beam. In this section, an additional loading type was investigated. The additional load type was a

combination of concentrated and distributed loading. The distributed loading is specified by ASCE 7-10 as 1.2 times the dead load plus 0.5 times the live load as a proper loading combination for extraordinary events, which applies to this case. For the combined case, the same distributed and concentrated loads were applied together. The results of the two loading types for the five story steel frame are presented in Figures 5-23 through 5-25. For all these models, displacement control analysis was adopted. The displacement control was set at the mid span point of the first floor double span beam for all the models.

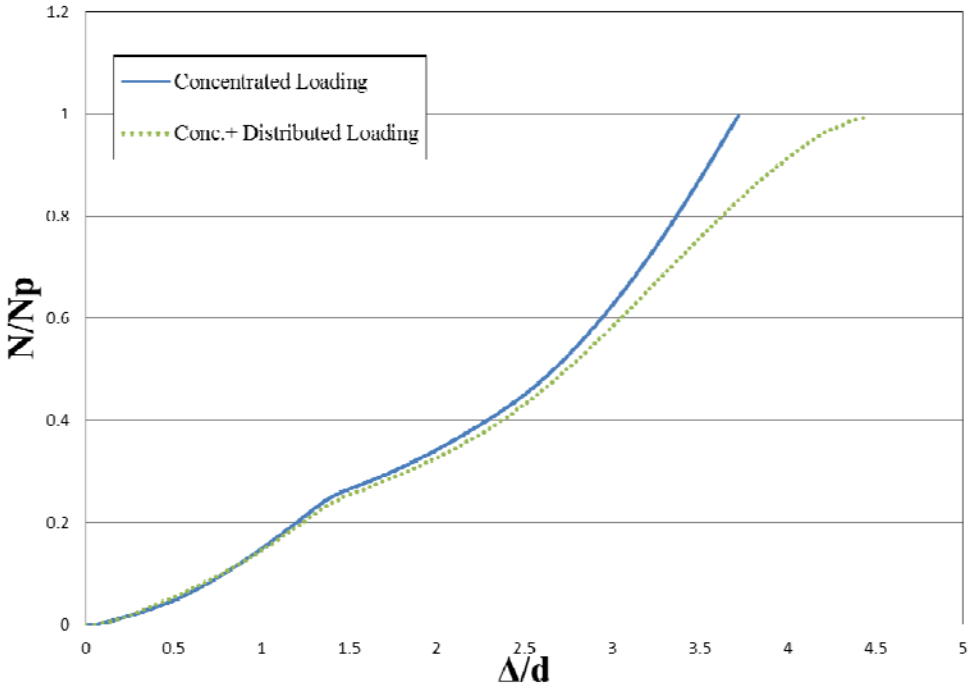

Figure 5-23: Effect of Loading Type - Axial Force versus Deflection

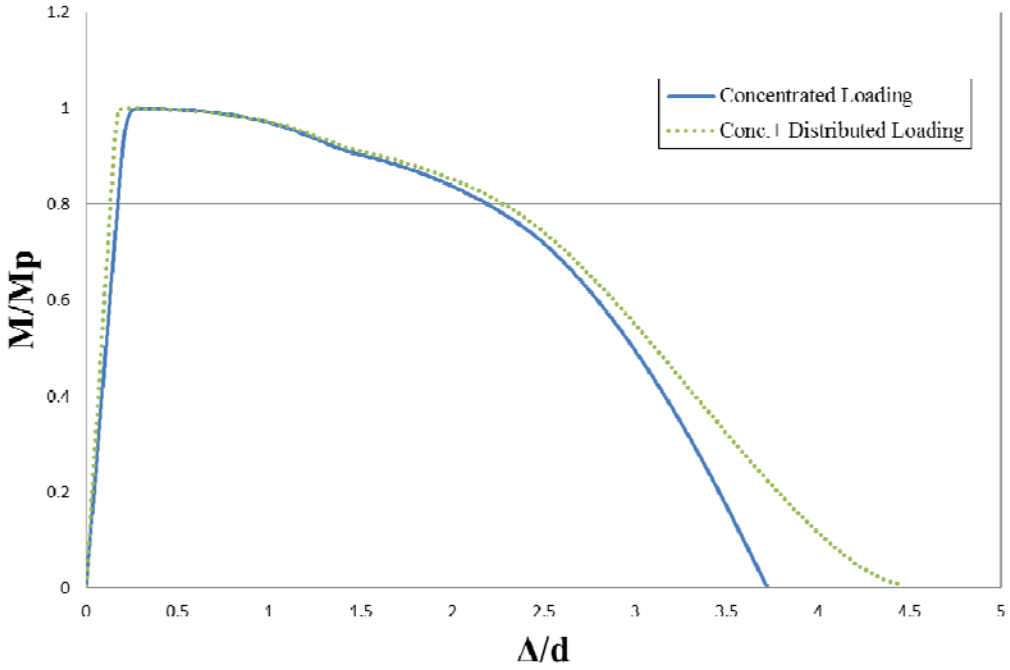

Figure 5-24: Effect of Loading Type - Moment versus Deflection

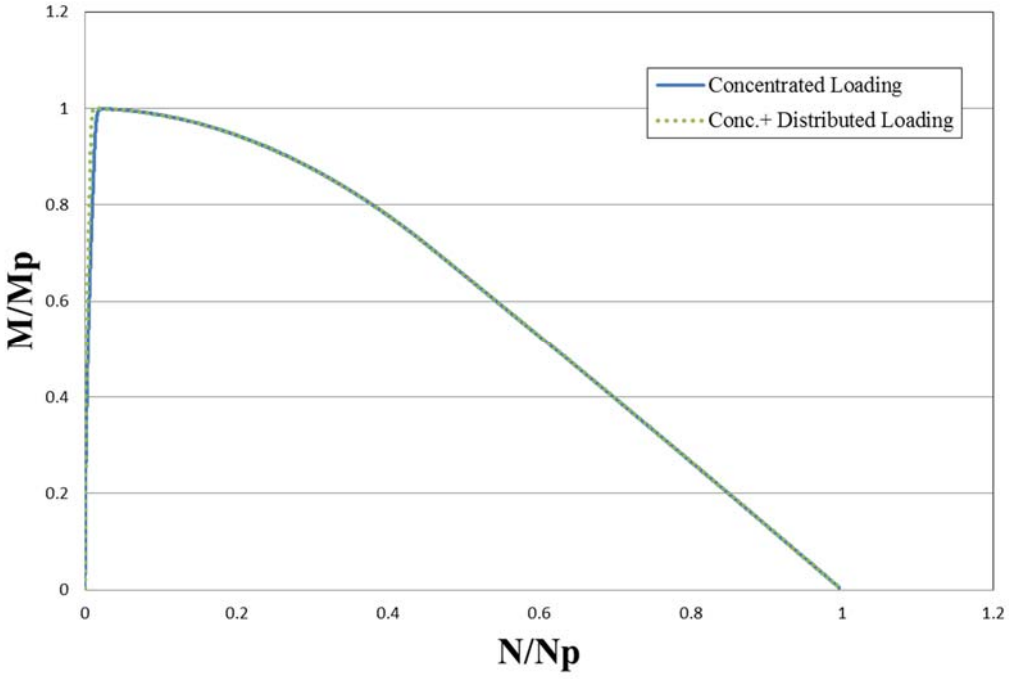

Figure 5-25: Effect of Loading Type - Interaction Diagram

Figure 5-23 shows the generated axial forces at the beam ends for the two loading types. The two loading types seemed to behave similarly up to a midspan vertical deflection of about 2.5d. Both loading types continued developing axial force all the way up to N_p. However, the combined case got to Np at a vertical deflection of about 4.5d, while the concentrated case got there at about 3.7d. The difference between the results can be attributed to the BRBs' contribution, the nature of the loading type, and the curvature of the double span beams. The combined loading started developing axial forces in a fashion similar to the concentrated loading type. However, the combined loading didn't stop generating axial load like the concentrated loading, because of the additional distributed loading it continued to generate more axial load at the beam end.

Figure 5-24 and Figure 5-25 show the generated moment and the interaction diagram at the beam end. The two loading techniques managed to get to plastic hinge formation point ($M=M_p$). Additionally, the concentrated and the combined case managed to get to full catenary action. The concentrated loading case got to zero moment at a midspan deflection of 3.7d, while the combined case got zero moment at midspan deflection of 4.5d. Those results agree with conclusions from the axial force plot of the two loading types. This section underlines the role that the type of loading plays in generating catenary demands, and the manner in which the loading type can impact the axial forces and moments at the double span beam ends.

5.5 Conclusions

This study focused on understanding the impact of BRBs on catenary action in steel frames and the overall steel frame load carrying capacity. Push-down analyses of

three, five and eight story steel frames with different configurations were performed. An eight story steel frame with BRBs was compared to a bare steel moment frame. The load carrying capacity of the frames and the developed forces in the adjacent lateral load resisting frames were investigated. The role of building height and its effect on the results was studied. Finally, three different BRB placement scenarios in a five story steel frame and three loading types were considered to study the effect of BRB placement and loading types on the overall results.

The comparison between the BRB frame and the bare eight story frame indicated that the braced frame had a higher load carrying capacity than the bare steel frame. The data also showed that the side frames in BRB frames resist more force than the bare steel frame due to the fact that BRBs increase the lateral stiffness of the side frames. It was noticed that building height has a significant impact on the load carrying capacity of the frames. On the other hand, the building height has a negligible effect on the catenary action development. Furthermore, when results of varying BRB placement scenarios were compared, it was shown that the placement of BRBs in the middle double span bay significantly increased the load carrying capacity of the steel frame. On the other hand, when BRBs were removed from that bay only and were kept everywhere else in the structure, the steel frames behaved similarly regardless of the BRB placement scenario. Furthermore, having four or two bays of BRBs had virtually no impact on the load carrying capacity of the frame. Finally, it was shown that loading type had a significant impact on the developed catenary forces. In conclusion, the findings of this study highlight the importance of accounting for the BRBs when calculating the developed

catenary action forces in the adjacent lateral load resisting systems. This will ensure more accurate and efficient design of the overall structure.

The conclusions of this study were based on the assumptions made in this dissertation and on the limited number of building heights and BRB placement scenarios that were presented. Hence, the conclusions in this study are limited to the scope of the research.

Chapter 6: Catenary Action in Steel Framed Structures with Concrete Slab

6.1 Overview

This chapter focuses on the contribution of the concrete slab to catenary action development in the steel beams and overall load carrying capacity of the structure. In the previous two chapters, the concrete contribution was not accounted for in the analysis of the steel frames with AAC infill and Buckling Restrained Braces. In this chapter, light is shed on the possible contribution of the concrete slab and how it may change the forces in the beams and adjacent lateral load resisting systems. Concrete slabs are very common in residential and commercial steel framed buildings. The interaction between AAC, BRB and concrete slabs in steel frames is also covered in this chapter.

6.2 Catenary Action Development

An eight story steel frame was designed using the commercial software package SAP2000 (Habibullah 2013) to obtain the sections for the frame. The frame shown in Figure 6-1 was designed for Seismic Design Category A (Atlanta, GA) with S_{DS} equal to 0.1447 and S_{D1} equal to 0.056. The design loads for the frame were determined based on the Minimum Design Loads for Buildings and Other Structures, ASCE (2010). A W16x26 section was chosen for all the beams in the frame to rule out the impact of beam variation on the development of catenary action along the height of the frame.

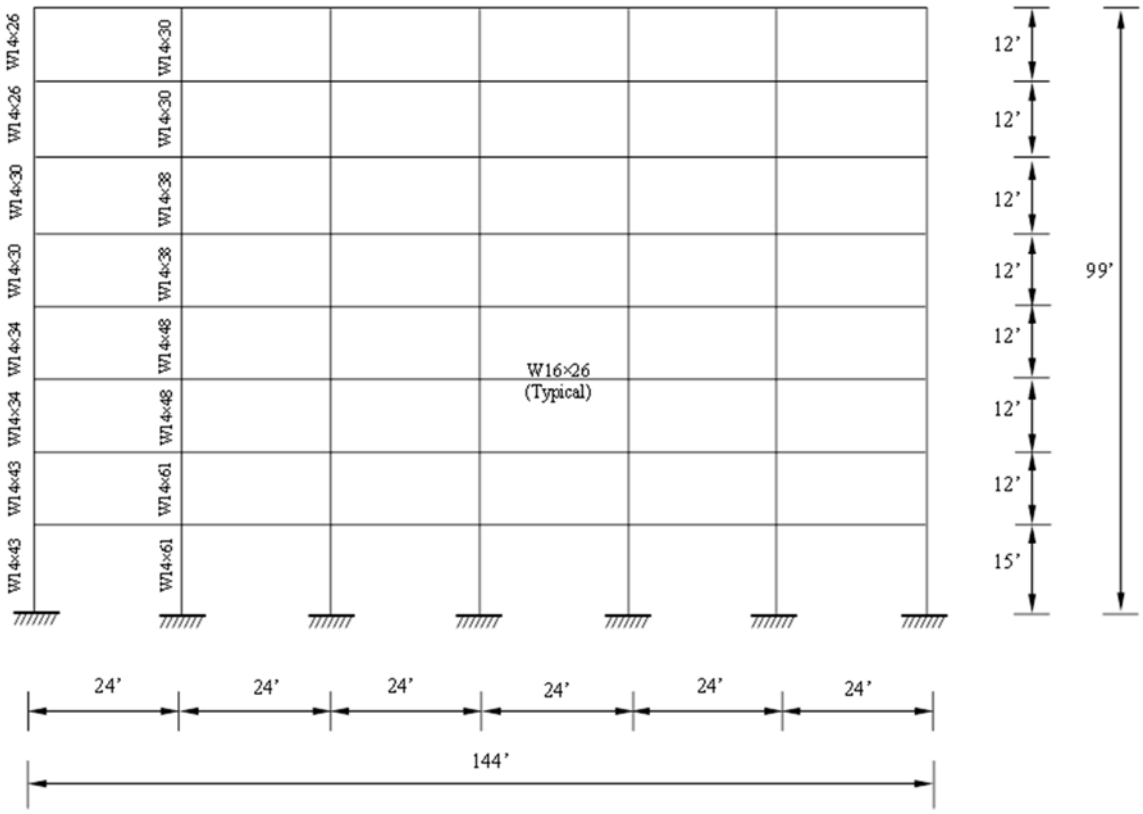

Figure 6-1: Eight Story Steel Frame Elevation

In order to study the impact of the concrete slab on catenary action demands in steel frames, two steel frames were analyzed using OpenSees. One was a bare steel frame while the other was steel frame with concrete slabs. In order to address progressive collapse, an interior bottom-story column was removed to simulate the missing column scenario. The two frames were subjected to a concentrated load at point "A" and were analyzed to study the difference between the case with and without concrete slabs. Figure 6-2 shows the elevation of the steel frame without and with concrete slabs. In Figure 6-2, point A is located directly above the removed column (mid-point of the double span beam at the first floor). Point A was highlighted because some of the data in the following sections was measured at this point.

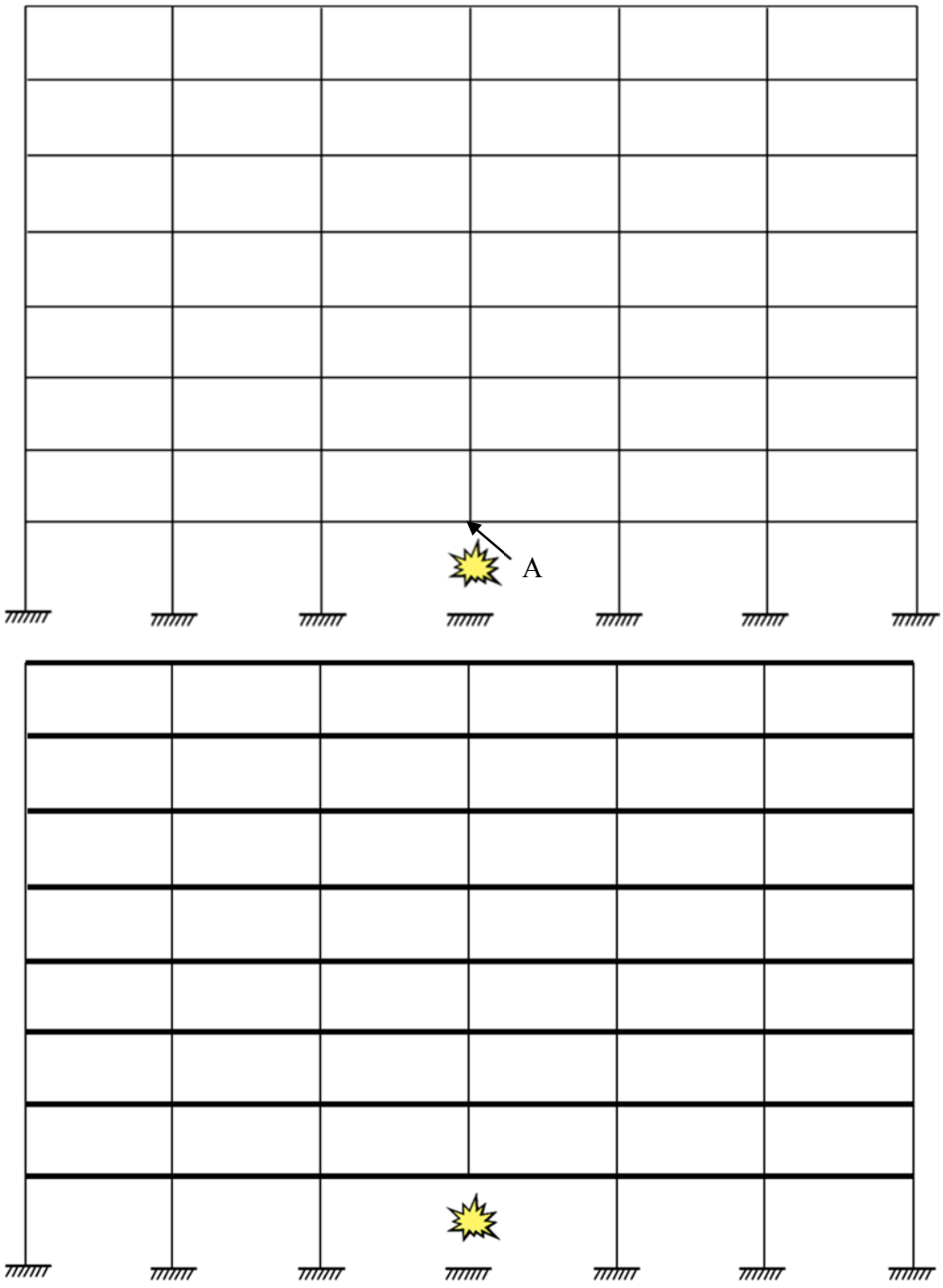

Figure 6-2: Eight Story Steel Frame without and with Concrete Slab

6.2.1 Analysis Results

Figures 6-3 through 6-8 show normalized plots of vertical load P, at point A, axial force N and bending moment M at the double span beam end. It was decided to monitor P, N and M at those locations in order to determine the load carrying capacity of the structure and the demand on theadjacent lateral load resisting system. The Conc. S models represent the steel frame with a concrete slab thickness of 8 inches and effective width of 72 inches. The Conc. W models represent the steel frame with a concrete slab thickness of 4 inches and effective width of 36 inches.

Vertical deflection Δ is measured at point A in Figure 6-2. In Figure 6-3 and Figure 6-4, the vertical load is normalized with respect to the flexural plastic collapse load, P_c, given as:

$$P_c = \frac{4M_P}{L} \tag{1}$$

where L is the span length of a single bay in the steel frame and M_p is the plastic yielding moment of the steel beam section. The axial force and moment are normalized with respect to plastic axial force, N_p, and plastic bending moment M_p, respectively. The vertical deflection is normalized with respect to the section depth, d.

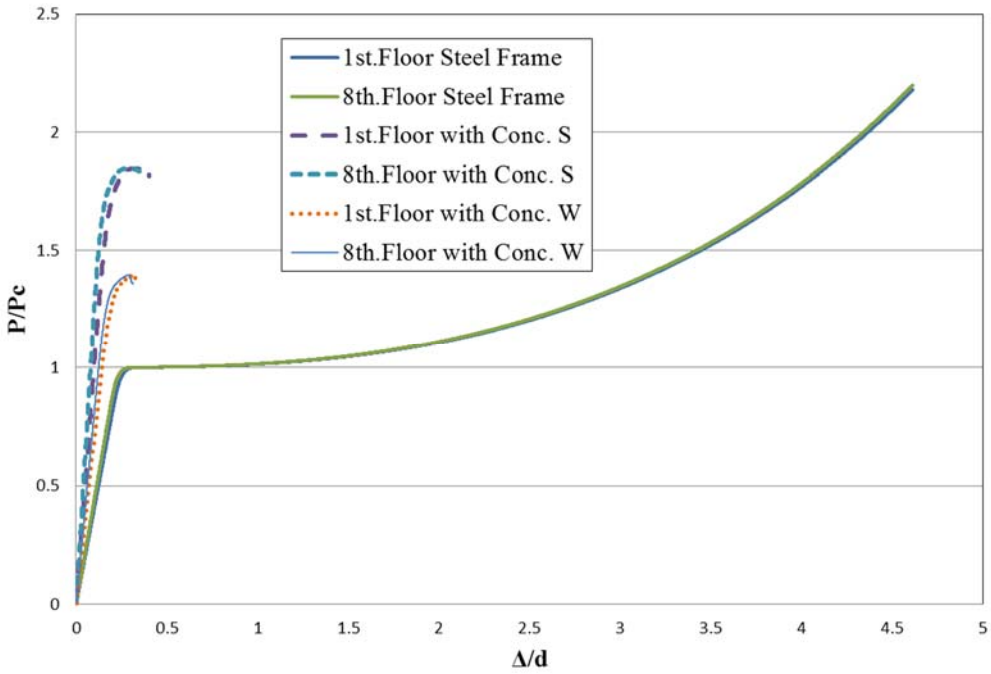

Figure 6-3: Effect of Concrete Slab - Vertical load with & without Concrete Slabs

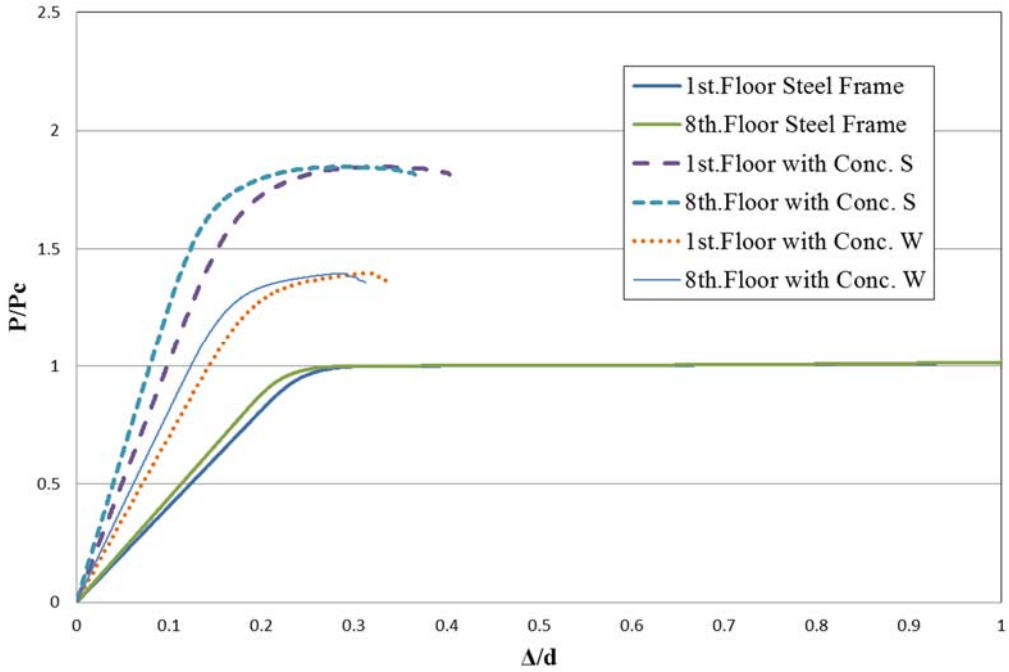

Figure 6-4: Vertical load with & without Concrete Slabs – Expanded View

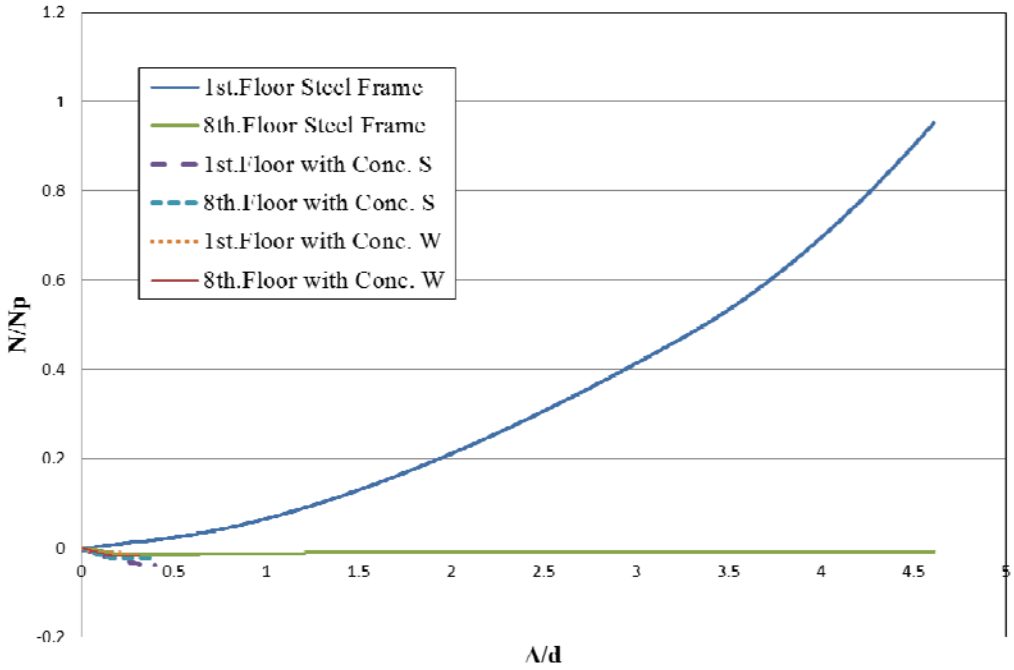

Figure 6-5: Axial force with & without Concrete Slabs

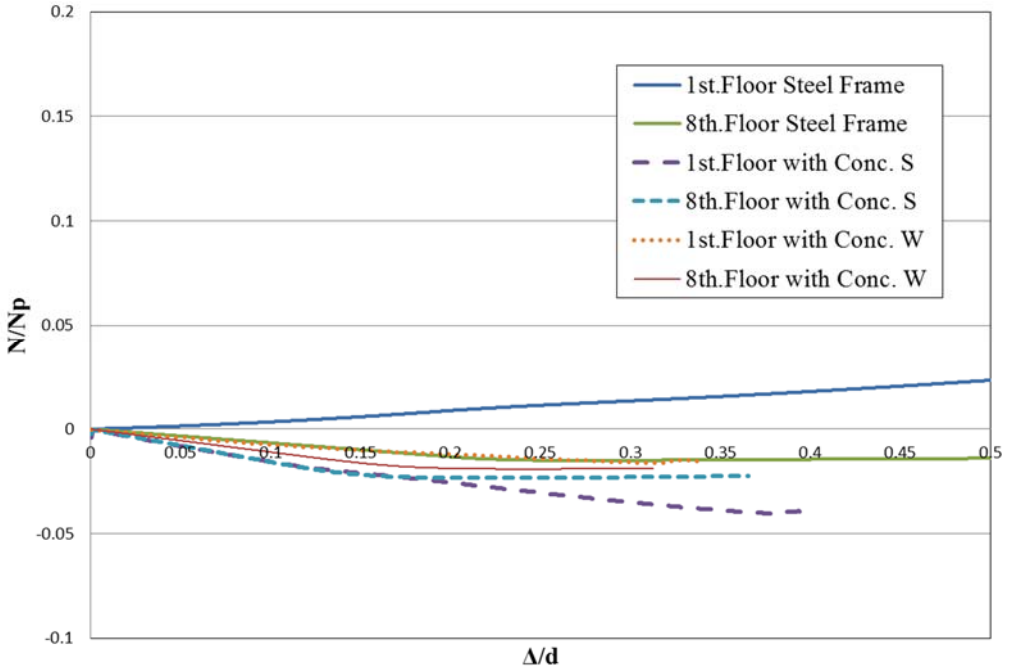

Figure 6-6: Axial force with & without Concrete Slabs - Expanded View

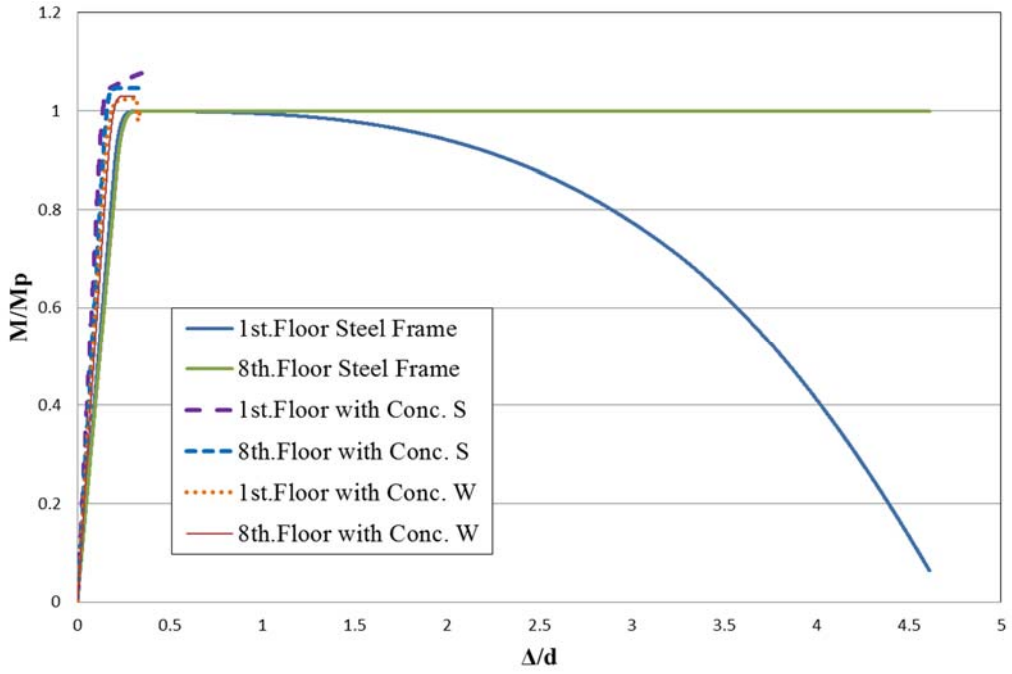

Figure 6-7: Moment versus Deflection

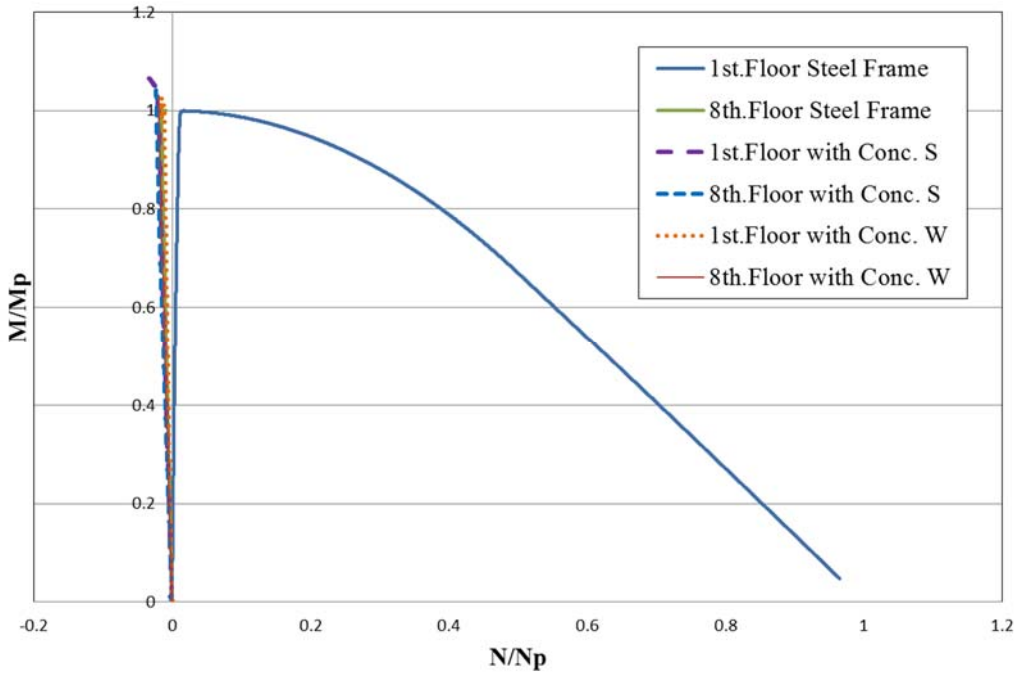

Figure 6-8: Moment versus Axial Force

Figures 6-3 through 6-8 show a comparison between the bare steel frame and the frame with concrete slabs. The results of the 1st, 3rd and 8th floors for the two frames are presented in three sets of figures to focus on the concrete slab contribution. Figure 6-3 and Figure 6-4 plot the vertical load P versus deflection at point "A" with different ranges of deflection. Figure 6-5 and Figure 6-6 plot the axial force at the beam end versus deflection at point "A". Figure 6-7 and Figure 6-8 plots the moment at the beam end versus deflection at "A" and axial force at the beam end. In order to highlight the difference in behavior of the floors with four and eight inch slab thicknesses, Figure 6-4 and Figure 6-6 were generated.

Figures 6-3 through 6-8 show that the concrete slabs have a significant impact on beam behavior. Figure 6-3 shows that the 1st and 8th floors of bare steel frame behave similarly. The two cases reach the plastic collapse load at a relatively low vertical deflection of about 0.25d. Afterwards, a transition from flexural behavior to catenary behavior starts occurring, leading to significant vertical deflection in the beams. The beams reach $2P_c$ at a midspan vertical deflection of about 4.5d. Figure 6-3 shows that a steel frame with concrete slabs can sustain higher load carrying capacity than the bare steel frame. Those high levels of load carrying capacity are achieved at very low deflection levels (about 0.2d). However, the bare steel frame can sustain loads for a deflection up to 4.5d compared to the steel frame with concrete slabs whose deflection only reached 0.4d.

It was observed that the floors with an eight inch concrete slab (1st & 8th floors) had approximately 1.3 times as much load carrying capacity as the 1st and 8th floors with four inch concrete slab frame as shown in Figure 6-4.

Figure 6-5 and Figure 6-6 show that the two steel frames with concrete slabs behave in a completely different way than the bare steel frame in regards to axial force development. While the 1st floor of the bare steel frame nearly reaches full catenary action, all the other floors are in compression rather than tension. The 8th floor of bare steel frame hardly develops any axial force at 4.5d due to the fact the generated axial forces in the steel frame diminish with height because of the contribution of the other floors and columns. However, the two steel frames with concrete slabs generate only compression, with no tension on either of the floors. Actually, the 1st floor eight inch slab develops the most compressive force of any case. This phenomenon can be attributed to the contribution of concrete slabs in the steel frame. The concrete slab on top of the steel beam develops compression while the steel beam develops tension force as the double middle span beam deflect. The two actions lead to a limited axial force in the beams. The contribution of the concrete slab and the developed axial forces is covered in detail in Figure 6-9.

Similar conclusions can be drawn from Figure 6-7 and Figure 6-8. They show that the bare steel frame starts developing catenary action at relatively small deflections and almost reaches pure catenary action (1st floor) when M=0 and $N=N_p$. However, the steel frames with concrete slabs can't achieve similar axial forces. Actually, the steel frames with concrete slabs achieve moments higher than the plastic collapse moment due to the existence of the concrete slab. In fact, a steel frame with concrete slabs, even with the limited deflection range, will be able to sustain more load than the bare steel frame due to the ductility and connections' limitations. This contributes to a higher load carrying capacity for the whole building.

Figure 6-9 shows the contribution of the concrete slab by itself (without the steel beam) for the two slab thicknesses. Obviously, the stronger slab (thicker slab with wider effective width) carries more axial force than the weaker slab (four inch slab). The eight inch concrete slab developed axial force up to about 425 kips in compression at a vertical midspan deflection of about 0.27d. The four inch slab though developed an axial force of only 190 kips in compression. This is less than half the axial force in the eight inch slab. Those findings confirms the earlier conclusions regarding the developed axial forces in the steel beams.

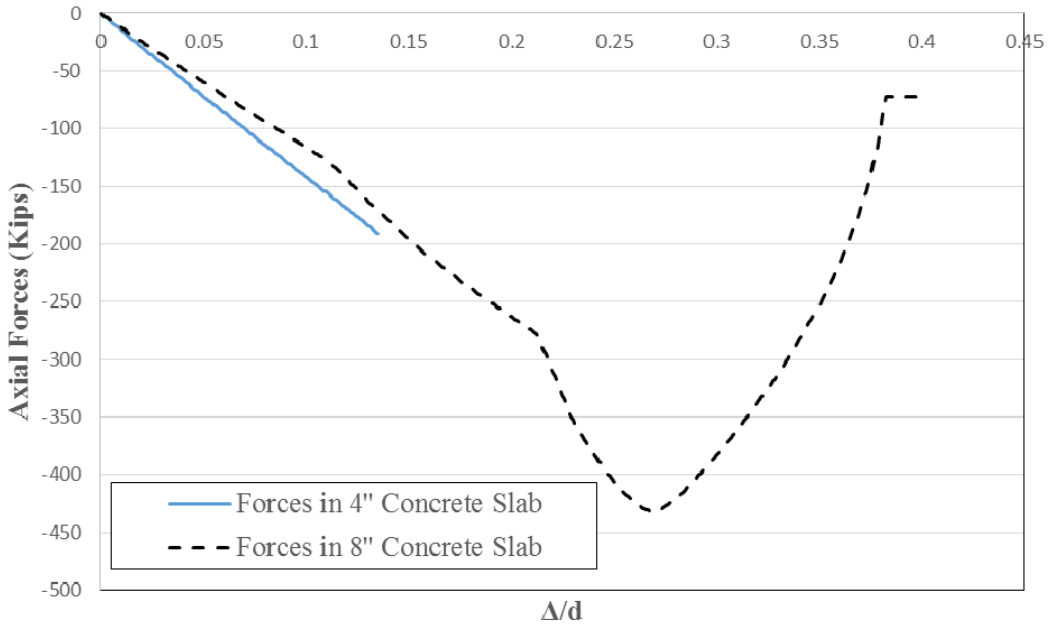

Figure 6-9: Forces in Concrete Slabs - Axial forces versus midspan deflection

6.3 Effect of Building Height

Three steel frames with concrete slabs were analyzed in order to study the impact of building height on the results. The eight, five and three story frames that were

designed are shown in Figure 6-10. The steel sections for the three and the five story steel frames are presented in Figure 6-11.

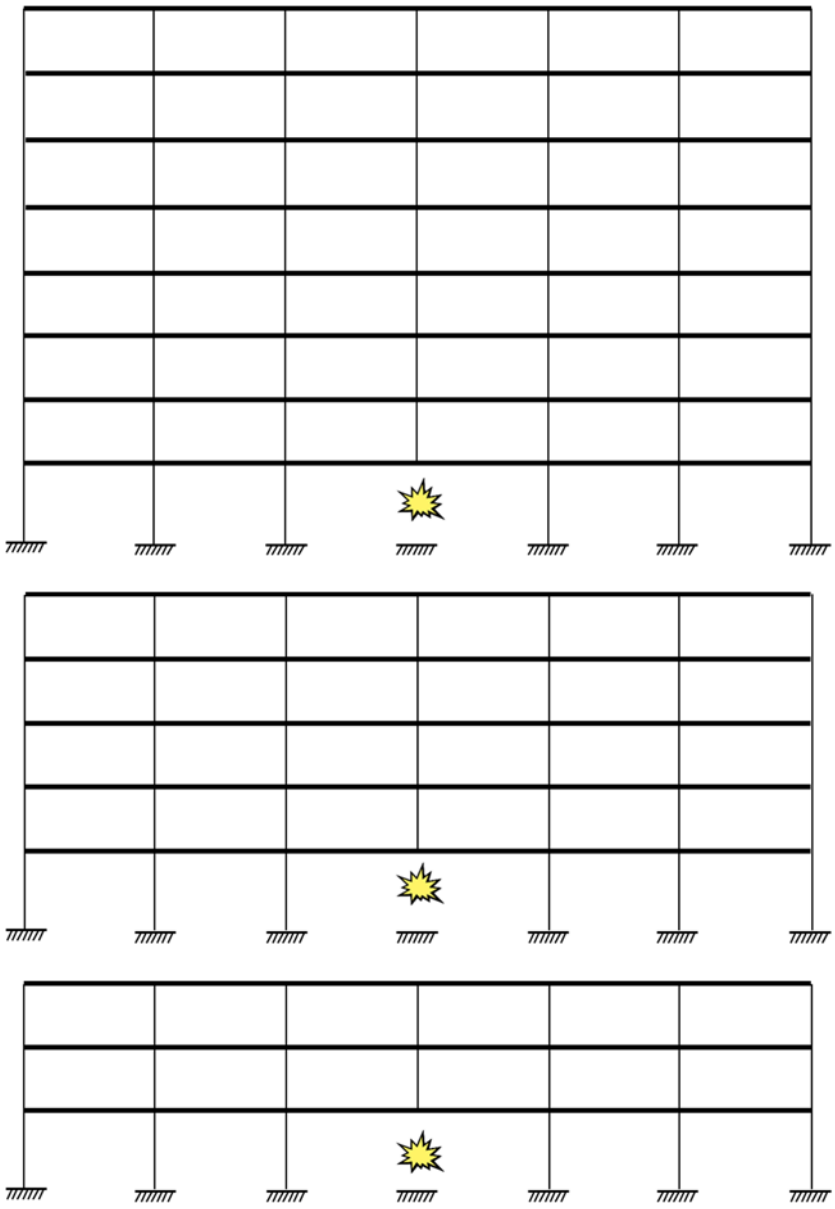

Figure 6-10: Eight, Five and Three Story Frames with Concrete Slabs

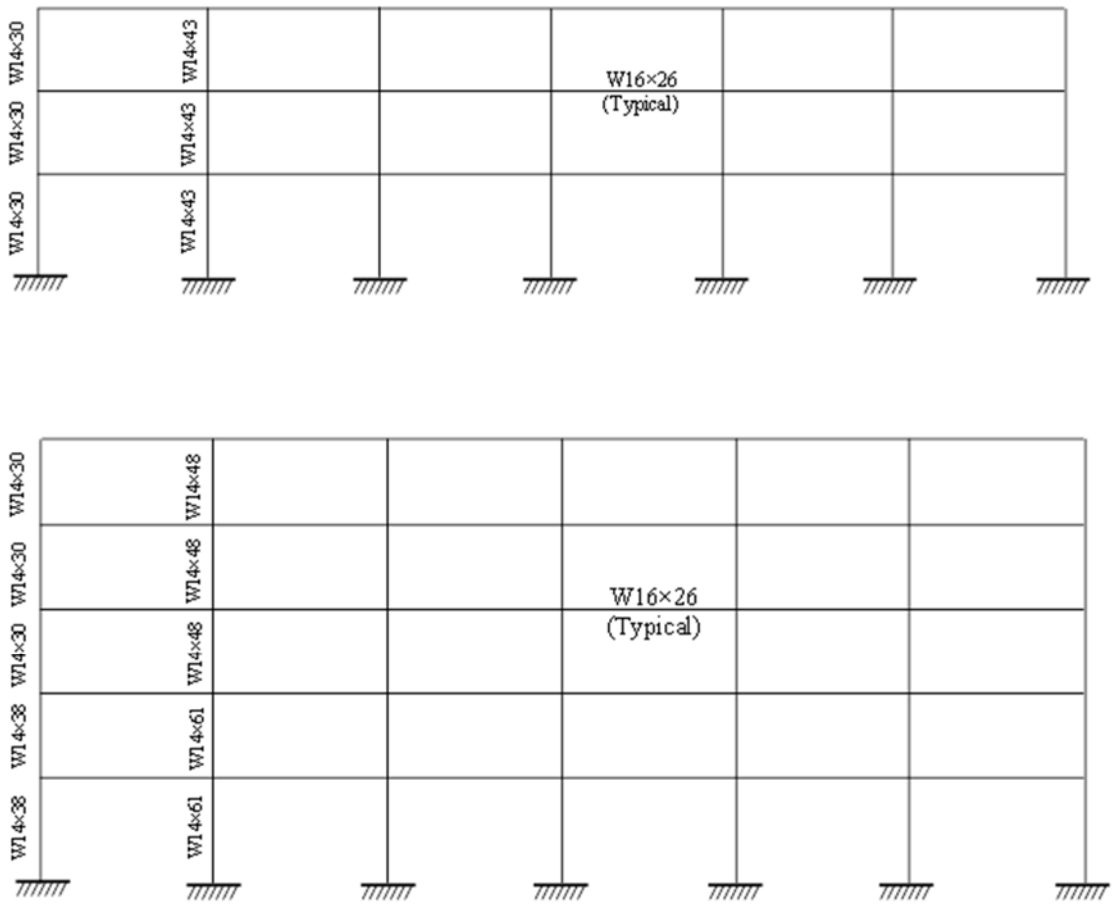

Figure 6-11: Three & Five Story Steel Frames Elevations

Six steel frames were modeled in OpenSees (three heights, each with two concrete slab thicknesses) and were subjected to a concentrated load at midspan of the first story beam. Plots showing the behavior of the different steel frames with concrete slabs are presented in the next set of figures. The axial forces and moment at the ends of the first story beams are presented in Figures 6-12 through 6-14.

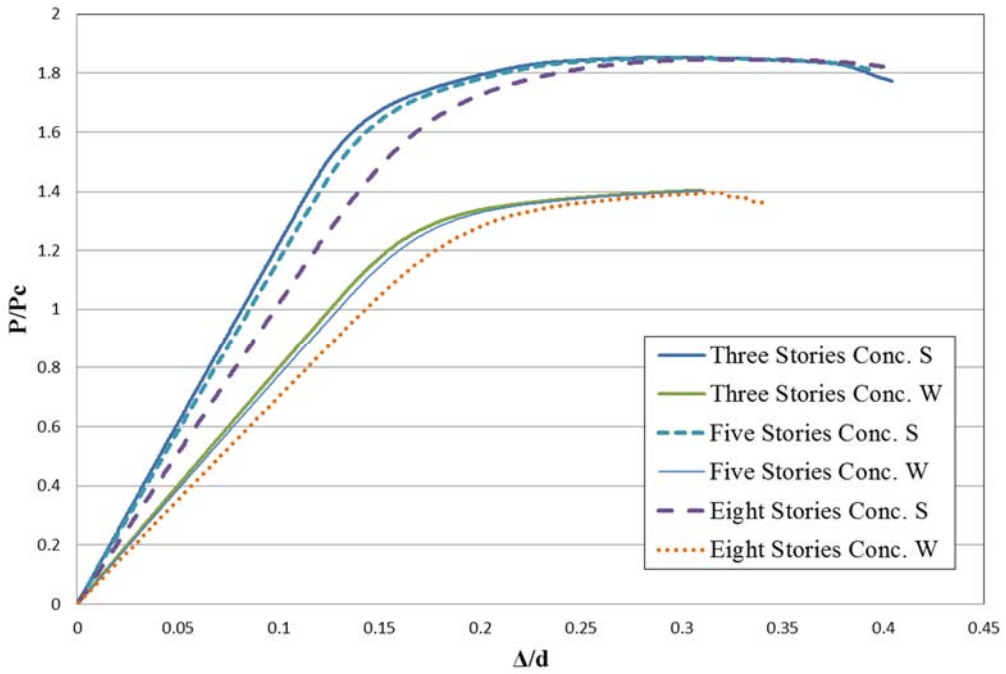

Figure 6-12: Vertical Load versus Deflection

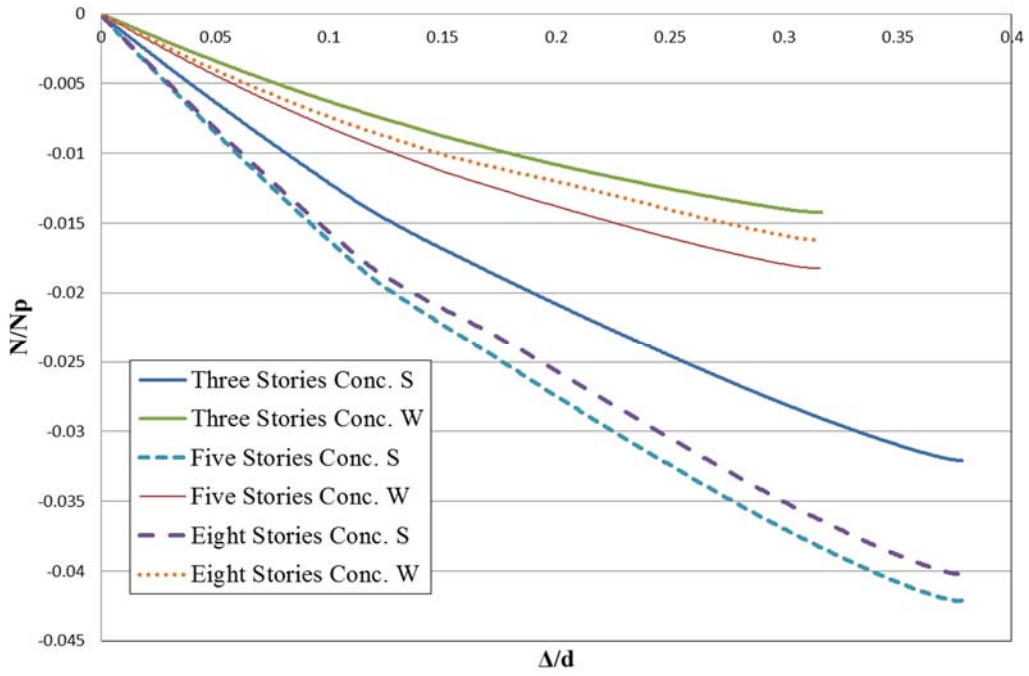

Figure 6-13: Axial Force versus Deflection

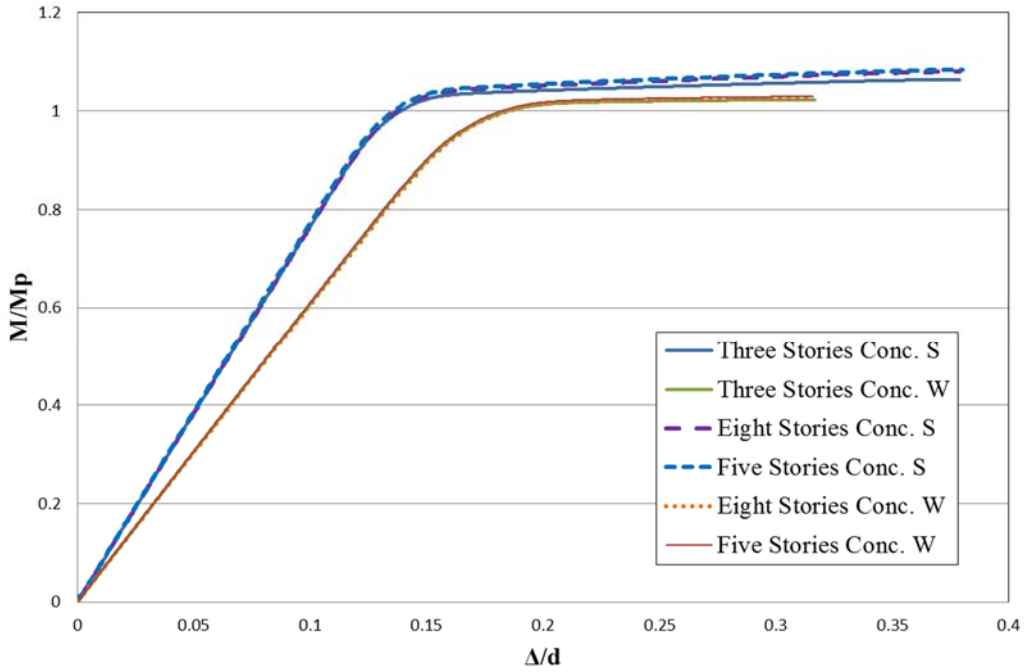

Figure 6-14: Moment versus Deflection

Figure 6-12 shows the load carrying capacities of the first story floors of the six steel frames with concrete slabs. The results show that the thickness of the concrete slab and the effective width have much more impact on the results than does the height of the frame. It can be observed that shorter frames tend to develop load carrying capacity at a faster rate compared to the taller frames. The three story steel frame with eight inch concrete slab achieves a load carrying capacity of 1.6 P_c at a vertical deflection of 0.14d while the eight story steel frame with eight inch concrete slab at the same deflection has a load carrying capacity of 1.4 P_c. This trend applies to the steel frames with four inch concrete slabs as well. The load carrying capacity of the 1st story floors of the eight inch concrete slabs at a vertical deflection of 0.3d is 1.3 times that of the 1st story floors with four inch concrete slabs for the same vertical deflection.

The generated axial forces and moments at the beam ends of the first floor beams of the three, five and eight story frames for the two concrete slab thicknesses are presented in Figure 6-13 and Figure 6-14. None of the 1st floor beams of the steel frames developed any significant axial forces. On the other hand, all the beams managed to get to moment levels higher than the plastic collapse moment of the bare steel frames. Again, the behavior of the beams can be attributed to the existence of the concrete slabs. First, the concrete slabs develop large compression forces, as can be seen in Figure 6-9, that minimize the overall axial forces in the beams. Second, the presence of concrete slabs increase the plastic collapse moment of the steel frames as the slabs contribute to the overall moment resistance of the steel frames.

The thickness of the concrete slab seems again to influence the behavior of the beams. The eight inch concrete slab frames developed more axial forces and sustained the loads to a higher deflection than the four inch concrete slab frames. For the eight inch concrete slab beams, the three story frame developed less axial forces and moments at the end of the beam than the five and eight story frames.

Those results are in agreement with the load carrying capacities of the frames from the previous plots. The impact of the concrete slabs had a bigger effect on the beam behavior than the frame height. However, as the height of the frame increases the other structural members (columns and beams) start to play a bigger role. That explains why there is more axial force in the beams of the 1st floor of the five story frames than the axial forces in the 1st floor beams of the eight story frames. That was the case for both of the two concrete slab thickness.

The axial forces and moments present in the beam ends of those steel frames support the fact that concrete slabs play a vital role in resisting the progressive collapse forces in steel frames regardless of frame height.

6.4 Effect of AAC & BRB Placement

In chapter four, the impact of the AAC infill on the catenary action demand in the steel frames was discussed. Chapter five focused on how the BRB existence in steel frames in highly seismic areas would affect the behavior of steel frames that are subjected to extreme load cases such as the missing column scenario. In order to tie the concrete slab contribution to the AAC and BRB cases, two placement scenarios (AAC Infill and a BRB) for the five story steel frame plus the five story frame with concrete slabs were considered. The different placement scenarios are shown in Figures 6-15 through 6-17. Finally, there is no AAC infill or BRB at the ground floor because it was assumed that the extreme event that destroyed the column also destroyed the AAC infill and BRBs.

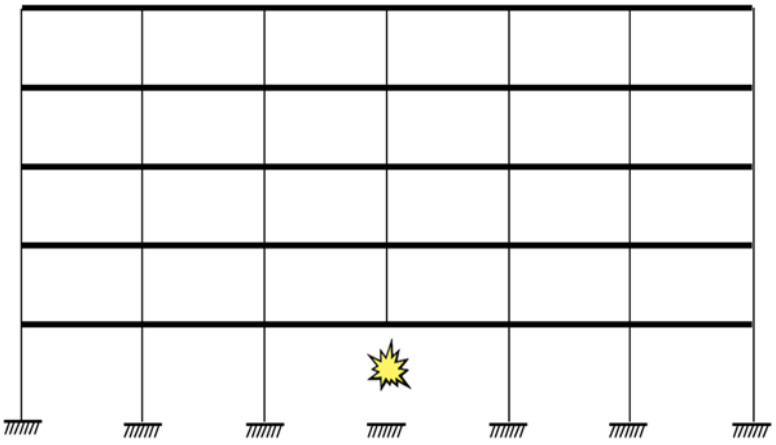

Figure 6-15: The Five Story Steel Frame with Concrete Slabs

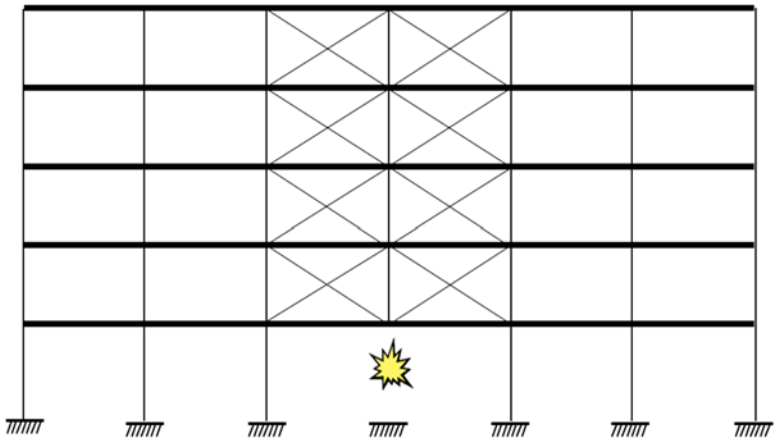

Figure 6-16: Five Story Frame with AAC Infill & Concrete Slabs

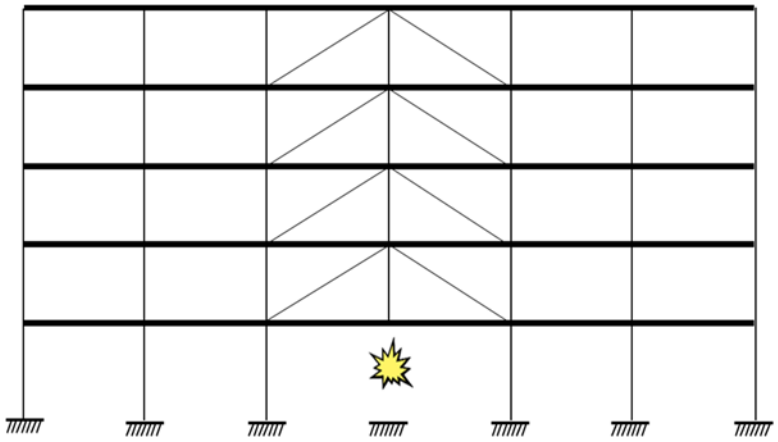

Figure 6-17: Five Story Frame with BRBs & Concrete Slabs

The three steel frames were analyzed in OpenSees to evaluate the impact of having a concrete slab along with AAC infill or BRB. The impact of those variable on the results was investigated. The results of the first story double span beams from the three scenarios are plotted in Figures 6-18 through Figure 6-21.

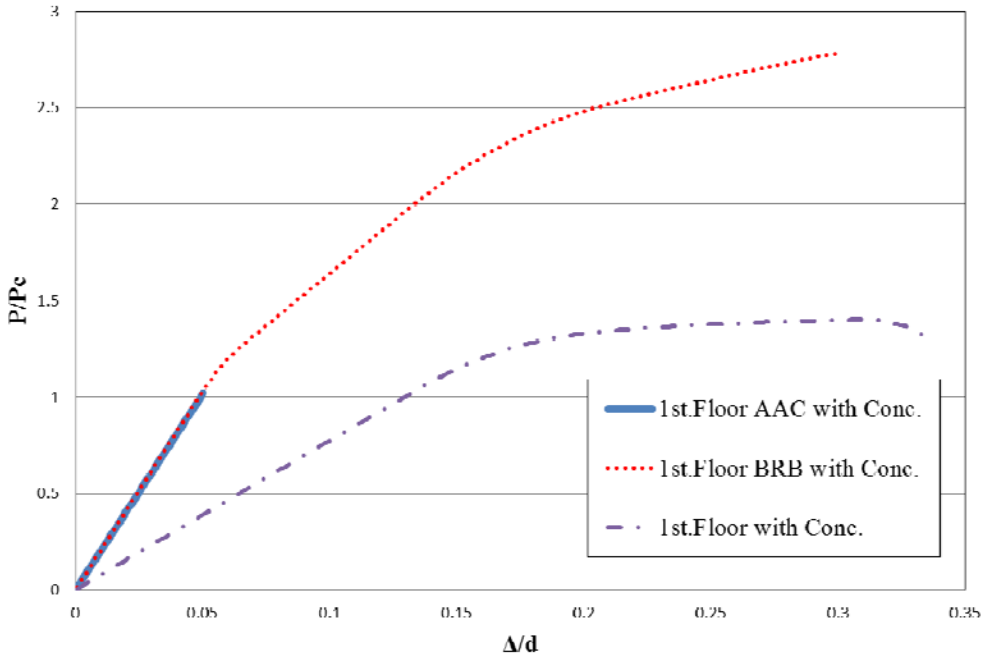

Figure 6-18: Vertical Load versus Deflection

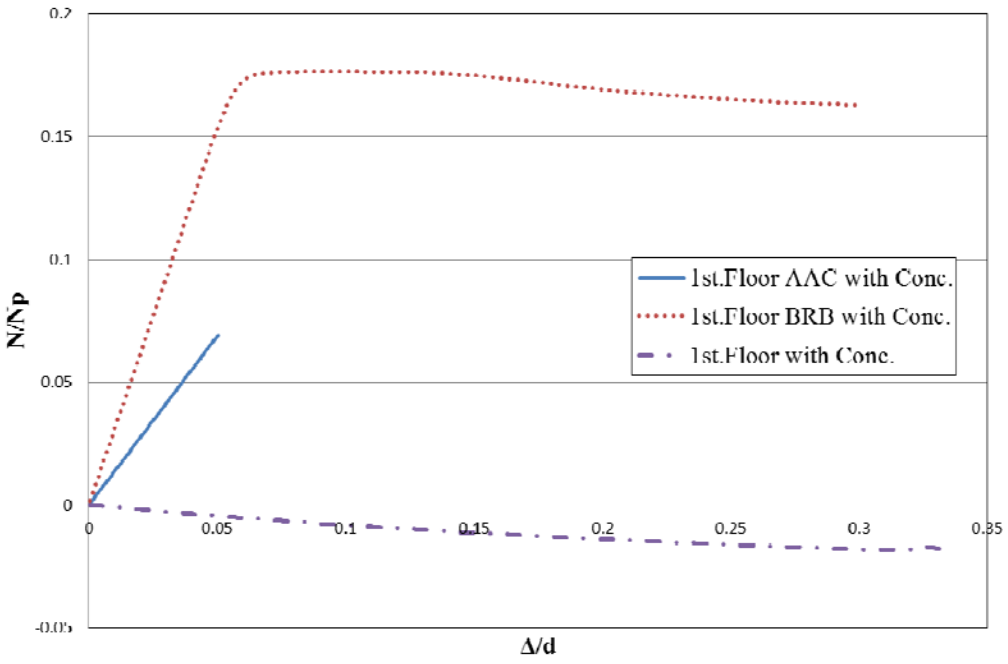

Figure 6-19: Axial Force versus Deflection

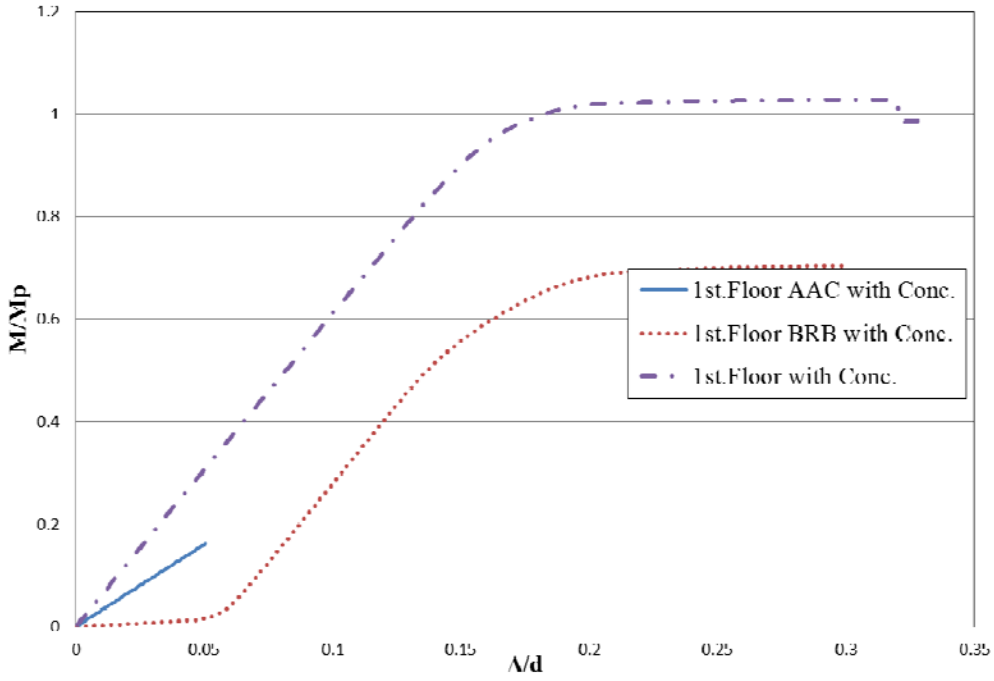

Figure 6-20: Moment versus Deflection

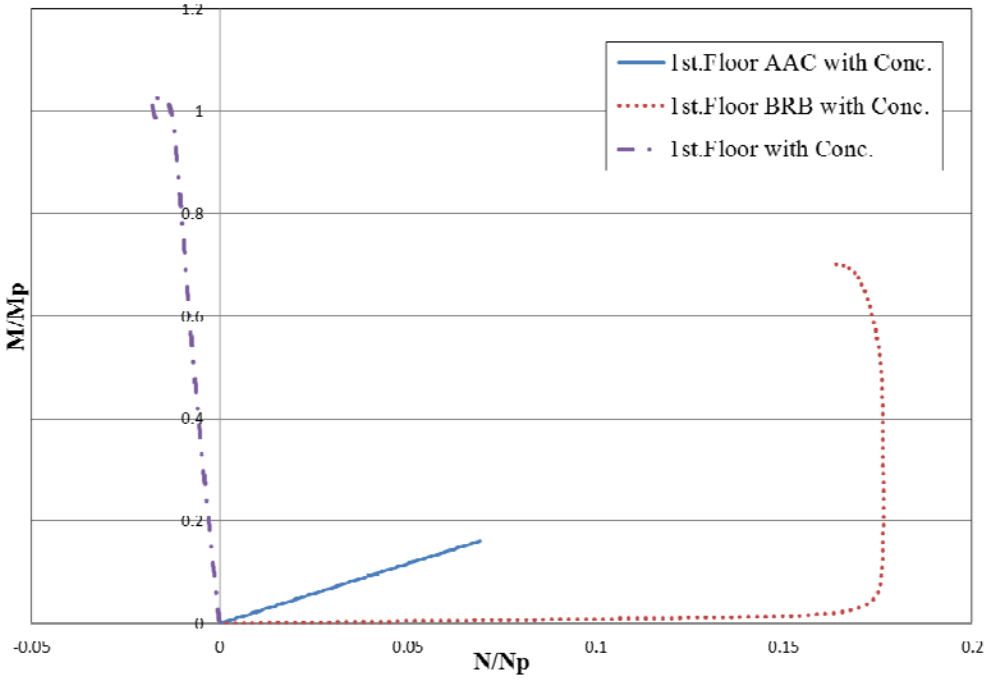

Figure 6-21: Interaction Diagram

Figure 6-18 shows the load carrying capacity of the three steel frames with the concrete slabs, AAC infill and BRB. The figure shows that the 1st floor beams behave significantly differently from each other. The 1st floor beam of the steel frame with AAC infill reaches a load carrying capacity of 1 P_c at a midspan deflection of about 0.35d. On the other hand, the 1st floor beam of the steel frame with BRBs reaches a load carrying capacity of 2.8 P_c at a midspan deflection of about 0.3d. The wide range of results highlights the impact of AAC infill and BRBs placement on the steel frame with concrete slabs. This difference in load carrying capacity can be attributed to the role played by the AAC struts on top of the double span beam. The AAC struts resist the additional loads resulting from the column loss and transfer the loads to the lateral load resisting system. Therefore, adding those struts (in the middle bay) increases the rate of load resistance as compared to the steel frame with concrete slab without AAC. However, the deflection of the double span beam is limited by the strength of the AAC infill.

The steel frame with BRBs is different. The BRBs in the middle bay increase the load carrying capacity by taking a part in resisting the additional loads resulting from the missing column scenario. The BRB case carries more load than the AAC infill case (remember that the BRBs can resist compression and tension while the AAC infill only resists compression). The BRB and AAC steel frames had a similar slope at the beginning, but as the deflection increased, the AAC case stopped while the BRB steel frame kept resisting loads up to 2.8P_c. This observation leads to the conclusion that, even with the concrete slab presence, the BRBs play a more significant role in the load carrying capacity of the steel frame than the concrete with AAC. Obviously, this

conclusion is based on the current placement of the AAC and BRB. In other words, the AAC and BRBs are most effective when placed above the damaged or removed column.

Figures 6-19 through 6-21 show the generated axial forces and moments at the beam ends of the 1st floor beam for the same three scenarios. Examination of the generated axial forces in the different frames help to clarify the beam behavior. The steel frame with concrete slabs only developed limited compression forces in the beam; again this can be attributed to the contribution of the concrete slab in load resistance. The steel frame with concrete slabs and AAC infill developed catenary action forces in the beam up to 0.07 N_p at a vertical midspan deflection of about 0.05d. Finally, the steel frame with concrete slabs and BRB developed tensile axial forces at a rate higher than the AAC case. At a vertical deflection of 0.06d, the axial forces at the beam end plateaued then stopped at a vertical deflection of 0.3d.

The existence of the concrete slab obviously limited the deflection of the beams. That behavior was not changed by adding AAC infill and BRBs. The main difference was that the AAC infill and the BRBs increased the developed axial tension forces in the beams, even with the concrete slabs. For the BRB case, the beam started generating high axial forces compared to the concrete only and AAC infill cases because of the BRB configuration and the fact that BRB can resist tension and compression forces. This beam behavior didn't last long as the deflection increased and the other floors with concrete slabs started contributing as well. The result was that the beam axial forces started plateauing and slightly decreasing. On the other hand, in the AAC infill case, the beam started developing axial forces at a constant rate, presumably up to the crushing of AAC infill. The reason the AAC is different from the concrete only case and the BRB case is

the way AAC infill is placed and the characteristics of the AAC. The AAC infill can only resist compression and it is basically connected to the middle bay beams at the beam ends and middle span.

Similar observations can be noted in Figure 6-20 and 6-21.The steel frame with concrete slabs generated moment at the beam end slightly higher than M_p as a result of the presence of concrete slab. The other two cases didn't get to M_p because of the presence of the AAC infill and the BRB.

6.5 Effect of Loading Type

In this section, responses from two loading types were investigated. The two types are concentrated loading and a combination of concentrated and distributed loading. For the concentrated load case, the plastic collapse load of the double span beam was applied as a concentrated load to the midspan point of the double span beam (Fig. 6-22).

ASCE 7-10 specifies 1.2 times the dead load plus 0.5 times the live load as a proper distributed loading combination for extraordinary events, which applies to this study. For the combined type of loading, the distributed and concentrated loads were applied simultaneously.

The results of four models (two loading types with two concrete slab thicknesses each) for the five story steel frame are presented in Figures 6-23 through 6-25.

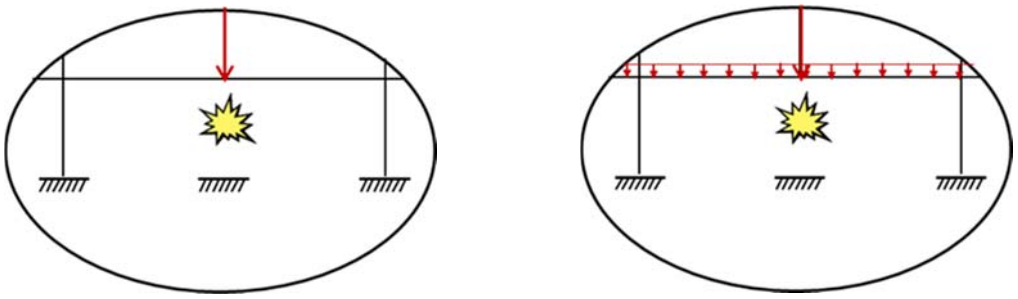

Figure 6-22: Concentrated and Combined Loading Techniques

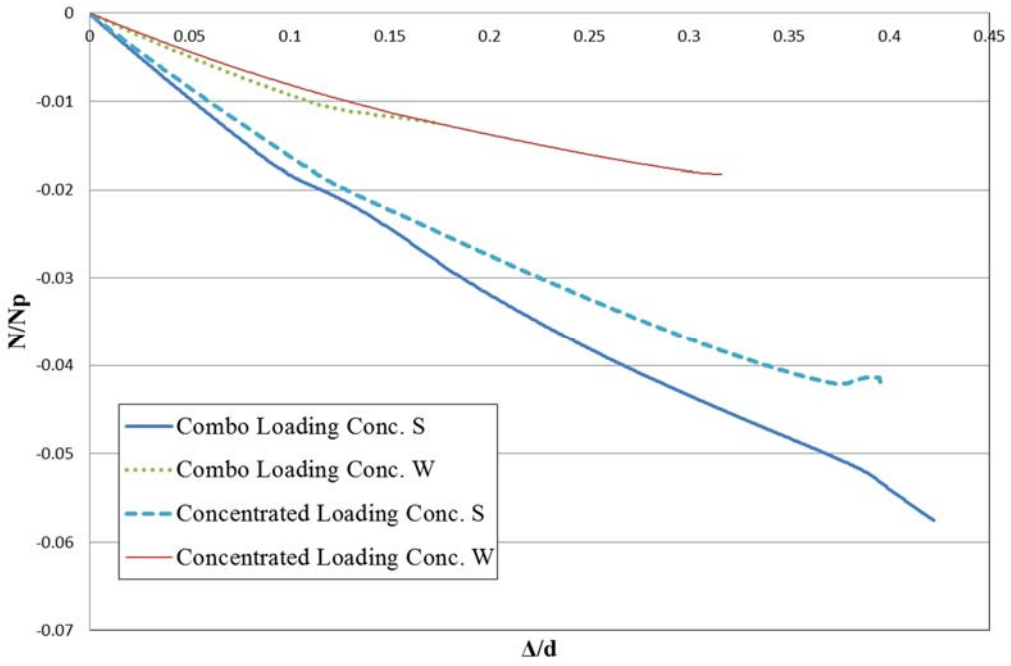

Figure 6-23: Effect of Loading Type - Axial Force versus Deflection

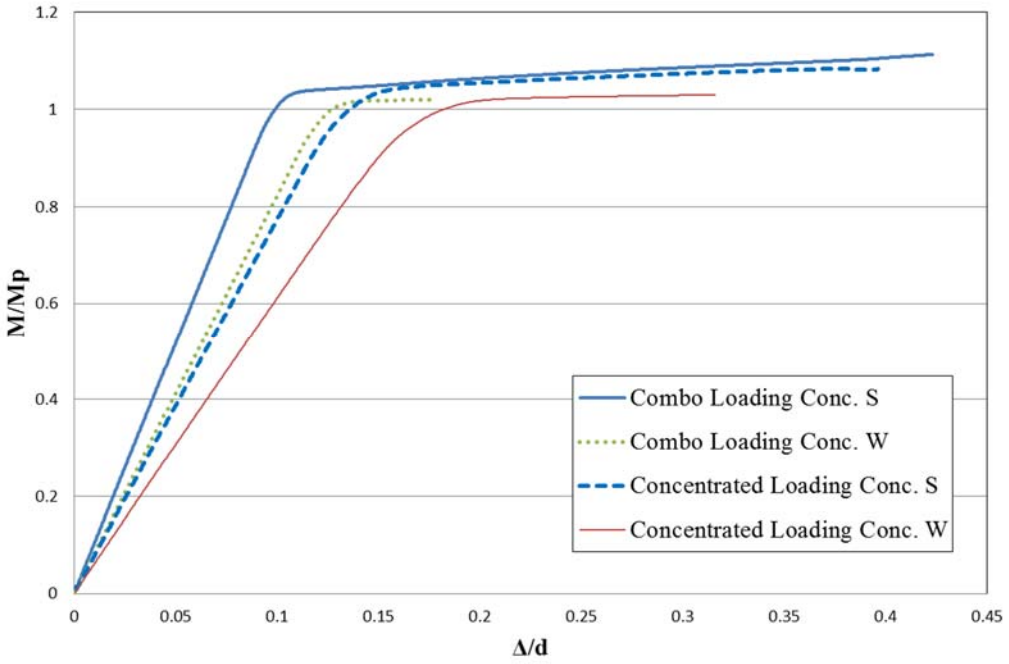

Figure 6-24: Effect of Loading Type - Moment versus Deflection

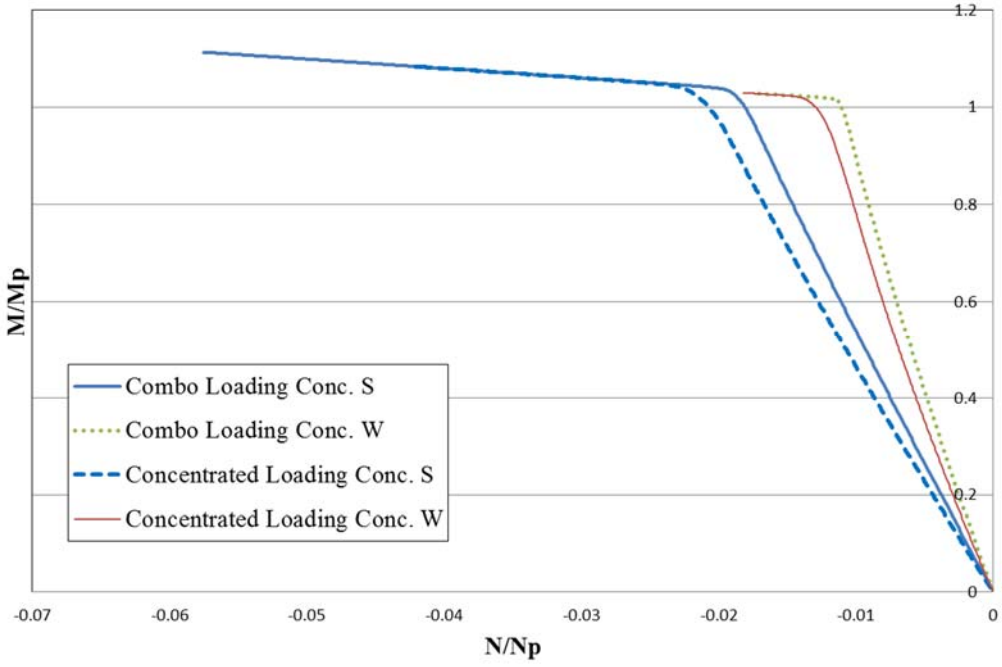

Figure 6-25: Effect of Loading Type - Interaction Diagram

The generated axial forces at the beam ends for the four steel frames are shown in Figure 6-23. The results show that the beam behavior is influenced by the concrete slab thickness and by the type of loading. The two steel frames with eight inch concrete slabs behave in a similar fashion, while the two steel frames with four inch concrete slabs behave similarly, but different from the eight inch concrete slab models.

The strong concrete slab models for the two loading types developed higher axial forces and sustained the loads to a larger vertical deflection than the weak concrete slab models, regardless of the loading type. For the weak concrete slabs, the two loading types initially shared a similar rate of developing axial forces. However, the concentrated load case developed axial forces up to 0.018 N_p at a vertical deflection of 0.3d while the combined case developed axial forces up to 0.012 N_p at a vertical deflection of 0.17d.

For the strong concrete slabs, the combined loading developed slightly higher axial forces than the concentrated loading. The difference between results can be attributed to the concrete slab contribution. For the weak concrete slab cases, the loading type had a minimal effect. On the other hand, for the strong concrete slab cases, the concrete slab had a greater contribution to the load carrying capacity and development of axial force in the beam. The strong concrete slabs started to resist the distributed load portion of the combined loading case early on.

Figure 6-24 and Figure 6-25 show the generated moment and the interaction diagram at the beam end. All four models were able to develop moment higher than M_p because of the concrete slab contribution. Again, the weak concrete slabs developed moment at beam ends barely above M_p. Meanwhile, the strong concrete slabs developed

moment at the beam ends of about $1.1M_p$. Those results are similar to those from the axial force plot of the two loading types.

6.6 Conclusions

The impact of concrete slabs on catenary action in steel frames and possible implications on the overall steel frame load carrying capacity was covered in this chapter. Push-down analyses of three, five and eight story steel frames with different concrete slabs were performed. Responses from an eight story steel frame with concrete slabs was compared to those from a bare steel moment frame. The load carrying capacity of the steel frames and the developed forces in the adjacent lateral load resisting frames were examined. The role of building height and its effect on the results was investigated. AAC infill and BRB placement scenarios of a five story steel frame and two loading types were considered to study their effect on the overall results.

The comparison between results from the steel frames with concrete slabs and the bare eight story frame indicated that the steel frames with concrete slabs had a higher load carrying capacity than the bare steel frame during the early stages after column loss. The data also showed that the concrete slabs make a significant contribution in resisting the catenary action demands in steel beams. Another observation was that the thicker and stronger the concrete slabs, the more they contribute to the load carrying capacity of the steel frame. It was also noticed that the building height had a lower impact on the results than did the slab thickness. Furthermore, after results from certain AAC infill and BRB placement scenarios were compared, the beam behavior showed that the placement of BRBs in the middle double span bay significantly increased the load carrying capacity of

the steel frame. Similarly, when AAC infill panels were added to the middle double span bay, the steel frame was able to sustain more load than the concrete only case, but the load was lower than those of the steel frame with BRBs. Finally two loading types were investigated: concentrated and combined loading, whose responses showed that loading type had less of an impact on the developed catenary forces compared to the concrete slab contribution. In conclusion, the findings of this section highlight the importance of accounting for concrete slabs when calculating the developed catenary action forces in the adjacent lateral load resisting systems.

The conclusions of this research were based on the assumptions made in this research and on the limited number of building heights and concrete slabs that were presented. Hence, the conclusions are limited to the scope of the study.

Chapter 7: Summary, Conclusions, and Recommendations

7.1 Summary

This research focused on understanding the impact of AAC infill, BRBs and concrete slabs on catenary action in steel frames and possible implications on the overall steel frame carrying capacity. In the first two chapters, the research topic was introduced and a literature review of catenary action demands was presented. Current design guidelines and how they address those forces were also described.

In the third chapter, the finite element modeling of the progressive collapse of the steel structures were detailed. The different material models, element types and sections were covered as well. The fourth chapter focused on catenary action in steel frames and the impact of AAC infill on the developed axial forces. The fifth chapter addressed catenary action in steel frames with BRBs in highly seismic regions. The impact of the BRBs on the developed catenary forces in the steel beams and on the overall frame behavior were the primary topic of this chapter.

Chapter six described the influence of the concrete slabs. In this chapter, the contribution of the concrete slab to the load carrying capacity of the steel frame and the resulting effects on the developed catenary forces were highlighted. Additionally, the influence of two types of infill, AAC infill and BRBs, were analyzed again, this time with concrete slabs.

To recap, push-down analyses of three, five and eight story steel frames with different configurations were performed. Eight story steel frames with AAC infill, buckling restrained braces and concrete slabs were compared to a bare steel moment frame. The load

carrying capacity of the frames and the developed forces in the steel beams were examined. The role of building height and its effect on results was studied. Finally, several placement scenarios in a five story steel frame and different loading types were considered to study the effect of AAC infill and BRB placement and loading types on the overall results.

For this study, SAP 2000 (commercial software package) was used to design all the steel frames. OpenSees (Open System for Earthquake Engineering Simulation), a software developed by the Pacific Earthquake Engineering Research (PEER) Center of the University of California at Berkeley, was used to analyze the models.

Finally, the results of this research emphasize the importance of AAC infill, BRBs, and concrete slabs on the developed catenary action forces in steel frames. Without accounting for the different types of infill and concrete slabs in steel structures, calculations of the catenary forces would be unrealistic and possibly over-conservative.

7.2 Conclusions

Based on the work performed in this research, the following conclusions regarding the behavior of the steel beams, adjacent side frames and overall structure were reached:

- The AAC infilled frame had a higher load carrying capacity than the bare steel frame.
- The AAC infilled frame generated a lower demand on the adjacent frame (i.e. developed lower axial forces at beam ends compared to the bare steel frame) due to the presence of AAC struts.
- Varying the building height, in the presence of AAC infill, had a significant

impact on the results.

- After results from four AAC placement scenarios were compared, the beam behavior showed that the placement of AAC struts in the middle double span bay limited the developed catenary action forces in the steel frame.
- Including even one floor of AAC struts above the removed column ensures improved load carrying capacity of the frame compared to including no AAC infill in that bay at all.
- The loading type (concentrated, distributed or a combined loading) had a significant impact on the developed catenary forces in AAC infilled frames.
- The BRB frame had a higher load carrying capacity than the bare steel frame.
- The side frames in BRB frames resist more forces than the bare steel frames due to the fact that BRBs increase the lateral stiffness of the side frames.
- Varying building height, in the presence of BRBs, has a significant impact only on the load carry capacity of the frames. On the other hand, the building height has a negligible effect on catenary action development.
- The beam behavior showed that placement of BRBs in the middle double span bay significantly increased the load carrying capacity of the steel frame. On the other hand, when BRBs were removed from that bay only and were kept everywhere else in the structure, the steel frames behaved similarly, regardless of the BRB placement scenario.
- Having four or two bays of BRBs had virtually no impact on the load carrying capacity of the frame.
- The loading type had a significant impact on the developed catenary forces in

buckling restrained braced frames.

- Concrete slabs in steel frames increase the load carrying capacity of the frame early on.
- Varying concrete slab thickness has a bigger impact on the results than the changing the frame height or loading types.
- The concrete slab plays a big role in resisting the axial forces in the beams.
- Accounting for AAC infill in the calculation of catenary action demands, can significantly reduce the strength and ductility requirements of the connections and adjacent steel frames.
- Taking BRBs into consideration when designing steel structures to resist progressive collapse will increase the load carrying capacity of the structure, but might add more demand on the side frames.
- Consideration of the concrete slabs in steel framed structures is critical to avoid unrealistic calculations of catenary actions forces in the steel beams.

7.3 Recommendations

The following items are recommended for continued research efforts:

- Perform analytical analyses on additional frame heights and placement scenarios for AAC infill and BRBs.
- Investigate the impact of other types of concrete infill on the catenary action development and compare it to that of the AAC infill.
- Study the effect of other types of bracing (like concentric braces) on the behavior of the steel frame and determine how they impact the results in comparison with those from BRBs.
- Investigate micro-modeling of moment-frame connections.
- Perform three dimensional analysis for simple shear connections.
- Study composite action between the concrete slabs and steel beams.

References

Alashker, Y., Li, H., & El-Tawil, S. (2011). Approximations in Progressive Collapse Modeling. *Journal of Structural Engineering*, 914-924.

American Society of Civil Engineers (ASCE). (2010). *Minimum Design Loads for Buildings and Other Structures.* Reston: American Society of Civil Engineers.

British Standards (BSi). (2006). *Eurocode 1: Actions on structures.* Brussels, Belgium: European Committee for Standardization .

Byfield, M., & Paramasivam, S. (2007). Catenary action in steel-framed buildings. *Structures & Buildings, 160*(5), 247–257.

Centre for the Protection of National Infrastructure (CPNI). (2011). *Review of International Research on Structural Robustness and Disproportionate Collapse.* London, UK: Department for Communities and Local Government.

Chen, J., Peng, W., Ma, R., & He, M. (2012). Strengthening of Horizontal Bracing on Progressive Collapse Resistance of Multistory Steel Moment Frame. *Journal of Performance of Constructed Facilities, 26*(5), 720-724.

De Souza, R. (2000). Force-Based Finite Element for Large Displacement Inelastic Analysis of Frames. *Ph.D Dissertation*. Berkeley, CA: University of California.

Escalera, V. (2011). Enhancing Progressive Collapse Resistance of Steel Building Frames using Thin Infill Steel Panels. *M.S.Thesis.* San Luis Obispo: California Polytechnic State University.

Gerasimidis, S., & Baniotopoulos, C. C. (2011). Evaluation of wind load integration in disproportionate collapse analysis of steel moment frames for column loss. *Journal of Wind Engineering and Industrial Aerodynamics*, 1162-1173.

Gong, Y. (2010). Analysis and Design for the Resilience of Shear Connections. *Canadian Journal of Civil Engineering*, 1581-1589.

Habibullah , A. (2013). *Structural Analysis Program 2000 (SAP2000).* Computers and Structures, Inc.

Hayes Jr, J., Woodson, S., Pekelnicky, R., Poland, C., Corley, W., & Sozen, M. (2005). Can Strengthening for Earthquake Improve Blast and Progressive Collapse Resistance ? *Journal of Structural Engineering, 131*(8), 1157-1177.

Humar, J., Lau, D., & Pierre, J. (2001). Performance of buildings during the 2001 Bhuj earthquake. *Canadian Journal of Civil Engineering, 28*(6), 979-991.

International Code Council, Inc. (2009). *International Building Code.* Country Club Hills, IL: Delmar Cengage Learning.

Izzuddin, B., & Nethercot, D. (2009). Design-oriented approaches for progressive collapse assessment: load-factor vs ductility-centred methods. *Proceedings of Structures Congress*, (pp. 1-10). Austin, Texas.

Joint ACI/ASCE/TMS Committee 530. (2008). *Building Code Requirements and Specification for Masonry Structures and Related Commentaries.* Boulder, CO: The Masonry Society.

Khandelwal, K., & El-Tawil, S. (2007). Collapse behavior of steel special moment resisting frame connections. *Journal of Structural Engineering, 133*(5), 646-655.

Khandelwal, K., & El-Tawil, S. (2011). Pushdown resistance as a measure of robustness in progressive collapse analysis. *Engineering Structures, 33*(9), 2653-2661.

Khandelwal, K., El-Tawil, S., & Sadek, F. (2009). Progressive collapse analysis of seismically designed steel braced frames. *Journal of Constructional Steel Research, 65*(3), 699-708.

Khandelwal, K., El-Tawil, S., Kunnath, S., & Lew, H. (2008). Macromodel-based simulation of progressive collapse: Steel frame structures. *Journal of structural engineering, 134*(7), 1070-1078.

Kim, J., & An, D. (2009). Evaluation of progressive collapse potential of steel moment frames considering catenary action. *The structural design of tall and special buildings, 18*(4), 455-465.

Kim, J., & Choi, H. (2004). Behavior and Design of Structures with Buckling-Restrained Braces. *Engineering Structures, 26*, 693-706.

Kim, J., & Kim, T. (2009). Assessment of progressive collapse-resisting capacity of steel moment frames. *Journal of Constructional Steel Research, 65*(1), 169-179.

Kim, J., Choi, H., & Min, K. (2011). Use of rotational friction dampers to enhance seismic and progressive collapse resisting capacity of structures. *The structural design of tall and special buildings, 20*(4), 515-537.

Kim, J., Park, J.-H., & Lee, T.-H. (2011). Sensitivity Analysis of Steel Buildings Subjected to Column Loss. *Engineering Structures*, 421-432.

Kim, T., Kim, J., & Park, J. (2009). Investigation of progressive collapse-resisting capability of steel moment frames using push-down analysis. *Journal of Performance of Constructed Facilities, 23*(5), 327-335.

Kim, T., Kim, U.-S., & Kim, J. (2010). Collapse resistance of unreinforced steel moment connections. *The Structural Design of Tall and Special Buildings*, 724-735.

Kwasniewski, L. (2010). Nonlinear dynamic simulations of progressive collapse for a multistory building. *Engineering Structures, 32*(5), 1223-1235.

Liu, Y.-S., & Li, G.-Q. (2004). Behavior of Steel Frames With and Without AAC Infilled Walls Subjected to Static and Cyclic Horizontal Loads. *13th World Conference on Earthquake Engineering*, (p. 1112). Vancouver, Canada.

Mahin, S., Uriz, P., Aiken, I., Field, C., & Ko, E. (2004). Seismic Performance of Buckling Restrained Braced Frame Systems. *13th World Conference on Earthqauke Engineering.* Vancouver, Canada.

Main, J. A., Sadek, F., & Lew, H. S. (2009). Assessment of Robustness and Disproportionate Collapse Vulnerability of Steel Moment-Frame Buildings. *Second International Workshop on Performance, Protection & Strengthening of Structures Under Extreme Loading (PROTECT2009).* Hayama, Japan.

Marchand, K. A., & Alfawakhiri, F. (2004). *Blast and Progressive Collapse.* Chicago, IL: American Institute of Steel Construction (AISC).

Mashhadiali, N., & Kheyroddin, A. (2013). Progressive collapse assessment of new hexagrid structural system for tall buildings. *The Structural Design of Tall and Special Buildings*.

Mazzolani, F., Corte, G. D., & D'Aniello, M. (2009). Experimental analysis of steel dissipative bracing systems for seismic upgrading. *Journal of Civil Engineering and Management*, 7-19.

McKenna, F., & Fenves, G. (2000). *Open system for earthquake engineering simulation (OpenSees).* Berkeley: University of California.

Mehrabi, A., Shing, P., Schuller, M., & Noland, J. (1996). Experimental evaluation of masonry-infilled RC frames. *Journal of Structural Engineering, 122*(3), 228-237.

Neuenhofer, A., & Filippou, F. (1998). Geometrically Nonlinear Flexibility-Based Frame. *Journal of Structural Engineering, 124*(6), 704-711.

Pirmoz, A. (2011). Performance of Bolted Angle Connections in Progressive Collapse of Steel Frames. *The Structural Design of Tall and Special Buildings*, 349-370.

Quiel, S. E., & Marjanishvili, S. M. (2012). Fire Resistance of a Damaged Steel Building that has been Designed to Resist Progressive Collapse. *Journal of Performance of Constructed Facilities*, 402-409.

Ravichandran, S. (2009). Design Provisions for Autoclaved Aerated Concrete (AAC) Infilled Steel Moment Frames. *Ph.D Dissertation*. Austin, Texas: The University of Texas at Austin.

Ravichandran, S., & Klingner, R. (2012). Behavior of Steel Moment Frames with Autoclaved Aerated Concrete Infills. *ACI Structural Journal, 109*(1), 83-90.

Sabelli, R. (2001). *Research on Improving the Design and Analysis of Earthqauke-Resistant Steel-Braced Frames.* Ockland, California: Earthquake Engineering Research Institute.

Sabelli, R., Mahin, S., & Chang, C. (2003). Seismic Demands on Steel Braced Frame Buildings with Buckling-Restrained Braces. *Engineering Structures, 25*(5), 655-666.

Sadek, F., Main, J. A., Lew, H. S., Robert, S. D., & Chiarito, V. (2009). Testing and Analysis of Steel Beam-Column Assemblies under Column Removal Scenarios. *Structures Congress* (pp. 1-10). Austin,TX: ASCE.

Song, B. I., Sezen, H., & Giriunas, K. A. (2010). Experimental and Analytical Assessment on Progressive Collapse Potential of Two Actual Steel Frame Buildings. *Structures Congress* (pp. 1171-1182). Orlando, FL: ASCE.

Tan, S., & Astaneh-Asl,, A. (2003). Use of steel cables to prevent progressive collapse of existing buildings. *Proceedings of Sixth Conference on Tall Buildings in Seismic Regions.* Los Angeles: University of California, Berkeley.

Tsai, M.-H. (2012). A performance-based design approach for retrofitting regular building frames with steel braces against sudden column loss. *Journal of Constructional Steel Research*, 1-11.

Tsai, M.-H., & Huang, T.-C. (2009). Effect of Interior Brick-infill Partitions on the Progressive Collapse Potential of a RC Building:Linear Static Analysis Results. *Engineering and Technology, 26*, 883-889.

United Facilities Criteria (UFC). (2010). *Design of Buildings to Resist Progressive Collapse (UFC 4-023-03).* Washington, D.C.: United States Department of Defense.

US General Services Administration. (2003). *Progressive collapse analysis and design guidelines for new federal office buildings and major modernization projects.* Washington (DC): US General Services Administration (U.S. GSA).

Vlassis, A. G., Izzuddin, B. A., Elghazouli, A. Y., & Nethercot, D. A. (2009). Progressive collapse of multi-storey buildings due to failed floor impact. *Engineering Structures*, 1522-1534.

Xu, G., & Ellingwood, B. R. (2011). Disproportionate Collapse Performance of Partially Restrained Steel Frames with Bolted T-stub Connections. *Engineering Structures*, 32-43.

Appendix A: Selected OpenSees Files

```
wipe all;


model basic -ndm 2 -ndf 3;


file mkdir EightStoriesBaseModelBRBResults;


node 11 0 0

node 12 0 180

node 13 0 324

node 14 0 468

node 15 0 612

node 16 0 756

node 17 0 900

node 18 0 1044

node 19 0 1188

node 21 288 0

node 22 288 180

node 23 288 324

node 24 288 468

node 25 288 612

node 26 288 756
```

node 27 288 900

node 28 288 1044

node 29 288 1188

node 31 576 0

node 51 1152 0

node 61 1440 0

node 62 1440 180

node 63 1440 324

node 64 1440 468

node 65 1440 612

node 66 1440 756

node 67 1440 900

node 68 1440 1044

node 69 1440 1188

node 71 1728 0

node 72 1728 180

node 73 1728 324

node 74 1728 468

node 75 1728 612

node 76 1728 756

node 77 1728 900

node 78 1728 1044

node 79 1728 1188

node 910 331.20 27.00

node 911 532.80 153.00

node 912 331.20 201.60

node 913 532.80 302.40

node 914 331.20 351.00

node 915 532.80 446.40

node 916 331.20 495.00

node 917 532.80 590.40

node 918 331.20 639.00

node 919 532.80 734.40

node 920 331.20 783.00

node 921 532.80 878.40

node 922 331.20 927.00

node 923 532.80 1022.40

node 924 331.20 1071.00

node 925 532.80 1166.40

node 926 1396.80 27.00

node 927 1195.20 153.00

node 928 1396.80 201.60

node 929 1195.20 302.40

node 930 1396.80 351.00

```
node 931 1195.20 446.40

node 932 1396.80 495.00

node 933 1195.20 590.40

node 934 1396.80 639.00

node 935 1195.20 734.40

node 936 1396.80 783.00

node 937 1195.20 878.40

node 938 1396.80 927.00

node 939 1195.20 1022.40

node 940 1396.80 1071.00

node 941 1195.20 1166.40



###Beams Nodes---###

for {set i 0} {$i<101} {incr i} {

set nodeTag [expr $i+101]

set xdim [expr $i*5.76+576]

node $nodeTag $xdim 180

}

for {set i 0} {$i<101} {incr i} {

set nodeTag [expr $i+202]

set xdim [expr $i*5.76+576]

node $nodeTag $xdim 324
```

```
}
for {set i 0} {$i<101} {incr i} {
set nodeTag [expr $i+303]
set xdim [expr $i*5.76+576]
node $nodeTag $xdim 468
}
for {set i 0} {$i<101} {incr i} {
set nodeTag [expr $i+404]
set xdim [expr $i*5.76+576]
node $nodeTag $xdim 612
}
for {set i 0} {$i<101} {incr i} {
set nodeTag [expr $i+505]
set xdim [expr $i*5.76+576]
node $nodeTag $xdim 756
}
for {set i 0} {$i<101} {incr i} {
set nodeTag [expr $i+606]
set xdim [expr $i*5.76+576]
node $nodeTag $xdim 900
}
for {set i 0} {$i<101} {incr i} {
set nodeTag [expr $i+707]
```

```
set xdim [expr $i*5.76+576]
node $nodeTag $xdim 1044
}
for {set i 0} {$i<101} {incr i} {
set nodeTag [expr $i+808]
set xdim [expr $i*5.76+576]
node $nodeTag $xdim 1188
}

puts "Nodes defined!!!"

fix 11 1 1 1;
fix 21 1 1 1;
fix 31 1 1 1;
fix 51 1 1 1;
fix 61 1 1 1;
fix 71 1 1 1;

puts "BC's defined!!!"

geomTransf Linear 1;
geomTransf Corotational 2;
```

```
uniaxialMaterial ElasticPP 1 29000 0.00172413;

uniaxialMaterial Elastic 2 29000;

uniaxialMaterial Steel02 3 36 29000 0.003 15 0.925 0.15;


#Section--W16x40#

set d 16.0;

set tw 0.305;

set bf 7.00;

set tf 0.505;

set nfdw 2998;

set nftw 1;

set nfbf 1;

set nftf 101;


set dw [expr $d-2*$tf]

set y1 [expr -$d/2]

set y2 [expr -$dw/2]

set y3 [expr  $dw/2]

set y4 [expr  $d/2]


set z1 [expr -$bf/2]

set z2 [expr -$tw/2]

set z3 [expr  $tw/2]
```

```
set z4 [expr  $bf/2]


#
section fiberSec 1 {
    #            nfIJ  nfJK    yI  zI    yJ  zJ    yK  zK    yL  zL
    patch quadr  1 $nfbf $nftf   $y1 $z4   $y1 $z1   $y2 $z1   $y2 $z4
    patch quadr  1 $nftw $nfdw   $y2 $z3   $y2 $z2   $y3 $z2   $y3 $z3
    patch quadr  1 $nfbf $nftf   $y3 $z4   $y3 $z1   $y4 $z1   $y4 $z4
  }
puts "Section 1 Defined!!"
###---Other Sections----####
#Section--W16x31#
set d 15.9;
set tw 0.275;
set bf 5.53;
set tf 0.44;
set nfdw 3004;
set nftw 1;
set nfbf 1;
set nftf 88;


set dw [expr $d-2*$tf]
set y1 [expr -$d/2]
```

```
set y2 [expr -$dw/2]

set y3 [expr  $dw/2]

set y4 [expr  $d/2]


set z1 [expr -$bf/2]

set z2 [expr -$tw/2]

set z3 [expr  $tw/2]

set z4 [expr  $bf/2]


#

section fiberSec 2 {

    #             nfIJ  nfJK    yI  zI    yJ  zJ    yK  zK    yL  zL

    patch quadr  1 $nfbf $nftf   $y1 $z4   $y1 $z1   $y2 $z1   $y2 $z4

    patch quadr  1 $nftw $nfdw   $y2 $z3   $y2 $z2   $y3 $z2   $y3 $z3

    patch quadr  1 $nfbf $nftf   $y3 $z4   $y3 $z1   $y4 $z1   $y4 $z4

  }

puts "Section 2 Defined!!"


#Section--W14x283#

set d 16.7;

set tw 1.29;

set bf 16.1;

set tf 2.07;
```

```
set nfdw 2512;
set nftw 1;
set nfbf 1;
set nftf 414;

set dw [expr $d-2*$tf]
set y1 [expr -$d/2]
set y2 [expr -$dw/2]
set y3 [expr  $dw/2]
set y4 [expr  $d/2]

set z1 [expr -$bf/2]
set z2 [expr -$tw/2]
set z3 [expr  $tw/2]
set z4 [expr  $bf/2]

#
section fiberSec 3 {
    #             nfIJ  nfJK    yI  zI    yJ  zJ    yK  zK    yL  zL
    patch quadr  1 $nfbf $nftf   $y1 $z4   $y1 $z1   $y2 $z1   $y2 $z4
    patch quadr  1 $nftw $nfdw   $y2 $z3   $y2 $z2   $y3 $z2   $y3 $z3
    patch quadr  1 $nfbf $nftf   $y3 $z4   $y3 $z1   $y4 $z1   $y4 $z4
  }
```

```
puts "Section 3 Defined!!"


#Section--W14x159#
set d 15.0;
set tw 0.745;
set bf 15.6;
set tf 1.19;
set nfdw 2524;
set nftw 1;
set nfbf 1;
set nftf 238;

set dw [expr $d-2*$tf]
set y1 [expr -$d/2]
set y2 [expr -$dw/2]
set y3 [expr  $dw/2]
set y4 [expr  $d/2]

set z1 [expr -$bf/2]
set z2 [expr -$tw/2]
set z3 [expr  $tw/2]
set z4 [expr  $bf/2]
```

```
#
section fiberSec 4 {
    #            nfIJ  nfJK    yI  zI    yJ  zJ    yK  zK    yL  zL
    patch quadr  1 $nfbf $nftf   $y1 $z4   $y1 $z1   $y2 $z1   $y2 $z4
    patch quadr  1 $nftw $nfdw   $y2 $z3   $y2 $z2   $y3 $z2   $y3 $z3
    patch quadr  1 $nfbf $nftf   $y3 $z4   $y3 $z1   $y4 $z1   $y4 $z4
  }
puts "Section 4 Defined!!"

#Section--W14x145#
set d 14.8;
set tw 0.68;
set bf 15.5;
set tf 1.09;
set nfdw 2524;
set nftw 1;
set nfbf 1;
set nftf 218;

set dw [expr $d-2*$tf]
set y1 [expr -$d/2]
set y2 [expr -$dw/2]
set y3 [expr  $dw/2]
```

```
set y4 [expr  $d/2]


set z1 [expr -$bf/2]
set z2 [expr -$tw/2]
set z3 [expr  $tw/2]
set z4 [expr  $bf/2]


#
section fiberSec 5 {
    #             nfIJ  nfJK    yI  zI    yJ  zJ    yK  zK    yL  zL
    patch quadr  1 $nfbf $nftf   $y1 $z4   $y1 $z1   $y2 $z1   $y2 $z4
    patch quadr  1 $nftw $nfdw   $y2 $z3   $y2 $z2   $y3 $z2   $y3 $z3
    patch quadr  1 $nfbf $nftf   $y3 $z4   $y3 $z1   $y4 $z1   $y4 $z4
  }
puts "Section 5 Defined!!"


#Section--W14x176#
set d 15.2;
set tw 0.83;
set bf 15.7;
set tf 1.31;
set nfdw 2516;
set nftw 1;
```

```
set nfbf 1;
set nftf 262;

set dw [expr $d-2*$tf]
set y1 [expr -$d/2]
set y2 [expr -$dw/2]
set y3 [expr  $dw/2]
set y4 [expr  $d/2]

set z1 [expr -$bf/2]
set z2 [expr -$tw/2]
set z3 [expr  $tw/2]
set z4 [expr  $bf/2]

#
section fiberSec 6 {
    #            nflJ  nfJK    yI  zI    yJ  zJ    yK  zK    yL  zL
    patch quadr  1 $nfbf $nftf   $y1 $z4   $y1 $z1   $y2 $z1   $y2 $z4
    patch quadr  1 $nftw $nfdw   $y2 $z3   $y2 $z2   $y3 $z2   $y3 $z3
    patch quadr  1 $nfbf $nftf   $y3 $z4   $y3 $z1   $y4 $z1   $y4 $z4
  }
puts "Section 6 Defined!!"
```

```
#Section--W14x132#
set d 14.7;
set tw 0.645;
set bf 14.7;
set tf 1.03;
set nfdw 2528;
set nftw 1;
set nfbf 1;
set nftf 206;

set dw [expr $d-2*$tf]
set y1 [expr -$d/2]
set y2 [expr -$dw/2]
set y3 [expr  $dw/2]
set y4 [expr  $d/2]

set z1 [expr -$bf/2]
set z2 [expr -$tw/2]
set z3 [expr  $tw/2]
set z4 [expr  $bf/2]

#
section fiberSec 7 {
```

```
    #            nfIJ  nfJK    yI  zI    yJ  zJ    yK  zK    yL  zL
    patch quadr  1 $nfbf $nftf   $y1 $z4   $y1 $z1   $y2 $z1   $y2 $z4
    patch quadr  1 $nftw $nfdw   $y2 $z3   $y2 $z2   $y3 $z2   $y3 $z3
    patch quadr  1 $nfbf $nftf   $y3 $z4   $y3 $z1   $y4 $z1   $y4 $z4
  }
puts "Section 7 Defined!!"



##---Define Elements-----------------------------------------##
##---Other Beams-------------------------------##
element elasticBeamColumn 101 12 22 11.8 29000 5000000 1;
element elasticBeamColumn 102 13 23 11.8 29000 5000000 1;
element elasticBeamColumn 103 14 24 11.8 29000 5000000 1;
element elasticBeamColumn 104 15 25 11.8 29000 5000000 1;
element elasticBeamColumn 105 16 26 11.8 29000 5000000 1;
element elasticBeamColumn 106 17 27 11.8 29000 5000000 1;
element elasticBeamColumn 107 18 28 11.8 29000 5000000 1;
element elasticBeamColumn 108 19 29 9.1 29000 5000000 1;
element elasticBeamColumn 201 22 101 11.8 29000 5000000 1;
element elasticBeamColumn 202 23 202 11.8 29000 5000000 1;
element elasticBeamColumn 203 24 303 11.8 29000 5000000 1;
element elasticBeamColumn 204 25 404 11.8 29000 5000000 1;
element elasticBeamColumn 205 26 505 11.8 29000 5000000 1;
```

element elasticBeamColumn 206 27 606 11.8 29000 5000000 1;

element elasticBeamColumn 207 28 707 11.8 29000 5000000 1;

element elasticBeamColumn 208 29 808 9.1 29000 5000000 1;

element elasticBeamColumn 501 201 62 11.8 29000 5000000 1;

element elasticBeamColumn 502 302 63 11.8 29000 5000000 1;

element elasticBeamColumn 503 403 64 11.8 29000 5000000 1;

element elasticBeamColumn 504 504 65 11.8 29000 5000000 1;

element elasticBeamColumn 505 605 66 11.8 29000 5000000 1;

element elasticBeamColumn 506 706 67 11.8 29000 5000000 1;

element elasticBeamColumn 507 807 68 11.8 29000 5000000 1;

element elasticBeamColumn 508 908 69 9.1 29000 5000000 1;

element elasticBeamColumn 601 62 72 11.8 29000 5000000 1;

element elasticBeamColumn 602 63 73 11.8 29000 5000000 1;

element elasticBeamColumn 603 64 74 11.8 29000 5000000 1;

element elasticBeamColumn 604 65 75 11.8 29000 5000000 1;

element elasticBeamColumn 605 66 76 11.8 29000 5000000 1;

element elasticBeamColumn 606 67 77 11.8 29000 5000000 1;

element elasticBeamColumn 607 68 78 11.8 29000 5000000 1;

element elasticBeamColumn 608 69 79 9.1 29000 5000000 1;

##---Columns--------------------------------##

element elasticBeamColumn 11 11 12 51.8 29000 2140 1;

element elasticBeamColumn 12 12 13 51.8 29000 2140 1;

element elasticBeamColumn 13 13 14 38.8 29000 1530 1;

```
element elasticBeamColumn 14 14 15 38.8 29000 1530 1;
element elasticBeamColumn 15 15 16 38.8 29000 1530 1;
element elasticBeamColumn 16 16 17 38.8 29000 1530 1;
element elasticBeamColumn 17 17 18 38.8 29000 1530 1;
element elasticBeamColumn 18 18 19 38.8 29000 1530 1;
element elasticBeamColumn 21 21 22 46.7 29000 1900 1;
element elasticBeamColumn 22 22 23 46.7 29000 1900 1;
element elasticBeamColumn 23 23 24 42.7 29000 1710 1;
element elasticBeamColumn 24 24 25 42.7 29000 1710 1;
element elasticBeamColumn 25 25 26 42.7 29000 1710 1;
element elasticBeamColumn 26 26 27 42.7 29000 1710 1;
element elasticBeamColumn 27 27 28 83.3 29000 3840 1;
element elasticBeamColumn 28 28 29 83.3 29000 3840 1;
element elasticBeamColumn 31 31 101 46.7 29000 1900 1;
element elasticBeamColumn 32 101 202 46.7 29000 1900 1;
element elasticBeamColumn 33 202 303 42.7 29000 1710 1;
element elasticBeamColumn 34 303 404 42.7 29000 1710 1;
element elasticBeamColumn 35 404 505 42.7 29000 1710 1;
element elasticBeamColumn 36 505 606 42.7 29000 1710 1;
element elasticBeamColumn 37 606 707 83.3 29000 3840 1;
element elasticBeamColumn 38 707 808 83.3 29000 3840 1;
element nonlinearBeamColumn 42 151 252 3 4 1;
element nonlinearBeamColumn 43 252 353 3 5 1;
```

```
element nonlinearBeamColumn 44 353 454 3 5 1;
element nonlinearBeamColumn 45 454 555 3 5 1;
element nonlinearBeamColumn 46 555 656 3 5 1;
element nonlinearBeamColumn 47 656 757 3 3 1;
element nonlinearBeamColumn 48 757 858 3 3 1;
element elasticBeamColumn 51 51 201 46.7 29000 1900 1;
element elasticBeamColumn 52 201 302 46.7 29000 1900 1;
element elasticBeamColumn 53 302 403 42.7 29000 1710 1;
element elasticBeamColumn 54 403 504 42.7 29000 1710 1;
element elasticBeamColumn 55 504 605 42.7 29000 1710 1;
element elasticBeamColumn 56 605 706 42.7 29000 1710 1;
element elasticBeamColumn 57 706 807 83.3 29000 3840 1;
element elasticBeamColumn 58 807 908 83.3 29000 3840 1;
element elasticBeamColumn 61 61 62 46.7 29000 1900 1;
element elasticBeamColumn 62 62 63 46.7 29000 1900 1;
element elasticBeamColumn 63 63 64 42.7 29000 1710 1;
element elasticBeamColumn 64 64 65 42.7 29000 1710 1;
element elasticBeamColumn 65 65 66 42.7 29000 1710 1;
element elasticBeamColumn 66 66 67 42.7 29000 1710 1;
element elasticBeamColumn 67 67 68 83.3 29000 3840 1;
element elasticBeamColumn 68 68 69 83.3 29000 3840 1;
element elasticBeamColumn 71 71 72 51.8 29000 2140 1;
element elasticBeamColumn 72 72 73 51.8 29000 2140 1;
```

```
element elasticBeamColumn 73 73 74 38.8 29000 1530 1;
element elasticBeamColumn 74 74 75 38.8 29000 1530 1;
element elasticBeamColumn 75 75 76 38.8 29000 1530 1;
element elasticBeamColumn 76 76 77 38.8 29000 1530 1;
element elasticBeamColumn 77 77 78 38.8 29000 1530 1;
element elasticBeamColumn 78 78 79 38.8 29000 1530 1;
##---BRBs--------------------------------##
element elasticBeamColumn 901 21 910 22.5 29000 1 1;
element truss 902 910 911 4.5 3;
element elasticBeamColumn 903 911 101 22.5 29000 1 1;
element elasticBeamColumn 904 22 912 20 29000 1 1;
element truss 905 912 913 4.0 3;
element elasticBeamColumn 906 913 202 20 29000 1 1;
element elasticBeamColumn 907 23 914 17.5 29000 1 1;
element truss 908 914 915 3.5 3;
element elasticBeamColumn 909 915 303 17.5 29000 1 1;
element elasticBeamColumn 910 24 916 15.0 29000 1 1;
element truss 911 916 917 3.0 3;
element elasticBeamColumn 912 917 404 15.0 29000 1 1;
element elasticBeamColumn 913 25 918 15.0 29000 1 1;
element truss 914 918 919 3.0 3;
element elasticBeamColumn 915 919 505 15.0 29000 1 1;
element elasticBeamColumn 916 26 920 10.0 29000 1 1;
```

element truss 917 920 921 2 3;

element elasticBeamColumn 918 921 606 10.0 29000 1 1;

element elasticBeamColumn 919 27 922 7.5 29000 1 1;

element truss 920 922 923 1.5 3;

element elasticBeamColumn 921 923 707 7.5 29000 1 1;

element elasticBeamColumn 922 28 924 5 29000 1 1;

element truss 923 924 925 1 3;

element elasticBeamColumn 924 925 808 5 29000 1 1;

element elasticBeamColumn 925 61 926 22.5 29000 1 1;

element truss 926 926 927 4.5 3;

element elasticBeamColumn 927 927 201 22.5 29000 1 1;

element elasticBeamColumn 928 62 928 20 29000 1 1;

element truss 929 928 929 4.0 3;

element elasticBeamColumn 930 929 302 20 29000 1 1;

element elasticBeamColumn 931 63 930 17.5 29000 1 1;

element truss 932 930 931 3.5 3;

element elasticBeamColumn 933 931 403 17.5 29000 1 1;

element elasticBeamColumn 934 64 932 15.0 29000 1 1;

element truss 935 932 933 3.0 3;

element elasticBeamColumn 936 933 504 15.0 29000 1 1;

element elasticBeamColumn 937 65 934 15.0 29000 1 1;

element truss 938 934 935 3.0 3;

```
element elasticBeamColumn 939 935 605 15.0 29000 1 1;
element elasticBeamColumn 940 66 936 10.0 29000 1 1;
element truss 941 936 937 2.0 3;
element elasticBeamColumn 942 937 706 10.0 29000 1 1;
element elasticBeamColumn 943 67 938 7.5 29000 1 1;
element truss 944 938 939 1.5 3;
element elasticBeamColumn 945 939 807 7.5 29000 1 1;
element elasticBeamColumn 946 68 940 5 29000 1 1;
element truss 947 940 941 1 3;
element elasticBeamColumn 948 941 908 5 29000 1 1;



##---The Beams---####
for {set i 0} {$i<100} {incr i} {
set eltag [expr $i+1101]
set inode [expr $i+101]
set jnode [expr $i+102]
element nonlinearBeamColumn $eltag $inode $jnode 3 1 2
}
for {set i 0} {$i<100} {incr i} {
set eltag [expr $i+1201]
set inode [expr $i+202]
set jnode [expr $i+203]
```

```
element nonlinearBeamColumn $eltag $inode $jnode 3 1 2
}
for {set i 0} {$i<100} {incr i} {
set eltag [expr $i+1301]
set inode [expr $i+303]
set jnode [expr $i+304]
element nonlinearBeamColumn $eltag $inode $jnode 3 1 2
}
for {set i 0} {$i<100} {incr i} {
set eltag [expr $i+1401]
set inode [expr $i+404]
set jnode [expr $i+405]
element nonlinearBeamColumn $eltag $inode $jnode 3 1 2
}
for {set i 0} {$i<100} {incr i} {
set eltag [expr $i+1501]
set inode [expr $i+505]
set jnode [expr $i+506]
element nonlinearBeamColumn $eltag $inode $jnode 3 1 2
}
for {set i 0} {$i<100} {incr i} {
set eltag [expr $i+1601]
set inode [expr $i+606]
```

```
set jnode [expr $i+607]
element nonlinearBeamColumn $eltag $inode $jnode 3 1 2
}
for {set i 0} {$i<100} {incr i} {
set eltag [expr $i+1701]
set inode [expr $i+707]
set jnode [expr $i+708]
element nonlinearBeamColumn $eltag $inode $jnode 3 1 2
}
for {set i 0} {$i<100} {incr i} {
set eltag [expr $i+1801]
set inode [expr $i+808]
set jnode [expr $i+809]
element nonlinearBeamColumn $eltag $inode $jnode 3 2 2
}

puts "Elements Defined!!"

recorder Node -file EightStoriesBaseModelBRBResults/Node252.out -time -node 252 -
dof 2 disp;
recorder Node -file EightStoriesBaseModelBRBResults/Node202.out -time -node 202 -
dof 1 3 disp;
```

recorder Node -file EightStoriesBaseModelBRBResults/Node302.out -time -node 302 -dof 1 3 disp;

recorder Node -file EightStoriesBaseModelBRBResults/Node151.out -time -node 151 -dof 2 disp;

recorder Node -file EightStoriesBaseModelBRBResults/Node101.out -time -node 101 -dof 1 3 disp;

recorder Node -file EightStoriesBaseModelBRBResults/Node201.out -time -node 201 -dof 1 3 disp;

recorder Node -file EightStoriesBaseModelBRBResults/Node353.out -time -node 353 -dof 2 disp;

recorder Node -file EightStoriesBaseModelBRBResults/Node555.out -time -node 555 -dof 2 disp;

recorder Node -file EightStoriesBaseModelBRBResults/Node303.out -time -node 303 -dof 1 3 disp;

recorder Node -file EightStoriesBaseModelBRBResults/Node858.out -time -node 858 -dof 2 disp;

recorder Element -file EightStoriesBaseModelBRBResults/ForceE1101-S1.out -time -ele 1101 section 1 force;

recorder Element -file EightStoriesBaseModelBRBResults/ForceE1151-S1.out -time -ele 1151 section 1 force;

recorder Element -file EightStoriesBaseModelBRBResults/ForceE1201-S1.out -time -ele 1201 section 1 force;

recorder Element -file EightStoriesBaseModelBRBResults/ForceE1251-S1.out -time -ele 1251 section 1 force;

recorder Element -file EightStoriesBaseModelBRBResults/ForceE1301-S1.out -time -ele 1301 section 1 force;

recorder Element -file EightStoriesBaseModelBRBResults/ForceE1501-S1.out -time -ele 1501 section 1 force;

recorder Element -file EightStoriesBaseModelBRBResults/ForceE1351-S1.out -time -ele 1351 section 1 force;

recorder Element -file EightStoriesBaseModelBRBResults/ForceE1801-S1.out -time -ele 1801 section 1 force;

recorder Element -file EightStoriesBaseModelBRBResults/ForceE901.out -time -ele 901 Force;

recorder Element -file EightStoriesBaseModelBRBResults/ForceE902.out -time -ele 902 axialForce;

recorder Element -file EightStoriesBaseModelBRBResults/ForceE903.out -time -ele 903 Force;

recorder Element -file EightStoriesBaseModelBRBResults/ForceE904.out -time -ele 904 Force;

recorder Element -file EightStoriesBaseModelBRBResults/ForceE907.out -time -ele 907 Force;

recorder Element -file EightStoriesBaseModelBRBResults/ForceE910.out -time -ele 910 Force;

recorder Element -file EightStoriesBaseModelBRBResults/ForceE913.out -time -ele 913 Force;

recorder Element -file EightStoriesBaseModelBRBResults/ForceE916.out -time -ele 916 Force;

recorder Element -file EightStoriesBaseModelBRBResults/ForceE919.out -time -ele 919 Force;

recorder Element -file EightStoriesBaseModelBRBResults/ForceE922.out -time -ele 922 Force;

recorder Element -file EightStoriesBaseModelBRBResults/ForceE903L.out -time -ele 903 localForce;

recorder Element -file EightStoriesBaseModelBRBResults/ForceE906L.out -time -ele 906 localForce;

recorder Element -file EightStoriesBaseModelBRBResults/ForceE909L.out -time -ele 909 localForce;

recorder Element -file EightStoriesBaseModelBRBResults/ForceE912L.out -time -ele 912 localForce;

recorder Element -file EightStoriesBaseModelBRBResults/ForceE915L.out -time -ele 915 localForce;

recorder Element -file EightStoriesBaseModelBRBResults/ForceE918L.out -time -ele 918 localForce;

recorder Element -file EightStoriesBaseModelBRBResults/ForceE921L.out -time -ele 921 localForce;

```
recorder Element -file EightStoriesBaseModelBRBResults/ForceE924L.out -time -ele
924 localForce;

pattern Plain 1 Linear {
load 151 0 -386.4477 0
}

constraints Plain;
numberer Plain;
system SparseGEN;
test NormDispIncr 1.0e-1 10;
algorithm Newton;
integrator DisplacementControl 151 2 -0.01;
analysis Static
analyze 100000;
loadConst -time 0.0;

puts "Done!"
```